UNIVERSITÀ
DEGLI STUDI
DI PADOVA

Sede Amministrativa: Università degli Studi di Padova
Dipartimento di Agronomia Animali Alimenti Risorse Naturali e Ambiente
(DAFNAE)

Scuola di dottorato di ricerca in: Scienze Animali e Agroalimentari
Indirizzo: Scienze Animali
XXVIII Ciclo

Apoplastic glutathione degradation by gamma-glutamyl transferase isoforms GGT1 and GGT2 is important for generative and vegetative development in *Arabidopsis thaliana*

Direttore della Scuola: Ch.ma Prof.ssa Viviana Corich
Coordinatore d'indirizzo: Ch.mo Prof. Roberto Mantovani
Supervisore: Ch.mo Prof. Antonio Masi

Dottorando: Sabrina Giaretta

Men love to wonder, and that is the seed of our science

(Ralph Waldo Emerson, 1883)

Table of contents

Index of figures ... **III**
Index of tables ... **IV**
Table of abbreviations ... **V**
Abstract ... **VII**
Riassunto ... **VIII**
1 Introduction ... **1**
1.1 Sulfur ... 1
1.2 Glutathione ... 2
1.3 Reactive oxygen species (ROS) as signaling molecules ... 5
1.3.1 ROS and PCD in development and growth ... 6
1.4 Gamma-glutamyl-transferase (GGT) in glutathione catabolism ... 7
1.4.1 Plant ... 7
1.4.2 Animal ... 9
1.5 Seed ... 10
1.5.1 Seed development ... 11
1.5.2 Assimilates transport ... 12
1.6 Aims of the project ... 13
2 Materials and methods ... **15**
2.1 Technical equipment and materials ... 15
2.1.1 Technical equipment ... 15
2.1.2 Chemicals ... 16
2.1.3 Software ... 16
2.1.4 Consumables ... 17
2.1.5 Enzymes and kits ... 17
2.1.6 Primers ... 18
2.2 Plant methods ... 19
2.2.1 Plant material ... 19
2.2.2 Soil cultivation ... 19
2.2.3 Surface sterilization of seeds ... 20
2.2.4 Growth of Arabidopsis on Petri plate under sterile conditions ... 20
2.2.5 Hydroponic culture ... 21
2.2.6 Detection of phenotypic differences between mutants ... 21
2.2.7 Germination rate ... 22
2.2.8 Pollen viability test ... 22
2.2.9 Crossing of *Arabidopsis thaliana* lines *sir1-1*, *ggt1*, *ggt2* and *ggct* ... 23
2.3 Molecular biology methods ... 23
2.3.1 Extraction of genomic DNA ... 23
2.3.2 Polymerase chain reaction (PCR) ... 24
2.3.3 Agarose gel electrophoresis ... 24
2.3.4 Generation of double *ggt1/ggt2* RNAi mutants ... 25
2.3.5 Total RNA extraction from plant tissue ... 26
2.3.6 Determination of RNA concentration and quality ... 28
2.3.7 First strand cDNA synthesis ... 28
2.3.8 Quantitative real time PCR ... 28
2.4 Biochemical methods ... 29
2.4.1 Protein extraction ... 29
2.4.2 Determination of protein concentration ... 29
2.4.3 SDS- polyacrylamide gel electrophoresis (PAGE) Tricine ... 30
2.4.4 Protein staining and quantification ... 30
2.4.5 Activity assay ... 30
2.5 Analytical methods ... 32
2.5.1 Acidic extraction of thiols ... 32
2.5.2 Determination of thiols ... 32
2.5.3 GSH depletion in liquid solution ... 33
2.5.4 Ascorbate ... 33
2.5.5 Determination of free amino acid ... 33

2.5.6 Analysis of total carbon, nitrogen, and sulfur content 34
2.6 Microscopic methods 34
2.6.1 Slide preparation for enzyme histochemical analysis 34
2.7 Statistical analysis 34
3 Results 36
3.1 Selection of *ggt1*/*ggt2* RNAi double mutants 36
3.1.1 Construct design, plant transformation and homozygote selection 36
3.1.2 Validation of *GGT1* and *GGT2* silencing on RNAi lines 37
3.2 *GGT1* and *GGT2* anatomical expression using Genevestigator and eFP Browser 39
3.3 Phenotypic characterization of generative tissue 44
3.3.1 Determination of GGT activity in seed 44
3.3.2 Seed yield and influential factors 46
3.3.3 Silique characterization 47
3.3.4 Germination rate 49
3.3.5 Seeds biochemical composition 50
3.3.6 Protein profile 53
3.3.7 Determination of *GGCT2;1* and *GGT4* transcripts in *ggt1* and *ggt2* seeds 53
3.4 Root biochemical and phenotypic characterization 54
3.4.1 Depletion of GSH from external solution 54
3.4.2 GGT activity *in vivo* and *in vitro* in root 56
3.4.3 GST activity in root 58
3.4.4 Root morphological and growth characterization 58
3.5 Phenotypic characterization in vegetative tissues 60
3.5.1 Rosette growth 60
3.5.2 Trichomes 61
3.5.3 Metabolites: thiols, ascorbate 61
3.6 Double mutants using *ggt1, ggt2*, *sir1-1*, *ggct2;1* 62
4 Discussion 65
4.1 GGT and seed development 65
4.1.1 GTT leads cys to the seed 66
4.1.2 GGT as ROS modulator in seed development 68
4.1.3 Oxidative stress in seed and germination 70
4.2 GGT and glutathione in vegetative tissues development 72
4.2.1 Root 72
4.2.2 Leaves and trichome 74
5 Conclusion 76
6 References 77
Publications 84
Acknowledgment - Ringraziamenti 85

Index of figures

Fig. 1 The ascorbate glutathione cycle 3
Fig. 2 Glutathione biosynthesis 4
Fig. 3 Glutathione degradation pathways 8
Fig. 4 Development stages of *Arabidopsis thaliana* seed 12
Fig. 5 Model of Stadler et.al showing the symplastic domain in Arabidopsis seed and the path of assimilates 13
Fig. 6 RNAi construct in pWatergate vector 25
Fig. 7 *GGT1* and *GGT2* relative expression in root of WT, *ggt1, ggt2,* L5 and L6 38
Fig. 8 Temporal and spatial localization of *GGT1* and *GGT2* expression in developing seed using eFP Browser 41
Fig. 9 Anatomical localization of *GGT1* and *GGT2* expression using Genenvestigator® 43
Fig. 10 Detection of GGT activity in dry seed and its localization in transversal section of green silique. 45
Fig. 11 Seed yield, 100-seed-weight, branches and time to bolting of wild-type, *ggt1*, *ggt2*, L5 and L6 47
Fig. 12 Silique characterization of wild-type, *ggt1*, *ggt2*, L5 and L6 48
Fig. 13 Germination rate on filter paper 50
Fig. 14 Total content of nitrogen, carbon and sulfur in mature seed 51
Fig. 15 Free amino acids composition of dry seeds of WT, *ggt1*, *ggt2*, L5 and L6 52
Fig. 16 Seed protein profile 53
Fig. 17 *GGCT2;1* and *GGT4* relative expression in mature seed of WT, *ggt1* and *ggt2* 54
Fig. 18 Percentage of glutathione degradation and cys-gly releasing by root of wild-type, *ggt1*, *ggt2*, L5 and L6 plant 56
Fig. 19 GGT activity in root of wild-type, *ggt1*, *ggt2*, L5 and L6 57
Fig. 20 GST activity in root of wild-type, *ggt1*, *ggt2*, L5 and L6 58
Fig. 21 Root growth curves 59
Fig. 22 Rosette growth phenotype 60
Fig. 23 Trichomes in first true leaves 61
Fig. 24 Rosette comparison between single and relative double mutants 64

Index of tables

Table 1 Primers for cloning 18
Table 2 Primers for genotyping 18
Table 3 Primer for qRT-PCR 18
Table 4 Transgene lines used in this thesis work 19
Table 5 Composition of ½ MS medium 20
Table 6 Combinations of the crossing performed 23
Table 7 Typical set up of PCR program 24
Table 8 Thiols content in dry seeds of WT, *ggt1*, *ggt2*, L5 and L6 51
Table 9 Root structure parameters 59
Table 10 Thiols and ascorbate levels in leaves of wild-type, *ggt1*, *ggt2*, L5 and L6 62

Table of abbreviations

5Opase	5-oxo-prolinase
ACC	1-aminocyclopropano
APES	3-aminopropyltriethoxysilane
APR	adenosine-5'-phosphosulfate reductase
APS	adenosine-5-phosphosulfate
APS	adenosine 5'-phosphosulfate
ASC	reduced ascorbate
ATP	adenosine triphosphate
ATPS	adenosine triphosphate sulfurylase
BSA	bovine serum albumin
Cat	catalase
Col-0	Arabidopsis thaliana ecotype Columbia-0
cys	cysteine
cys-gly	cysteinyl-glycine
DAF	days after flowering
ddH_2O	double distilled water
DEPC	diethylpyrocarbonate
DHA	dehydroascorbate
dNTP	deoxynucleotide solution mix
EDTA	ethylenediamine tetraacetic acid
FW	fresh weight
gDNA	genomic DNA
GGCT	gamma-glutamyl cyclotrasferase
GGMN	glutamic acid γ-(4-methoxy-β-napthylamide)
GGT	gamma-glutamyl transpeptidase
GPNA	γ-glutamyl-p-nitroanilide
GR	glutathione reductase
GSH	reduced glutathione
GSH1	γ-glutamylcysteine ligase
GSSG	oxidized glutathione
GST	glutathione-S-transferase
H_2O_2	hydrogen peroxide
HO_2^-	hydroperoxide radical
Homocys	homocysteine
HO^-	hydroxyl radical
HPLC	high performance liquid chromatography
Kan	kanamycin
kDa	kilo Dalton

kPa	kilo Pascal
Met	methionine
MS	Murashige & Skoog
NADPH	nicotinamide adenine dinucleotide phosphate
NASC	nottingham arabidopsis stock center
NOX	NADPH oxidases
O_2^-	superoxide radical
OAS	O-acetyl serine
OCT	optimal cutting temperature medium
PAGE	polyacrylamide gelelectrophoresis
PCD	programmed cell death
PCR	polymerase chain reaction
PdK	pyruvate orthophosphate dikinase
pWG	pWatergate
pWG-GGT	pWatergate vector carry in GGT target sequence
qRT-PCR	quantitative realtime polymerase chain reaction
RbcS	rubisco
RNAi	RNA interference
ROS	reactive oxygen species
rpm	round per minute
S	sulfur
S^{2-}	sulfide
SAT (serat)	serine acetyltransferase
SBD-F	ammonium 7-fluoro 2,1,3- benzooxadiazole-4-sulfonate
SDS	sodiumdodecylsulfate
SerBor	Serine-Borate
Sir	sulfite reductase
SMM	S-methyl-methionine
SO_3^{2-}	sulfite
SOD	superoxide dismutase
SULTR	sulfate transporter
T-DNA	transferred DNA used for insertional mutagenesis
TAIR	the Arabidopsis information resource
TEMED	N,N,N',N'-Tetramethylethylenediamine
Tris	2-amino-2-(hydroxymethyl)propane-1,3-diol
w/v	weight per volume
WT	wild-type

Abstract

Gamma-glutamyl transferase (GGT) is the unique enzyme able to degrade glutathione (GSH) in extra cytosolic spaces. In plant cell GGT1 and GGT2 isoforms are located in the apoplast, bound to the cell wall and to the plasma membrane respectively. GGT1 is expressed in whole plants mainly in leaves and in the vascular system, whereas more specific expression concerns GGT2 that is found in seed, trichome, pollen and weakly in root. However their role in plant physiology is still waiting to be defined. Glutathione, the substrate of GGT, is one of the most multifunctional molecule in biology, being the most important redox buffer and in plants one of the major source of reduced sulfur. Glutathione is a constituent of the phloem sap, but the mechanisms of its phloem loading and unloading are largely unknown. Obtaining and characterizing the *ggt1/ggt2* RNAi double mutant allows to add more clues than the relative single mutants and to shutdown possible compensatory expression between the two isoforms. In this work the selection and characterization of previously obtained *ggt1/ggt2* RNAi lines has been performed. The silencing level of both *GGT1* and *GGT2* transcript was verified by qRT-PCR and the total GGT activity analyzed. Furthermore phenotypic characterization was carried out; firstly, the GGT contribution in cysteine delivery to the seed and in seed development and composition was investigated. The *ggt1/ggt2* RNAi plants showed lower seed yield due to reduced silique number and silique length. However thiol content and 2S albumin storage proteins did not change in mutant seeds. It can be concluded that GGT silencing results in metabolic readjustments leading to allocation of resources to less, but fully viable seeds. The fact that GGT uses GSH as a substrate poses the question whether altered resource allocation results from impairment of cysteine delivery to sink tissues and cells, or from redox imbalances which may result in altered glutathione metabolism. The latter might correlate with the observed proline accumulation, which suggests the occurrence of oxidative stress affecting also the germination rate, which resulted delayed. The vegetative growth was also slightly slowed down with a reduced growth rate of rosette diameter and root length. Trichomes, the leaf hair characterized by high level of GSH, were also less in number than wild-type. Moreover the GSH depletion by roots in *ggt* mutants suggests cooperation between the two isoforms. In conclusion the simultaneous

GGT1 and GGT2 silencing induces the decrease of number of organs with high GSH demand (seed and trichome), oxidative stress in seeds and slightly affects vegetative growth. Further information about GGT will be provided by the double mutants obtained in this thesis work through the crossing between *ggt* mutants with *sir1-1,* that has reduced sulfur flux, and with *ggct2;1,* that lacks cytosolic GSH degradation.

Riassunto

La gamma-glutammil transferasi (GGT) è l'unico enzima in grado di degradare il glutatione (GSH) nelle regioni extra citosoliche. Le isoforme GGT1 e GGT2, nelle cellule vegetali, sono localizzate nell'apoplasto; ancorate rispettivamente alla parete cellulare e alla membrana plasmatica. La GGT1 è espressa in complesso in tutta la pianta, principalmente nelle foglie e nel sistema vascolare; mentre la GGT2 ha un'espressione più specifica e la si trova principalmente nei semi, nei tricomi, nel polline e in misura minore nelle radici. Tuttavia il loro ruolo nella fisiologia vegetale non è ancora stato chiarito. Il glutatione, substrato della GGT, è una delle molecole più versatili in biologia; infatti è tra i più importanti regolatori dello stato redox cellulare e nelle piante una delle principali fonti di zolfo ridotto. Il glutatione è un normale costituente della linfa nel floema, ma i meccanismi del suo caricamento e scaricamento floematico non sono ancora chiari. Ottenere e caratterizzare un doppio mutante *ggt1/ggt2* RNAi permetterebbe di aggiungere più informazioni rispetto a quelle fornite dai singoli mutanti, evitando inoltre possibili meccanismi compensatori tra le due isoforme. In questo lavoro sono state selezionate e caratterizzate le linee *ggt1/ggt2* RNAi, generate già in precedenza. Il livello di silenziamento di entrambi i trascritti *GGT1* e *GGT2* è stato verificato mediante qRT-PCR e l'attività totale della GGT è stata quantificata. Inoltre è stata condotta una caratterizzazione fenotipica; in primo luogo è stato studiato il contributo che potrebbe avere la GGT nel rilasciare cisteina al seme e in particolare la sua rilevanza nello sviluppo e nella composizione del seme. Le piante *ggt1/ggt2* RNAi hanno mostrato una minore produzione di semi dovuta al ridotto numero di silique e della loro lunghezza. Tuttavia nessun cambiamento è stato riscontrato nel contenuto di tioli e nelle proteine di riserva albumina 2S dei

semi mutanti. In conclusione il silenziamento della GGT induce un riaggiustamento metabolico che porta ad una redistribuzione delle risorse in un numero inferiore di semi, ma quanto meno vitali. Il fatto che la GGT usi il GSH come substrato solleva la questione sul fatto che l'alterata ridistribuzione delle risorse sia dovuto o a deficit nel rilasciare cisteina ai tessuti/cellule sink, o a scompensi redox che possono portare ad alterazioni nel metabolismo del glutatione. Quest'ultima possibilità potrebbe essere correlata con l'accumulo di prolina rilevato nei semi *ggt1/ggt2* RNAi, suggerendo la presenza di uno stress ossidativo che va influenzare negativamente anche il tasso di germinazione, risultato ritardato. Anche la crescita vegetativa *ggt1/ggt2* RNAi è risultata leggermente rallentata con una riduzione del diametro della rosetta e della lunghezza delle radici. I tricomi, i peli fogliari caratterizzati da alti livelli di GSH, erano anch'essi in numero minore rispetto al *wild-type*. Inoltre nei mutanti *ggt* il consumo di GSH da parte delle radici suggerisce una cooperazione tra le due isoforme. In conclusione il contemporaneo silenziamento di *GGT1* e *GGT2* induce una riduzione nel numero degli organi che hanno un'alta domanda di GSH (semi e tricomi), uno stress ossidativo nei semi e in misura minore influenza la crescita vegetativa. Nuove interessanti informazioni sulle GGT potranno essere estrapolate tramite lo studio dei doppi mutanti generati in questo lavoro, ottenuti incrociando i mutanti *ggt* con *sir1-1*, il quale ha un ridotto flusso di zolfo, o con *ggct2;1*, nel quale manca la degradazione citosolica del GSH.

1 Introduction

1.1 Sulfur

All living organisms need sulfur (S) that is a key element in many biochemical processes. Sulfur is an essential macronutrient for plant growth, development and response to environmental changes. The reduced form, sulfide, is a component of several macromolecules: amino acids such as cysteine (Cys), methionine (Met), homocysteine (Homocys), antioxidant molecules like glutathione (GSH) and thioredoxin, vitamins and coenzymes, phytochelatins used for heavy metal detoxification, sulfur lipids, glucosinolates, iron-sulfur clusters. The strong nucleophile property makes sulfide optimal mediator of redox reactions, including: catalysis, activation of reactive groups (e.g. coenzyme A), disulfide bonds formation and electron transfer via iron-sulfur clusters.

The sulfur assimilation in plant begins with the root uptake of sulfate from the soil by specific sulfate transporters (SULTRs). Sulfate is further translocated through the xylem and phloem to the shoot. In plastids sulfate is incorporated into adenosine-5-phosphosulfate (APS) which is reduced by glutathione-dependent reaction to sulfite (SO_3^{2-}) and then to sulfide (S^{2-}) by the enzyme sulfite reductase (SiR), finally the combination with the activated form of serine, O-acetyl serine (OAS), produces cysteine (Cys) (Takahashi et al., 2011). Development and several stresses influence sulfur assimilation, for instance when high level of cysteine and methionine are required for protein synthesis, such as in developing seeds (Tabe and Droux, 2001) and trichomes (Gutiérrez-Alcalá et al., 2000). Cysteine synthesis occurs almost constitutively and ubiquitously in plant cells (in plastids, cytosol and mitochondria) and is the major regulator in the primary sulfur metabolism (Hell and Wirtz, 2011). Cysteine is the exclusive precursor of most of all the other S-derived compounds in downstream metabolism and is mainly stored in form of glutathione.

Glutathione is the major reservoir of cysteine and consequently of reduced sulfur (Noctor et al., 2011). When cysteine is supplied, the intracellular excess of cysteine is transiently stored as glutathione. In contrast, the sulfate-starved condition induces the decrease of glutathione levels before those of cysteine. Glutathione may thus act as an internal “barometer” of plant sulfur status

(Kopriva and Rennenberg, 2004). It regulates several steps involved in sulfur assimilation, such as specific transporters and enzymes, e.g. ATP sulphurylase 1 (APS1) (Vauclare et al., 2002). Furthermore glutathione may link changes in sulfur nutrition to resistance to some pathogens (Höller et al., 2010) and response to oxidative stress such as exposure to ozone (Bick et al., 2001). Therefore cysteine and glutathione are closely interconnected in a global network. Glutathione has been considered the main form of long distance transport of reduced sulfur (Rennenberg and Herschbach, 2014). However sulfate is phloem mobile and its assimilation has been found in lupine seed (Tabe and Droux, 2001). S-methyl-methionine (SMM) has been also found to be important sulfur distributor form in the phloem (Bourgis et al., 1999), however SMM is not indispensable in sulfur transport (Kocsis et al., 2003). How SMM and GSH are loaded into the phloem and unloaded to sink plant organ, remains at the moment unknown.

1.2 Glutathione

Glutathione (GSH; γ-L-glutamyl-L-cysteinyl-glycine) is the main low-molecular-weight thiol in most organisms. It is a tripeptide of glutamate, cysteine and glycine, where the carboxyl side chain of the glutamate is linked to the amino group of cysteine by an unusual peptide bond called γ-glutamyl bond that confers resistance to protease attack. Moreover the nucleophile property conferred by the sulfur group of cysteine, gives to glutathione the capability to undergo numerous redox reactions. Glutathione is a multifunctional metabolite in plant, some of its roles include: anti-oxidant defense, sequestering of heavy metals and xenobiotics, reserve and long-distance transport of reduce sulfur, stress signaling and plant growth regulation. Moreover it is the precursor of phytochelatins, glucosinolates and it is necessary for maturation of iron-sulfur proteins and used as cofactor in cysteine biosynthesis. It is indispensable for plant development, mutant lacking of the first enzyme of its biosynthesis show embryo lethality (Cairns et al., 2006) and mutants with reduced glutathione level have serious growth impairments (Vernoux et al., 2000).

In all organisms glutathione is known for its antioxidant function against reactive oxygen species (ROS) to prevent excessive oxidation of cell components. Unlike many other antioxidants, glutathione is stable and is recycled from the oxidized

(GSSG) to the reduced (GSH) form at high rates by specific glutathione reductase (GR) through the reducing potential of NADPH. GRs are present in most of the cellular compartments but not in the apoplast. In addition ascorbate (ASC or AA) participates in maintaining the redox cell balance in the mutual ascorbate glutathione cycle (Fig. 1), where glutathione is used to regenerate oxidized ascorbate (DHA) (NOCTOR, 2006). In the cytosol the glutathione pool is maintained at high level in reduced state, typically 1:20 of GSSG:GSH ratio is measured in leaves in physiological condition. This ratio tends to increase when oxidative stress occurs, indeed the GSSG:GSH ratio is usually a nice estimation of the intracellular redox environment and used as marker of plant stress (NOCTOR et al., 2012).

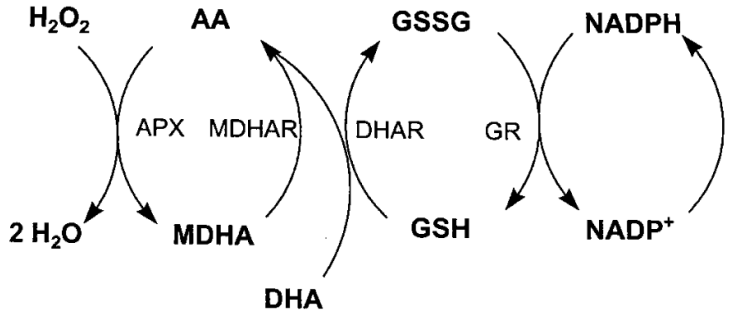

Fig. 1 The ascorbate glutathione cycle
The enzymes participating in the ascorbate glutathione cycle: APX ascorbate peroxidase; MDHA monodehydroascorbate reductase; DHAR dehydroascorbate reductase and GR glutathione reductase; (May et al., 1998).

In Arabidopsis the biosynthesis of glutathione (Fig. 2) takes place in chloroplast and in cytosol in two ATP-depending steps. The first step is exclusively located in the chloroplast and involves the formation of γ-glutamylcysteine (γ-EC) out of glutamate and cysteine catalyzed by γ-glutamylcysteine synthetase (GSH1; also referred to as γ-ECS in some literature, EC 6.3.2.2). In the second step glycine is added to γ-glutamylcysteine to form glutathione by glutathione synthetase (GSH2; also referred to as GSHS in some literature, EC 6.3.2.3.) in plastids and cytosol. It has been shown that the restriction of the second step to the cytosol is sufficient for normal plant development (Pasternak et al., 2008), while the first step located in the plastid is active only in diurnal, which causes γ-EC accumulation during the night (Masi et al., 2002).

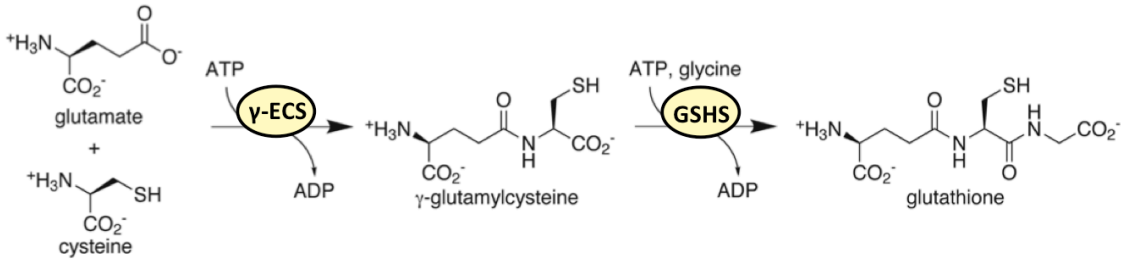

Fig. 2 Glutathione biosynthesis
Substrates and products of the reactions catalyzed by glutamate-cysteine ligase (GCL) and glutathione synthetase (GS) are shown. Figure modified from (Galant et al., 2011).

In plant cell, glutathione is in millimolar concentrations (1-5 mM) exceeding free cysteine by 10- to 50-fold. Through the glutathione subcellular localization using the immunogold cytochemistry technique (Zechmann et al., 2008; Zechmann, 2014), was found that, after its biosynthesis in chloroplast, glutathione is further distributed to various organelles. Indeed the highest glutathione content was detected in mitochondria, followed by nuclei, cytosol, peroxisomes and with the lowest density in the plastids, whereas no specific labeling was found in the apoplast and in the vacuole. However glutathione can be detected through different techniques also in these last compartments even if at very low level and mainly in the oxidized form (Vanacker et al., 1998; Ohkama-Ohtsu et al., 2007a). The low glutathione level reported in vacuole and in the apoplast is correlated with the localization of two-glutathione degradation pathway led by γ-glutamyl-transferase (GGT) (Ohkama-Ohtsu et al., 2007a; Ohkama-Ohtsu et al., 2008), which suggests rapid glutathione degradation in these two compartments. Indeed, in the apoplast of *ggt1* mutant, leaf cell glutathione accumulates more than in wild-type (Tolin et al., 2013). Moreover glutathione is usually transported into the vacuole mainly in the conjugated form during the detoxification process. Glutathione S-transferase (GST) is mainly involved in this latest process, GST catalyzed the conjugation between the thiol group of glutathione and an electrophilic group which is commonly found in xenobiotic or toxic compound and secondary metabolites. Glutathione was also detected at high level in nuclei where is involved in DNA protection against oxidative stress, in the progression of the cell cycle (Diaz Vivancos et al., 2010) and in gene transcription regulation especially related to defense responses (Mou et al., 2003; Gomez et al., 2004).

Glutathione is considered the main source of reduce sulfur, it is translocated through the phloem in different organs (Lappartient and Touraine, 1996; Herschbach et al., 2000; Kuzuhara et al., 2000) and it has been also found moving in the vascular system as complex with toxic metal as cadmium (Mendoza-Cózatl et al., 2008). During leaf senescence, nutrient mobilization to the seed occurs to salvage nutrients stoked in leaves (Himelblau and Amasino, 2001) and it has been shown that, during the cereal grain development, most of the sulfur decreased in leaf can be attributed to glutathione diminishment (Anderson and Fitzgerald, 2001) Recent studies have added new evidences about the existence of a GSH transporter called OPT4, which could be involved in GSH unloading from the phloem into siliques (Zhang et al., 2015). This transporter is located on the cell membrane and is expressed throughout the vasculature of leaves, stem, roots and moreover in the funiculus and siliques. Decreased GSH content has been found in siliques of *opt4* mutant, suggesting OPT4 involvement in GSH unloading to siliques. However no growth defect phenotype has been observed in *opt4* mutant and the substrate specificity is still unclear since OPT4 has low affinity for GSH and is able to transport additional oligopeptides.

1.3 Reactive oxygen species (ROS) as signaling molecules

Reactive oxygen species (ROS) include a group of molecules originated from incomplete reduction of oxygen, such as: superoxide (O_2^-), hydroperoxide (HO_2^-), hydroxyl (HO^-) radicals and hydrogen peroxide (H_2O_2). ROS are normal products of aerobic metabolism and are produced in all cell compartments during several processes such as photosynthesis in chloroplast and respiration in mitochondria. ROS have a bivalent effect: at high level they damage the cell and at worst induce cell death, whereas at low level they work as signaling molecule. Complex network of antioxidant enzymes, antioxidants, pro-oxidant enzymes and molecules are tightly coordinated to maintain ROS level under control. The intensity, frequency modulation, duration and origin location of ROS signal are regulated by cell mechanisms and trigger specific process as development, stress responses and acclimation. In the apoplast there is an important production of O_2^- by NAD(P)H oxidases (NOX) and H_2O_2 by NAD(P)H peroxidase, bound to the membrane and to the cell wall respectively. Apoplast ROS accumulation is connected to events

involved in environmental stimuli, such as the hypersensitive response to pathogen, but it also regulates cell growth and development (Shapiguzov et al., 2012). Unlike the other ROS, H_2O_2 is mobile and can migrate quite far from the site of generation; moreover it can pass thought the membrane by specialized aquaporins called peroxoporin (Bienert et al., 2006).

1.3.1 ROS and PCD in development and growth

Several developmental processes are regulated by ROS, in summary are included: embryogenesis, aleurone cell death, root and leaf elongation, root hair growth, trichome development, tracheary elements differentiation and senescence (Gapper and Dolan, 2006; Gechev et al., 2006).

Most of ROS signaling that has been shown to be involved in development is generated by NADPH oxidases (NOX). It has been demonstrated that NOX, through ROS modulation, activates the Ca^{2+} channel that leads to cell expansion that in turn influences the root elongation and root hair growth (Foreman et al., 2003). Moreover, several studies suggested that leaf expansion and shape are under control of ROS produced by NOX (Rodríguez et al., 2002; Schopfer et al., 2002; Sagi et al., 2004). In contrast H_2O_2 may have inhibitory effect on growth by downregulating auxin-responsive genes (Gechev et al., 2005). Cell wall is also shaped by ROS in order to support the cell expansion (Liszkay et al., 2004). Hydroxyl radical has been shown promote cell wall loosing by scission of xyloglucan polymers (Fry, 1998), while H_2O_2 is correlated to tightening of cell wall (Brisson et al., 1994).

Programmed cell death (PCD) is the process leading to destroy the cell, mediated by intracellular controlled program. In many cases ROS induce the PCD to control a number of developmental processes including aleurone cell death, embryogenesis and morphogenesis. PCD is fundamental to remove and shape temporary, surplus tissue and organ during embryogenesis both in animal and plant (Baehrecke, 2002; Bozhkov et al., 2005). Despite the wide knowledge in animal, the molecular mechanisms that regulate PCD in plant embryo are still unknown. Recent studies demonstrate that a member of cysteine protease named metacaspase executes PCD during plant embryogenesis (Bozhkov et al., 2005). Suspensor is example of temporary organ that at the end of its role decays by PCD event (Yeung and Meinke, 1993; Kawashima and Goldberg, 2010). Moreover the

two external layers of the inner integument undergo PCD during differentiation of the seed coat, and by the time the seed is mature the final destiny of all cell layers is to die (Haughn and Chaudhury, 2005). The specific time course of the various layers' death reveals that PCD is a regulated program as a part of the differentiation process.

1.4 Gamma-glutamyl-transferase (GGT) in glutathione catabolism

1.4.1 Plant

Gamma-glutamyl transferase (GGT; E.C. 2.3.2.2) is the main enzyme that degrades glutathione to cysteinyl-glycine (cys-gly) and glutamate. GGT catalyzes the break down of γ-glutamyl bound and transfers the γ-glutamyl group to a range of appropriate acceptors: to H_2O in slightly acid state that is physiological or to amino acids in basic condition (Storozhenko et al., 2002). GGT is not the unique enzyme that is able to degrade glutathione; alternative pathway led by γ-glutamyl cyclo-transferase (GGCT) and 5-oxo-prolinase (5Opase) exists in the cytosol (Ohkama-Ohtsu et al., 2008; Paulose et al., 2013). However the two degradation pathways operate in different locations: GGTs dominate the extra cytosolic compartments (apoplast, vacuole), while GGCT is restricted to the cytosol. Four GGT isoforms are known: GGT1 and GGT2 are both located in the apoplast, bound to the cell wall and to the membrane respectively (Ohkama-Ohtsu et al., 2007a); GGT3 has been considered nonfunctional since it lacks the sequence for the catalytic activity; GGT4 is the vacuolar isoform and is involved in degradation of glutathione conjugates supporting the detoxification processes (Vanacker et al., 1998; Ohkama-Ohtsu et al., 2007b). While the role of GGT4 is almost explained, the significance of GGT1 and GGT2 on plant physiology is still nebulous. These two latest isoforms take part in the γ-glutamyl cycle (Masi et al., 2015) in which GSH is recycled between apoplast and cytosol as occurs in animals (Meister and Anderson, 1983). In this cycle, not completely characterized yet in plants, GGT1 and GGT2 degrade GSH in glutamate and cysteinyl-glycine in the apoplast, then cysteinyl-glycine is further cleaved by an unknown dipeptidase; the

single amino acids are transported into the cytosol and then used to newly biosynthesize GSH which is extruded again to the external environment (Fig. 3).

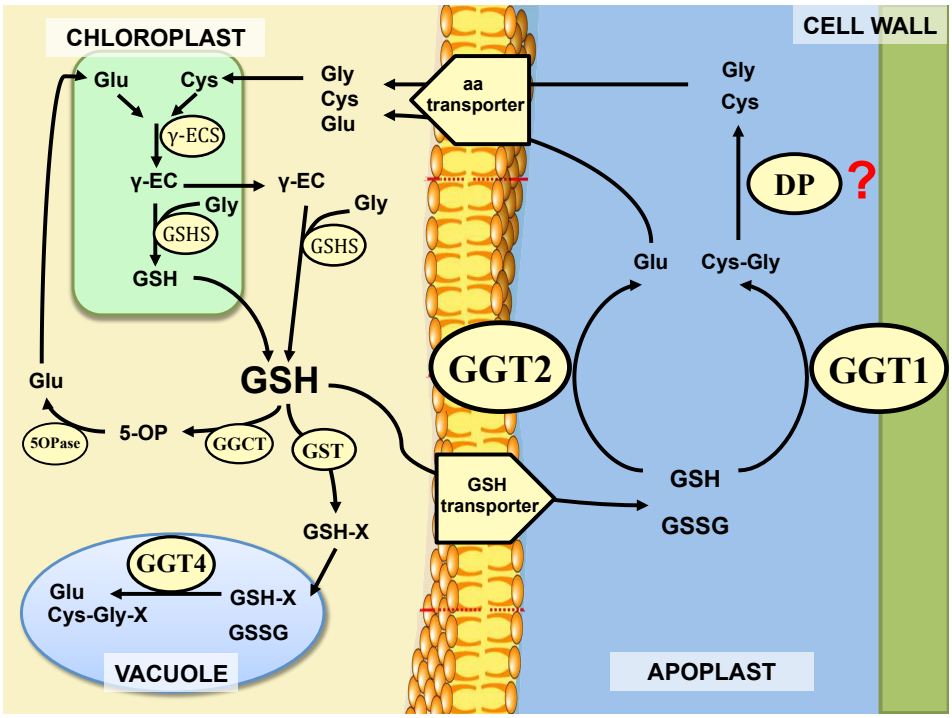

Fig. 3 Glutathione degradation pathways
Glutathione (GSH) is extruded in the apoplast where GGT1 and GGT2 break down the gamma-glutamyl bound. Cysteinyl-glycine (cys-gly) released by GGT is cleaved by an unknown dipeptidase (DP), then single amino acids are transported inside the cell. Gamma glutamyl cyclo-transferase (GGCT) and 5-oxo-prolinase (5Opase) are involved the cytosolic GSH degradation. In the vacuole GGT4 degrades the glutathione S-conjugates in the detoxification process.

Despite GGT1 and GGT2 sequences conserve high similarity, different pattern of expression discerns both isoforms. GGT1 is expressed in almost all tissue especially in leaves, root and in the vascular system, whereas GGT2 expression is restricted to few sites: seed, pollen, trichome and weakly in root. The expression patterns of all GGT isoforms are not restricted to individual organ but are temporally and spatially limited. Histochemical localization of GGTs:GUS fusion protein was performed in the same year by two distinct research group (Martin et al., 2007; Ohkama-Ohtsu et al., 2007a) and revealed the specific GGTs expression in very sensitive manner. GGT1:GUS expression was evident since the early stage of development after germination, first in shoot and later in root of the little seedling. In adult leaves GGT1:GUS was expressed mainly in the vascular system, that has been also confirmed in other work where intense GGT activity is detected in vascular bundles and epidermal cell layer of leaves (Destro et al., 2011). While

GGT1:GUS is almost expressed in whole plant, GGT2:GUS has a narrow spatial and temporal expression. It is essentially present in three sites: seed, pollen and trichomes (Martin et al., 2007). The ovule is the predominant organ where GGT2:GUS is expressed from before fertilization till mature seed. In particular it is expressed in the endosperm, integument, embryo and intense GUS staining in the suspensor and in funiculus was reveled (Ohkama-Ohtsu et al., 2007a). In roots GGT2 is usually expressed at low level; however overexpression of its transcript and enhancement of activity has been shown to be induced after GSH supplementation or accumulation in the apoplast as indirect consequence in *ggt1* mutant (Destro et al., 2011)

Recently, studies in *ggt1* mutant proteome have suggested GGT1 as sentinel of the redox status in the apoplast. Proteins involved in stress defense and with antioxidant action are switched on in *ggt1* leaves even under normal physiological condition (Tolin et al., 2013). Moreover oxidative stress induced by UV-B radiation in leaves (Trentin et al., 2015) and diamide in root (Ferretti et al., 2009) accelerates the extrusion and degradation rate of glutathione lead by GGT. All these evidences are underlined by the fact that GSSG is the primary substrate of GGT1 (Ohkama-Ohtsu et al., 2007a) suggesting that after ROS oxidant action, GSSG is subjected to a rapid turnover by GGT and subsequently a sort of message is internalized to the cell (Masi et al., 2015).

1.4.2 Animal

In animal GGT works to maintain sufficient levels of cysteine and glutathione into cells, in addition it is also involved in xenobiotics' detoxification after their excretion outside the cell. GGT is expressed on the luminal surface of excretive and absorptive cells of glands and ducts throughout the body and the highest level of GGT activity is found in the kidney (Hanigan and Frierson, 1996). Cysteine is an essential amino acid in animal and is rate-limiting for glutathione biosynthesis. GGT recovers cysteine from extracellular space by GSH degradation and this provides to maintain intracellular glutathione and cysteine level. GGT induction in cancer cells allows high intracellular GSH level and provides advantage for tumor development and drug resistance (Hanigan, 2014). Instead the lethal phenotype of GGT-knockout mice is due to continuous excretion of glutathione without any recovering of it that further leads to cysteine deficiency

(Lieberman et al., 1996). In mouse and human the single gene of GGT is transcribed from several promoters to multiple mRNAs that generate the same protein (Chikhi et al., 1999). The control of more than one promoter allows tight and flexible gene expression, because it increases the number of regulatory elements. Therefore tissue, development and stress specific expression is typical of genes controlled by multiple promoters.

GGT study in bovine eye lenses has proposed that the generation of cysteine-glycine in the extracellular space results in inhibition of glutathione extrusion outside the cell (De Donatis et al., 2010). It was also suggested that cysteinyl-glycine produced from GSH degradation by GGT, mediates generation of reactive forms of oxygen such as H_2O_2. Both the low glutathione level and the cysteinyl-glycine act as pro-oxidant which induce growth-inhibitory effects (Perego et al., 1997; Pompella et al., 2007). Reactive oxygen species formation through Fe^{3+} reduction has been also shown as a consequence of cysteinyl-glycine released by GGT (Stark et al., 1988; Stark et al., 1993). In addition the oxidation of cell surface protein thiols has been revealed in cell with enhanced GGT activity, while the oxidation has been prevented after GGT inhibition (Paolicchi et al., 2002). On the other hand protein thiolation with cysteinyl-glycine has been shown as additional factor of membrane protein thiol modification (Corti et al., 2005). Studies in lymphoma cells have shown that continue GGT-dependent H_2O_2 production acts as sort of “life signal” that support proliferation and prevent apoptosis. In accordance with this evidence, low levels of ROS, in particular H_2O_2, are mitogenic and support survival pathways *. Imbalance in cellular GSH-to-GSSG ratio in favour of the oxidized species (GSSG), promoted by ROS or GSH export, constitutes an important signal that could induce the cell apoptosis (Circu and Aw, 2008; Franco and Cidlowski, 2009).

1.5 Seed

Seeds are a key global food, because they account for the majority of calories and nutrients consumed by humans and animal. Hence improved seed quality and yield is a global aim for agriculture.

1.5.1 Seed development

The seed is generated by double fertilization event. Fusions of sperm cells with the egg cell generate the zygote embryo, with the central cell the endosperm. The seed development can be divided into three distinct regions: the embryo, the endosperm, and the seed coat.

Cell division of zygote and accumulation of organic substances and water characterize the embryogenesis that finally results in the embryo formation. Late during the maturation phase, no cell division event occurs anymore. Instead the embryo cells expand their volume and accumulate storage macromolecules in the cotyledon and become tolerant of desiccation. The suspensor serves as a conduit between the embryo and the endosperm, it transports to the embryo proper nutrients and molecules involved in growth regulation to support embryo development (Yeung and Meinke, 1993; Kawashima and Goldberg, 2010b). Suspensor is in symplastic continuity with the embryo till the globular stage (Kim et al., 2005), then it will further interrupt at the heart stage when suspensor begins to degenerate (Yeung and Meinke, 1993).

The primary endosperm cell undergoes nuclear but not cell divisions, and three subregions are formed: micropylar, which is close to the young embryo; peripheral, in the center of the endosperm region; and chalazal, at the pole opposite to the embryo. Cellularization of the endosperm, in which cell walls form around nuclear cytoplasmic domains of the endosperm, proceeds in a wave-like manner from the micropylar to chalazal end. The endosperm supports the embryo during the early stages of seed development, but later its storage substances are transferred in the cotyledon and at the end of seed development the endosperm is absorbed.

Finally, the seed coat originates from maternal ovule integument which further divides and differentiates into the distinct cell layers: the outer- and the inner-integument. The seed coat transfers assimilates from the maternal plant and serves to protect the embryo throughout seed development. Integuments undergo a complex process of differentiation to form seed coat, which can be divided into two subregions: the chalazal seed coat, proximal to the funiculus; and distal seed coat, that surround all the seed. Initially cell expansion and division are common events and then each cell layers follow a distinct developmental program. Several

modifications occur in the extracellular space: secondary metabolites formation, programmed cell death, cell wall thickening, mucilage secretion in the apoplast (Western et al., 2000)

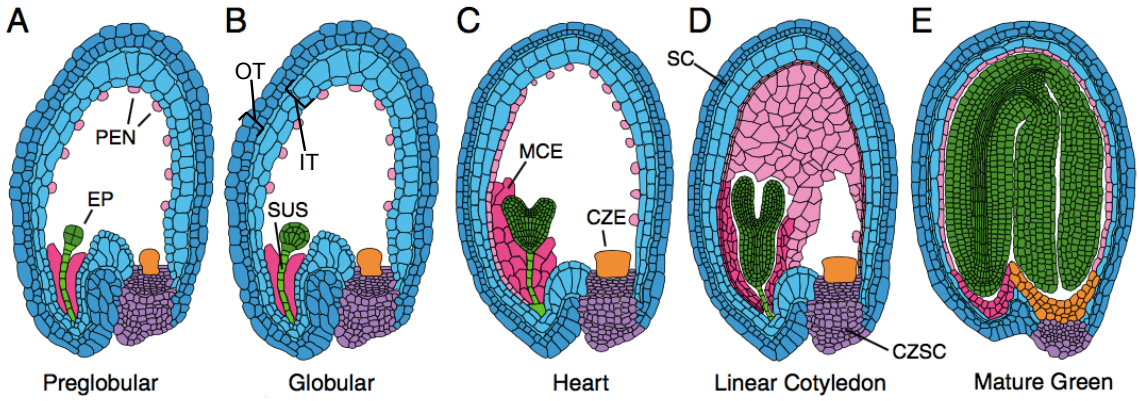

Fig. 4 Development stages of *Arabidopsis thaliana* seed
Representation of development seed stages: (A) preglobular stage, (B) globular stage, (C) heart stage, (D) linear cotyledon stage, (E) and mature green stage. Different seed subregions are indicated: peripheral endosperm (PEN), embryo proper (EP), outer integument (OT), inner integument (IT), suspensor (SUS), micropylar endosperm (MCE), chalazal (CZE), seed coat (SC), and chalazal seed coat (CZSC); (Belmonte et al., 2013).

1.5.2 Assimilates transport

In plants, there are two main types of vascular tissues: the xylem gets water and its mineral solutes from the roots; the phloem transports the sap, solution rich of nutrients and photosynthesis products, away from source tissue (e.g. leaves, root) to sink tissues (e.g. developing organ, seeds). During development fruits and seeds are strong sink competitors and they monopolize the nutrients available in the phloem. The vascular system reaches the seeds by the funiculus that connects the mother plant to the chalazal seed coat. This seed subregion is the first point of entry of nutrients arrived from maternal vascular system, and it is specialized for seed filling proccess. Indeed transcriptional analyses in chalazal seed coat have discovered several genes associated with phloem unloading, sucrose efflux transporters, amino acid transport, water transport genes and plasma membrane intrinsic protein (Becker et al., 2014). Post phloem symplastic vascular extension exists in the outer integument of seed coat, where all the cells are connect by plasmodesmata, creating a flux of assimilates around the seed coat. Later centripetal movement of assimilates through the apoplast crosses the inner integument and finally reaches the endosperm, since outer and inner integuments are not simplastically connected (Fig. 5) (Stadler et al., 2005).

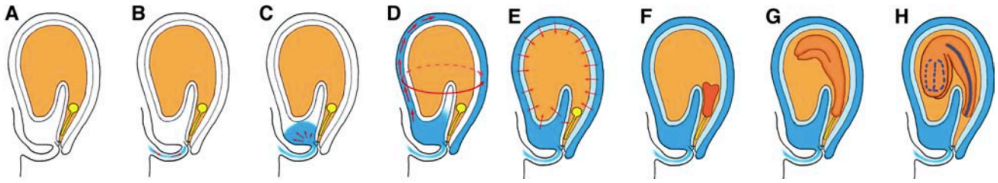

Fig. 5 Model of Stadler et.al showing the symplastic domain in Arabidopsis seed and the path of assimilates
(A) Seeds are connected to the mother plant by funiculus (B) and the flux of assimilates pass through it. (C) Assimilates unloading in the chalazal seed coat (D) and their moving in the outer integument (E) and toward endosperm. (F) At the early heart stage the simplastic continuity between suspensor and embryo is interrupted. (G) During the transition from heart to midtorpedo stage, the simplastic connectivity between epidermis and inner cell layers of the embryo is gradually reduced. (H) In the mature embryo the developing stele in the root and the hypocotyl begins to form an independent domain; (Stadler et al., 2005).

The suspensor has a nutritive function for the young embryo, connecting the micropylar endosperm with the embryo properly (Kawashima and Goldberg, 2010a). Suspensor lacks a cuticle and can easily exchange nutrients from endosperm through apoplast, moreover has a negative osmotic potential that provides a driving force to take up metabolites from the apoplast into the symplast (Lee and Yeung, 2010). The suspensor is in symplastic continuity with the embryo during the globular stage that will interrupt at the heart stage when suspensor begins to degenerate. This disconnection occurs at the time of hypophysis formation led by auxin signal. Up to this stage, the embryo is in symplastic continuity and nutrients can move freely between cells. Afterwards, when the suspensor degenerates, the embryo will take up nutrients directly from the endosperm through the apoplast (Morley-Smith et al., 2008).

1.6 Aims of the project

In these last years, several studies were conducted in order to characterize the gamma-glutamyl transferase (GGT) isoforms in plants. Many aspects about their localization and activity have been discovered, but less has been elucidated about their role in plant physiology. Several hypothetic functions have been suggested: redox protection against ROS in the apoplast, cysteine unloading from phloem to the sink tissue by glutathione (GSH) degradation, and redox sentinel in the apoplast as source of signaling addressed to the cell. GGT1 and GGT2 are the

isoforms located in the apoplast and compensatory overexpression of *GGT2* in *ggt1* mutant root was found previously (Destro et al., 2011). Hence single mutants do not achieve completely abolishment of apoplastic GGT activity in plant. Moreover the genes of *GGT1* and *GGT2* are consecutive; hence the creation of a double knocked out mutant by crossing is not possible. Then the challenge to generate and characterize *ggt1/ggt2* double mutant by RNA interference has been a way to find new clues to define the role of apoplastic GGT.

Glutathione is one of the major transport form of reduced sulfur and a constituent of the phloem sap, but the mechanisms of its phloem loading and unloading are largely unknown. GSH is the substrate of GGT and it has been shown to induce GGT2 expression and activity. Therefore our attention was focused on the tissues where GSH demand is higher and where it has physiological relevance such as seed. Improving the seed nutritional composition and yield has always been a global challenge for agriculture; in particular several attempts were conducted to enhance sulfur-containing amino acid (cysteine, methionine) content in seeds. In previous studies intense GGT1 expression was found in vascular system while GGT2 was found in the funiculus and in the suspensor of seed (Ohkama-Ohtsu et al., 2007a). Therefore generative tissue will be characterized here, to comprehend if GGT affects seed yield and composition.

In addition, characterization of vegetative development will be performed. Particular attention will assume trichome, where both GGT isoforms are expressed and a high GSH content is present, and root where the ability of different *ggt* mutants to deplete GSH in solution will be tested.

Finally the last aim is to cross *ggt1* and *ggt2* mutants with *sir1-1* and *ggct2;1* in order to investigate the effect of reduce flux of sulfur and the absence of cytosolic GSH degradation pathway respectively in *ggt* mutants.

2 Materials and methods

2.1 Technical equipment and materials

2.1.1 Technical equipment

HPLC System:	
Autoinjector 234	Gilson, France
Intelligent Spectrofluorometer 821-FP	Jasco, Japan
Luna 3 µ C18(2) 150 x 4.60 mm	Phenomenex, USA
Luna 5 µ C18(2) 150 x 4.60 mm	Phenomenex, USA
System Gold^{R} 126 Solvent Module	Beckman Coulter, Brea, CA
Analytical balance E42	Gibertini, Milano
Arium^{R} 611UV	Sartorius, Goettingen
BioSpectrometer kinetic	Eppendorf, Hamburg
Centrifuge 5424 R	Eppendorf, Hamburg
Chemical hood Cl18mnb	Labotech, Milano
ChemiDOC™ XRS+ Image System	BioRad, München
Dubnoff bath	Isco
Epson expression 10000XL	Seiko Epson Corporation, Japan
FiveEasy pH Meter	Mettler Toledo, Columbus, OH
GeneAmpR PCR System 9700	Applied Biosystem, Singapore
GENi System	Syngene, Cambridge, UK
Growth chamber	Cavallo, Milano
Horizontal electrophoretic chamber	Elettrofor, Rovigo
Leica DC300F camera	Leica Microsystems, Bensheim
Leica DM4000B digital microscope	Leica Microsystems, Bensheim
Mini-PROTEAN® Tetra Cell	BioRad, München
NanoDrop ND-2000	Peqlab, Erlangen
Ohaus^{R} Adventurer^{R} APRV70	Sigma-Aldrich, Steinheim
Olympus VR-340	Olympus Imaging Corp., China
Power Pac Basic	BioRad, München
Rotor-Gene Q	Qiagen, Hilden
Sterile hood HF A 48	Gelaire, Sidney

Table Centrifuge 5415 C	Eppendorf, Hamburg
Tissuelyser	Qiagen, Hilden
Unimax 1010	Heidolph, Schwabach
V-530 UV/VIS Spectrophotometer	Jasco, Groß-Umstadt

Further devices corresponded to usual laboratory equipment.

2.1.2 Chemicals

100 bp DNA Ladder	Invitrogen, Carlsbad, CA
Agar	Sigma-Aldrich, Steinheim
APES (A 3648)	Sigma-Aldrich, Steinheim
Bradford reagent	Applichem, Darmstatd
ColorBurst™ Electrophoresis Marker (C1992)	Sigma-Aldrich, Steinheim
dNTPs	Sigma-Aldrich, Steinheim
Fast Garnet GBC Sulfate salt (F8761)	Sigma-Aldrich, Steinheim
GGMN (G0141)	Sigma-Aldrich, Steinheim
GPNAL (G6133)	Sigma-Aldrich, Steinheim
GSH (G4251)	Sigma-Aldrich, Steinheim
Kanamycine (11815)	Invitrogen, Paisley
OCT	Cellpath, Newtown, UK
Polyvinylpyrolidone 40,000 (PVP-40)	Sigma-Aldrich, Steinheim
Sulfodiazine sodium (S6387)	Sigma-Aldrich, Steinheim
SYBR® Safe DNA Gel Stain	Invitrogen, Carlsbad, CA
TRIreagent	Sigma-Aldrich, Steinheim

Further chemicals corresponded to usual laboratory equipment.

2.1.3 Software

ChromCard board and software	Carlo Erba, Italy
Image J 1.48	NIH, United State
Image Lab™ Software	BioRad, München
Leica Image Manager 50 software	Leica Microsystems, Bensheim

NanoDrop ND-2000	Thermo Fisher Scientific, USA
R Development Core Team, 2015	R Foundation, Vienna
ReadCube	Labtiva Inc., Cambridge
Rotor-Gene® Q Series Software	Qiagen, Hilden
SigmaPlot 8.0	SPSS Inc., Munich
Vector NTI 9	Invitrogen, Karlsruhe
Winrhizo pro 2007.d	Regent Instruments Inc., Canada

Web based software tools and website:

BLAST nucleotide	blast.ncbi.nlm.nih.gov/Blast.cgi?PROGRAM=blastn &PAGE_TYPE=BlastSearch&LINK_LOC=blasthome
Clustal Omega	www.ebi.ac.uk/Tools/msa/clustalo/
eFP Browser	http://bar.utoronto.ca/efp/cgi-bin/efpWeb.cgi
Gene Investigator	https://genevestigator.com/gv/ (Hruz et al., 2008)
OligoCalc	www.basic.northwestern.edu/biotools/OligoCalc.html
TAIR	https://www.arabidopsis.org/

2.1.4 Consumables

Micropore™ 3 M 1.25 cm x 9.1 m	Gima, Milano
Strip tubes and caps, 0.1 ml	Qiagen, Hilden

Further consumables corresponded to usual laboratory equipment.

2.1.5 Enzymes and kits

Direct-zol ™ RNA MiniPrep	Zymo Research, Irvine, CA
DreamTaq DNA Polymerase	Thermo Scientific, Walldorf
Gateway system	Invitrogen, Carlsbad, CA
High-Capacity cDNA Reverse Transcription Kit	Applied Biosystem, Foster city
pWatergate	CSIRO, Australia
QIAEX II Gel Extraction Kit®	Qiagen, Hilden
Rotor-Gene SYBR® Green PCR Kit	Qiagen, Hilden

2.1.6 Primers

Suitable primers for genotyping or real-time PCR were designed using OligoCalc and BLAST nucleotide tool (2.1.3) and synthetized by Sigma-Aldrich. Lyophilized primers were resuspended in ddH2O to a stock concentration of 100 µM and a working concentration of 10 µM.

Table 1 Primers for cloning

N°	Description	Sequence
62	FW attB1	GGGGACAAGTTTGTACAAAAAAGCAGGCTGCAAAACGCTAACGCTGTGA
63	RW attB2	GGGGACCACTTTGTACAAGAAAGCTGGGTCAAGCCGTGTATAGACCCGC

Table 2 Primers for genotyping

N°	Description	Sequence
1	ggt2-069311 FW	CGTTCTGTGATTAATCTCTCTGG
2	3199_ggt2-069311 RW correct	GAACGCCTACTGACAAGGATC
3	At6-FW	AATTTTGTTTTCGGGAAAGTTCGA
4	At6-RW	CGCCTACTGATAAGGCTCCTTTCTT
5	LB	GGCAATCAGCTGTTGCCCGTCTCACT
47	GGCT2;1 FW	TTTAAATTGAGCAGTGGGGTG
48	GGCT2;1 RW	TGAGGGCTTCGAAAAGTATTG
49	LBb1.3	ATTTTGCCGATTTCGGAAC
38	1981_SiR FW	CGCTTCTTCTGGCTAGCC
39	606_SiR RW	AGGCGATTCAAAAAGCATCTC
40	432_GALB1	CCCATTTGGACGTGAATGTAGACAC
23	cat	AAGGGTCCTAACCAAGAAAATGAA
24	ocs	GATCTGAGCTACACATGCTCAGGT
25	arbcs	CACTCCAAAGCTTGTTCTCATTGT
26	pdk	TCTTCTTCGTCTTACACATCACTTGTC

Table 3 Primer for qRT-PCR

N°	Description	Sequence
18	gGT4 X anti	GCTGGCTTTCCATCTTTTCGAGGATC
19	gGT4 X sense	CCACGATCAATGGCGATCACATAGG
33	GGT2qRT_4/5exFW	GGTGGCAAATGGGGTCAGAT
35	GGT2qRT_5.2exRW	GACAGCATTATTGCCCCAAAGTA
43	2459_PP2a FW	CTTCTCGCTCCAGTAATGGGATCC
44	2460_PP2a RW	GCTTGGTCGACTATCGGAATGAGAG
53	GGT1qRT_iRNA1ex FW	GTTAAGATAGCTGGTGGGAAAG
54	GGT1qRT_iRNA1/2.2ex RW	CATTACCTCCATACATATTCTCAG
60	2546_SiR_RT_f	TTGAAAAGGTTGGTCTGGACTAC
61	2547_SiR_RT_r	GGTGTTCCTCCTAGCCAAAC

2.2 Plant methods

2.2.1 Plant material

For this thesis, *Arabidopsis thaliana* ecotype Col-0 (family: *Brassicaceae*, order: *Capparales*, class: *Dicotyledonae*, subdivision: *Angiospermae*) was used as the wild-type control. In the characterization studies two T-DNA insertion lines for *GGT1* (At4g39640) and *GGT2* (At4g39650) were used: *ggt1* (080363) (Martin et al., 2007) and *ggt2* (069311), established at the Salk Institute and obtained from the Nottingham Arabidopsis Stock Center (NASC). Four double knock down RNAi lines for *GGT1* and *GGT2* were also used in the same study: L2, L4, L5, L6 (2.2.9). The T-DNA insertion lines used for the crossing, in addition to *ggt1* and *ggt2*, were for *SiR* (At5g04590) and *GGCT2;1* (At5g26220): *sir1-1* (550A09) obtained from the GABI-Kat collection center (Khan et al., 2010) and *ggct2;1* (117578) provided by the Salk Institute and obtained from NASC (Paulose et al., 2013).

Table 4 Transgene lines used in this thesis work

Line	Gene locus	Stock name	Type	Antibiotic resistance	Reference
ggt1	At4g39640	SALK_080363	T-DNA, KO	Kanamycin	(Martin et al., 2007)
ggt2	At4g39650	SALK_069311	T-DNA, KO	Kanamycin	
sir1-1	At5g04590	GK-550A09	T-DNA, KD	Sulfadiazine	(Khan et al., 2010)
ggct2;1	At5g26220	SALK_117578	T-DNA, KO	Kanamycin	(Paulose et al., 2013)

2.2.2 Soil cultivation

Arabidopsis seeds were sowed in soil (Potground H) and stratified 2-3 days in the dark at 4 °C. Then they were transferred to germinate and growth in growth chamber (Cavallo) in short day condition (8.5 h day light) at 50 % relative humidity and a light intensity of 100 –120 m^{-2} s^{-1}. During the day the temperature was kept at 22°C and at 18°C during the night. After two weeks the plants were picked out in single pots and growth in short day condition. Plants were moved to long day condition (14 h of day light, same environmental parameters as in short day) for seeds propagation after 7 – 8 weeks from sowing.

For the determination of the bolting time the plants were left in short day condition till the inflorescence emergence and then transfer to long day condition.

2.2.3 Surface sterilization of seeds

Arabidopsis seeds were sterilized for growth on Petri plates and hydroponic cultures: seeds were incubated with 1 ml 70 % ethanol for 2 min followed by 15 min with 1 ml 5 % hypochlorite. Finally were washed five times with ddH_2O.

2.2.4 Growth of Arabidopsis on Petri plate under sterile conditions

Plants were growth on Petri plate under sterile conditions for root harvesting in order to extract RNA, to measure GGT and GST activity *in vitro* and for the morphological and growth root characterization. Seeds were sterilized (2.2.3) and sowed on half strength MS medium (Table 5) supplemented with 1 % sucrose, 1.4% agar and the pH adjusted to 5.8 with KOH. For RNA and enzyme activity analysis several seeds were sowed on the top of the plate whereas for the root characterization 6 seeds were sowed separately. After 3 days of stratification at 4 °C the plates were placed vertically into growth chamber in short day condition (2.2.2). Roots were harvested after 2 – 3 weeks for RNA extraction (2.3.5) and 4 weeks for enzyme activity assay (2.4.5); finally were frozen in liquid nitrogen and stored at -80 °C.

Table 5 Composition of ½ MS medium

Macroelements	Microelements
1.5 mM $CaCl_2$	50 µM FeNaEDTA
0.63 mM KH_2PO_4	0.05 µM $CoCl_2 \cdot 6H_2O$
9.40 mM KNO_3	0.05 µM $CuSO_4 \cdot 5H_2O$
0.75 mM $MgSO_4 \cdot 7H_2O$	50 µM H_3BO_3
10.31 mM NH_4NO_3	2.5 µM KI
	50 µM $MnSO_4 \cdot H_2O$
	0.5 µM $Na_2MoO_4 \cdot 2H_2O$
	15 µM $ZnSO_4 \cdot H_2O$

2.2.5 Hydroponic culture

Hydroponic culture was established for the GSH depletion experiment (2.5.3). Seeds were sterilized (2.2.3) and germinated in micro centrifuge tubes on half strength MS medium (Table 5) supplemented with 1 % sucrose, 0.6 % (w/v) agar and inserted in blue-tip-boxes full of 0.5 L of ½ MS solution. After three days of stratification at 4 °C, boxes were placed in growth chamber in short day condition (2.2.2). After two weeks, plants were transferred to 50 ml falcon tube with 45 ml of ½ MS liquid medium that was replaced every week to provide optimal supply of nutrition. At the age of 7 weeks, the night before the experiment, the liquid medium was replaced with distilled H_2O to create a starving condition.

2.2.6 Detection of phenotypic differences between mutants

The phenotypic characterization of the mutant lines was based on the standard parameters found in literature(Boyes et al., 2001; Bolle, 2009).

For seed and silique characterization plants grown in growth chamber (2.2.2) were used. The bolting time was determined in at least 12 plants grown under short day condition and plant was considered bolted when the flower bud was visible in the center of the rosette. The seed yield, the 100-seed-weight and the number of siliques was measured from several batches of plants grown in growth chamber in different periods. The number of seeds per siliques was counted without opening the siliques, but after making them transparent by overnight incubation in 0.2 M NaOH and 1 % SDS solution. Three siliques were used for each of the at least five plants examined. A digital caliper was used to measure the silique length; we considered at least 10 siliques from 3 different branches of five plants and the siliques were at least at 10 daf.

For root morphology and growth rate characterization plants grown in petri dishes were used (2.2.4), where 6 seeds were sowed in each of the 5 plates per genotype. The images were acquired every 2 – 3 days for 4 weeks by Epson expression 10000 XL (2.1.1) professional scanner. The image format was in A3, black and white at 400 DPI of resolution. The morphological root parameters were analyzed by the Winrhizo pro 2007.d software (2.1.3).

Documentation of rosette growth was performed with the camera Olympus VR-340 (2.1.1) on black velvet. The pictures were taken ones a week from the fourth to the eleventh week after sowing. Rosette diameter was measured three times by using the image software Image J 1.48 (2.1.3). The number of trichomes was counted from the first two true leaves of plants almost 2 – week – old, according to (Larkin et al., 1996). The relative images were taken by stereomicroscope equipped with camera and software.

2.2.7 Germination rate

Germination test was performed sowing at least 50 seeds on sterile filter paper closed into petri dishes and imbibed of sterile ddH_2O. For each genotype four different batches of seeds from different plants were used and sowed separately. Not sterilized seeds were imbibed on sterile ddH_2O before sowing and stratified for 4 days at 4 °C, then grown under short day condition (2.2.2). Seeds were considered germinated when the radicle was protruded and the number of germinated seed was monitored every day for four days and finally the seventh day.

2.2.8 Pollen viability test

Flowers of 4–6 week flowering plant (open flower with white petals developing) were removed from the plant and the anthers taken off the stamen. Pollen grains were released from the anther and put on a microscope slide. Pollen viability test was performed with Alexander's staining solution: 10 ml of ethanol, 10 ml malachite green (1 % w/v in 95 % ethanol), 25 ml glycerol, 5 g phenol, 5 g chloral hydrate, 50 ml acid fuchsin (1 % w/v in ddH_2O), 0.5 ml orange G (1 % w/v in ddH_2O), 2 ml glacial acetic acid, and 50 ml ddH_2O according to (Alexander, 1969). The slide was covered and heated gently from the bottom using a lighter until the solution begins to simmer. The analysis of pollen staining occurred on the same or next day by transmitted light microscopy (2.1.1).

2.2.9 Crossing of *Arabidopsis thaliana* lines *sir1-1*, *ggt1*, *ggt2* and *ggct*

The mutant lines *sir1-1* and *ggct2;1* used in the crossbreeding with *ggt1* and *ggt2* were provided by the Center of Organismal Studies of the University of Heidelberg. Plants grown in short day conditions were transferred at the same moment to long day conditions to induce the synchronization of the flowering time, except for *sir1-1* that was transferred in long day condition 2 weeks before the others lines (2.2.2). At the time of the crossing, flower with immature anthers of the maternal cross parent was chosen and was opened under stereomicroscope. The flower of the paternal plant with mature anthers was used as pollen donor and the pollen was transferred by rubbing the anthers on the stigma of the maternal cross parent. The combinations of crossing performed are listed in Table 6. The seedling obtained in F_2 were screened by using double selective media supplemented with kanamycin and sulfadiazine (2.1.2) for the plants in combination with *sir1-1*, and just with kanamycin for the plants in combination with *ggct2;1*. The survived plants were genotyped by PCR (2.3.2) with respective primers (2.1.6) to find the homozygote individuals.

Table 6 Combinations of the crossing performed

Line 1	Line 2
sir1-1	*ggt1*
sir1-1	*ggt2*
sir1-1	*ggct2;1*
ggct2;1	*ggt1*
ggct2;1	*ggt2*

2.3 Molecular biology methods

2.3.1 Extraction of genomic DNA

Genomic DNA (gDNA) was isolated from 30 mg rosette leaf. According to (Edwards et al., 1991) leaves were ground and suspended in 0.4 ml Edwards buffer (0.2 M Tris-HCL pH 7.5, 250 mM NaCl, 25 mM EDTA, 0.5 % SDS). Then the homogenate was mixed vigorously for 10 sec and was centrifuged for 5 min at RT at 13,000 rpm. 0.3 ml supernatant was transferred into a fresh tube and DNA was precipitated by addition of 0.3 ml isopropanol. After incubation at room

temperature for 2 min, the solution was centrifuged at 13,000 rpm for 10 min and the supernatant discarded. The resulting sediment was washed in 0.7 ml 70 % ethanol, pelleted again at 13,000 rpm for 3 min. Ethanol was discarded and the DNA sediment was air-dried for at least 30 min and resolved in 30 µl sterile H_2O.

2.3.2 Polymerase chain reaction (PCR)

The genotype of plants was screened by PCR amplification of the respective fragment for the T-DNA insertion or the RNAi construct. The polymerase chain reaction was performed in a final volume of 20 µl which contained 2 µl Taq polymerase buffer, 0.4 µl dNTPs, 0.5 µl forward primer, 0.5 µl reverse primer, 1.25 units Taq polymerase (2.1.2). One – two µl of isolated gDNA (2.3.1) from the plant of interest were added to the reaction as template.

Table 7 Typical set up of PCR program

Cycles	Step	Temperature	Time
1	Initial denaturation	95 °C	3 min
35	Denaturation	95 °C	30 sec
	Annealing	55-58 °C	30-45 sec
	Elongation	72 °C	60-95 sec
1	Final elongation	72 °C	10 min

2.3.3 Agarose gel electrophoresis

PCR products were separated by horizontal electrophoresis in 1 % – 2 % agarose gels. For preparation of gels, agarose was melted in 1× TAE buffer (40 mM Tris acetate pH 8.3, 1 mM EDTA). The melted agarose was cooled down to 45 °C and SYBR® Safe DNA Gel Stain 10000 X (2.1.2) was added. DNA was mixed with 6 X loading dye (0.25 % bromophenol blue, 0.25 %, xylene cyanole, 40 % glycerol) prior loading of the sample on the gel. The molecular weight standard 100 bp DNA ladder (2.1.2) was used as reference. Separation of DNA fragments was achieved by applying a voltage of 100 – 150 V for approximately 1 h, using 1× TAE as running buffer. The DNA bands were visualized under UV light using GENi gel documentation system (2.1.1).

2.3.4 Generation of double *ggt1/ggt2* RNAi mutants

The double knockdown *ggt1/ggt2* RNAi lines were obtained in cooperation with Dr. Dinesh Prasad of the Department of Biotechnology BIT Mesra, INDIA.

2.3.4.1 Construction of silencing vector

The target sequence for the induction of RNAi in Arabidopsis was amplified by adapter PCR and introduced into the hairpin RNA-expressing pWatergate vector (CSIRO Plant industry) using the Gateway system (Invitrogen, Carlsbad, CA, USA). The target sequence was a fragment of *GGT2* gene of 363 bp from nucleotides 104 to 467 and was amplified using the primer containing attB1 and attB2 recombination sites. The amplified PCR product was first cloned into the donor vector pDON221 (Invitrogen) to create an entry clone and after sequence verification, the gene specific sequence was transferred to the binary T-DNA destination vector pWatergate (pWG) in reactions mediated by BP and LR Clonase reaction (Invitrogen). The resulting recombinant construct, pWG-GGT, was then introduced into *A. tumefaciens* C58C1 harboring the pMP90 helper plasmid via a freeze–thaw method.

A

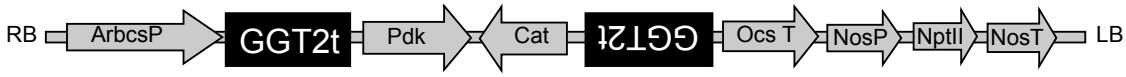

B

5’ – GCAAAACGCTAACGCTGTGAAAAATCTGCAAAGTATTGTTGCGTATCACGGTGCGGTTG
CGACAGACGATGGACGGTGTTCTGCAATAGGGACGAATGTTCTTCGTCAAGGAGGAAACGC
GATTGATGCGTCGGTGGCTGCTGCTCTTTGTTTGGGCGTTGTCAGTCCCGCATCTAGCGGTA
TAGGCGGTGGAGCGTTTACAATGATTAAGCTAGCTAATGGCACGGAAGTTGCTTATGATTCC
AGAGAAACCGCTCCTCTAAGCGCCACTGAGGATATGTATGGTGATAATCCTGAGCGAAAGAA
GAAAGGATCCTTGTCAGTAGGCGTTCCCGGGGAAGTCGCGGGTCTATACACGGCTTG – 3’

Fig. 6 RNAi construct in pWatergate vector
(A) Schematic representation of the hairpin-RNA construct in vector pWG-GGT. The hairpin structure consisting of a GGT2t sequence (B), the pyruvate orthophosphate dikinase (Pdk) intron, catalase intron (Cat) and the GGT2t in reverse orientation was inserted (mediated by LR clonase reaction) between the Arabidopsis rubisco promoter (Arbcs) and the octopine synthase terminator (Ocs T) of the pWatergate vector. RB, right border; NosP, nopaline synthase promoter; Npt II, neomycin phosphotransferase II; NosT, nopaline synthase terminator; LB, left border. (B) The gamma-glutamyl transpeptidase 2 target (GGT2t) correspond to 363 bp fragment between nucleotides 104 to 467 of *GGT2* cDNA sequence.

2.3.4.2 Generation of transgenic plants

Arabidopsis plants were transformed using the floral dip method (Zhang et al., 2006). *A. tumefaciens* carrying pWG-GGT were grown to stationary phase at 28°C in liquid YEB medium supplemented with 50 mg/L gentamycin and 100 mg/L spectinomycin. These bacteria were then sedimented by centrifugation at 5,000 x g for 15 min at 28°C and resuspended in transformation buffer containing 5 % (w/v) sucrose, half-strength MS salts, half-strength Gamborg's B5 vitamins, 44 mM benzyl aminopurine and 0.02 % (v/v) Silwet L-77 (Lehle seeds). Healthy flowering wild type plants were immersed in the cell suspension, infiltrated for 10 min under a vacuum of 40 kPa, and then covered with plastic wrap for overnight to prevent dehydration. The plants were grown and seeds were collected in bulk from the dried siliques. To select transgenic plants (T1 generation), the seeds from the infiltrated plants were germinated and tested for their antibiotic resistance on MS solid medium supplemented with 50 mg/L kanamycin. RNAi construct insertions in the kanamycin-resistant plants were verified by PCR amplification of genomic DNA.

2.3.4.3 Selection of homozygote RNAi lines

Several individual plants from the six RNAi selected lines (T2 generation) were cultivated on soil separately and kept to seed propagation. At least 100 seeds of 10 batches (except L6 for which 4 individuals were used) of each RNAi lines (L2, L4, L5, L6) were sowed separately in MS solid medium (2.2.4) supplemented with 50 mg/L kanamycin and growth in sterile short day condition (2.2.2). The seed batch in which the 100 % of seed germinated were survived was considered as homozygote batch.

2.3.5 Total RNA extraction from plant tissue

Total RNA was extracted from 50 mg of root using TRIzol® (2.1.2) and Direct-zol ™ RNA MiniPrep (2.1.5). The sample was ground in fine powder with mortar and pestle in liquid nitrogen then transferred in centrifuge tube in which was added 1 ml of RNA Extraction Buffer (100 mM Tris HCl pH 9.5, 150 mM NaCl, 0.5 % ß-mercaptoethanol) and vigorously mixed 1 min. The mixture was then centrifuged

5 min at 11000 g and 400 µl of supernatant was transferred in two new centrifuge tube and combined with 800 µl TRIzol® and mixed 1 min. Further 200 µl chloroform was added to the solution, mixed by inversion for 30 sec and incubated 5 – 15 min at RT. The sample was centrifuged for 15 min at 15000 g at 4 °C. After centrifugation three phases were created, the aqueous upper phase (approx. 700 µl) was collected and loaded on column of the Direct-zol ™ RNA MiniPrep Kit for the purification steps. The manufacturer's protocol was followed and the DNAse digestion was performed on column in order to minimized DNA contamination. Twenty-five µl of RNAase-free H_2O were added onto the membrane, incubate 5 min and RNA was eluted in a new centrifuge tube after 1 min at 10000 g of centrifuge. The RNA was quantified using NanoDrop ND 2000 (2.1.1), finally frozen in liquid nitrogen and stored at -80 °C.

For RNA extraction from seeds, the following protocol according to (Chang et al., 1993) was used. The extraction buffer (0.1 M Tris-HCl, pH 8.0, 2 % hexadecyltrimethylammonium bromide, 2 % PVP-40, 25 mM EDTA, 2 M NaCl) was preheated in a water bath at 65 °C and subsequently 0.1 ml β-mercaptoethanol were added to 5 ml extraction buffer. After combining the seed powder and the buffer, the homogenate was mixed for 1.5 min and incubated at 65 °C for 10 min. The reaction set was centrifuged at RT and 6000 g for 20 min. The supernatant was collected and combined with 5 ml of chloroform/isoamyl alcohol (24:1). The solution was mixed and the centrifugation step was repeated as described above. The whole supernatant was transferred to a fresh tube, 5 ml of 5 M LiCl was added and RNA was precipitated overnight at 4 °C. The samples were centrifuged with 6000 g at 4 °C for 30 min. The supernatant was removed and the sediment was resuspended in 0.6 ml resuspension buffer (10 mM Tris-HCl, pH 8.0, 1 M NaCl, 0.5 % SDS, 1 mM EDTA) which was preheated to 60 °C. The solution was transferred to a fresh tube and incubated at 60 °C until the sediment was resolved in buffer. Therefore 0.6 ml of chloroform/isoamyl alcohol (24:1) were added to the sample followed by centrifugation at 14000 g at 20°C for 10 min. The supernatant was mixed with 0.5 ml of chloroform/isoamyl alcohol (24:1) in a new tube and centrifugation was repeated as previously described for 15 min. After centrifugation, the supernatant was transferred into a new tube with 1.2 ml ice-cold 100% ethanol and incubated for 1 h at -80 °C to precipitate RNA. After centrifugation at 13000 g and 4 °C for 30 min, the supernatant was

discarded carefully and the sediment washed with ice-cold 70 % ethanol and centrifuged twice at 13000 g and like before for 10 min. Sediment was dried at RT and resuspended in 50 µl RNase-free DEPC-treated water. For all treatments and buffers, DEPC-treated water was used.

After RNA isolation, total RNA yield and quality was measured with NanoDrop 2000 spectrophotometer (2.1.1) as described in 2.3.6.

2.3.6 Determination of RNA concentration and quality

The amount of RNA was determined spectrophotometrically at 260 nm using the NanoDrop 2000 spectrophotometer (2.1.1). The ratios A260 nm/A280 nm and A260 nm/A230 nm were compared to estimate protein and polysaccharide impurities, the values should be between 1.8 and 2.1. RNA samples with the values included in 1.8 and 2.1 range and with at least 100 ng of concentration were used for cDNA synthesis (2.3.7).

2.3.7 First strand cDNA synthesis

RNA was converted into cDNA using the High-Capacity cDNA Reverse Transcription Kit (Applied Biosystem, 2.1.5), according to the manufacturer's instructions using 1 – 2 µg of total RNA. The synthesized cDNA was then diluted 1:2 with ddH_2O.

2.3.8 Quantitative real time PCR

Quantitative real timer-PCR (qRT-PCR) analysis was performed using the SYBR mix (Rotor-Gene SYBR® Green PCR Kit 2.1.5) in the Rotor-Gene Q cycler (2.1.1). The reaction was performed in a total volume of 20 µl containing 2 – 4 µl cDNA, 10 µl SYBR mix, 2 µl primer mix (5 µM each), ddH_2O to the final volume. For quantification, Rotor-Gene® Q Series Software (2.1.3) was used. Raw expression data were normalized using *PP2a* as reference gene (for primer list see Table 3).

2.4 Biochemical methods

2.4.1 Protein extraction

2.4.1.1 Protein extraction from Arabidopsis vegetative tissues (leaves, root)

Proteins were extracted from 200 mg of tissue ground in fine powered by mortar and pestle in liquid nitrogen. Therefore the Protein Extraction Buffer (40 mM TrisHCl pH 8, 3 % Triton, 1mM PMSF, 1mM Benzamidine, 1M NaCl) was added in 1:5 (mg/µl) ratio. The homogenate was then transferred in centrifuge tube and incubated under agitation at RT for at least 1 h. The supernatant was taken after centrifuge for 12 min at 13.000 rpm at 4°C. Protein quantification was determined by using Bradford reagent (2.4.2). For enzymatic activity assay (2.4.5) the sample was stored at -20 °C. For SDS-PAGE analysis (2.4.3) the protein was precipitated by overnight incubation with 100 % acetone in 1 : 4 ratio at -20 °C. The sample was centrifuge 3 min at 10.000 rpm at 4°C then washed twice with 1 ml of 80 % acetone. Finally the pellet was dried under fume hood and stored at -20 °C.

2.4.1.2 Protein extraction from Arabidopsis seeds

Approx. 5 mg of seeds were ground using the Qiagen TissueLyser (2.1.1) for 1 min at 30 Hz. One ml of hexane was added at the smashed sample and the samples were then centrifuge for 3 min at 10000 rpm at 4°C for 3 times to remove the lipid material. The pellet was then dried under fume hood then solubilized with 0.5 ml Protein Extraction Buffer (2.4.1.1) and incubated 2 h in agitation. The further steps were conducted as well as in paragraph 2.4.1.1.

2.4.2 Determination of protein concentration

Protein concentration was determined according to (Bradford, 1976). Protein extract was diluted 1:20 with ddH_2O and 100 µl were mixed with 1 ml of Bradford reagent (2.1.2) and incubated 15 min at RT. Absorbance was measured at 595 nm with the BioSpectrometer kinetic (2.1.1). Protein sample concentrations were quantified using a BSA standard calibration curve created with 0.01 – 0.2 $\mu g\ \mu l^{-1}$ BSA standard samples.

2.4.3 SDS- polyacrylamide gel electrophoresis (PAGE) Tricine

SDS-PAGE tricine is electrophoretic technic that allow a sensible separation of low molecular weight proteins, smaller than 30 kDa. The SDS-PAGE tricine gel consist in a separating gel of 16.5 % T, 3 % C Acryl/Bisacrylamide and a stacking gel of 4 % T, 3 % C Acryl/Bisacrylamide according to (Schägger, 2006). The gel was prepared and casted in the Mini-PROTEAN® Tetra Cell (Bio-Rad) 2.1.1. Protein samples were provided with a respective volume of 2 × Laemmli buffer [0.625 M Tris HCl pH 7.8; 2 % (w/v) SDS; 20 % (w/v) glycerine; 0.01 % (w/v) bromophenol blue; 5 % (v/v) β- mercaptoethanol]. Before loading, samples were denaturated for 5 min at 95 °C. ColorBurst™ Electrophoresis Marker (Sigma Aldrich) was used as marker for molecular size. Electrophoresis was performed with a cathode buffer (0.1 M Tris; 0.1 M tricine; 0.1 % (w/v) SDS; pH 8.25) poured inside the electrophoretic chamber and with an anode buffer (0.2 M Tris; pH 8.9) outside, at a current of 20 mA for approx. 3 - 5 h.

2.4.4 Protein staining and quantification

After protein separation by SDS PAGE Tricine, the proteins were stained in colloidal Coomassie staining solution overnight on a horizontal shaker. The background of the gels was destained four times by incubation with Coomassie destaining solution (20 % ethanol, 10 % acetic acid). Gels were aquirred after equilibration in water by using the ChemiDOC™ XRS+ Image System (BioRad, 2.1.3). The bands intensity was quantified from the digital image by using Image Lab™ Software (BioRad, 2.1.3) and normalized against the total lane densitometry.

2.4.5 Activity assay

2.4.5.1 Determination of GGT activity *in vitro*

The GGT activity was assayed *in vitro* according to (Huseby and Strömme, 1974), where the release of *p*-nitroanilide by the GGT from γ-glutamyl-*p*-nitroanilide (GPNA) substrate was measured spectrophotometrically. The reaction mix was prepared with 200 µl of protein extract, 1 ml of solution A (4.6 mM GPNA in 100

mM NaH_2PO_4 pH 8.0) and 100 µl of solution B (575 mM gly-gly in 100 mM NaH_2PO_4 pH 8.0) directly in cuvette. Therefore the absorbance at 407 nm was measured every 5 min for 1 h.

2.4.5.2 Determination of GGT activity *in vivo*

The GGT activity in roots was measured *in vivo* as described in (Ferretti et al., 2009) and adapted from the procedure to determine GGT activity *in vitro* (2.4.5.1). Pool of roots from 4 - week - old seedling grown on ½ MS media (2.2.4) were cut and placed into test tube containing 5 ml of solution A (4.6 mM GPNA in 100 mM NaH_2PO_4 pH 8.0) and 0.5 ml of solution B (575 mM gly-gly in 100 mM NaH_2PO_4 pH 8.0). The solution was cycled through piping from the test tube to the spectrophotometer cell using a peristaltic pump operated at a flow rate of 3 ml min^{-1}. The change in absorbance at 407 nm induced by releasing *p*-nitroaniline into the assay medium was recorded for 10 min.

2.4.5.3 Enzyme histochemical detection of GGT activity

Tissue sections were previously prepared and stored at -80°C (2.6.1). The staining was performed according the procedure describe in (Rutenburg et al., 1969). The slides were air dry overnight before the fixation procedure which were incubated in cold pure acetone for 15 sec, then in 50 % acetone for 30 sec and finally washed 3 times in ddH_2O. Therefore the slides were immersed 60 – 90 min in a freshly prepared staining solution containing 0.46 mM γ-glutamyl-4-methoxy-2-naphthylamide (GGMN) as a substrate, 6.3 mM glycyl-glycine (gly-gly) as γ-glutamyl acceptor in phosphate buffer pH 7.4 and 0.35 mg/ml Fast Garnet GBC (2.1.2). After staining the images were immediately acquired using Leica DM4000B digital microscope, equipped with a Leica DC300F camera and Leica Image Manager 50 software (2.1.1).

2.4.5.4 Determination of GST activity *in vitro*

GST was measured by spectrophotometric method according to (Habig et al., 1974). Forty µl of protein extract was combined with the GST reaction mix (50

mM PBS pH 6.5, 1 mM CDNB, 1 mM GSH, 1 mM EDTA) directly in the cuvette and the change in absorbance at 340 nm was measured for 5 min.

2.5 Analytical methods

2.5.1 Acidic extraction of thiols

Thiols were extracted from vegetative tissue (leaves) by grounding the tissue in liquid nitrogen by mortar and pestle and by homogenizing it with Acidic Extraction Buffer (0.1 M HCl, 1 mM EDTA) in 1:4 ratio (w/v). Each sample was transferred in a centrifuge tube and centrifuged for 8 min at 12000 rpm and the supernatant was taken. For generative tissue approx. 5 mg of seeds were ground using the Qiagen TissueLyser (2.1.1) for 1 min at 30 Hz. One ml of hexane was added at the smashed sample and the samples were then centrifuge for 3 min at 10000 rpm at 4°C for 3 times to remove the lipid material. The pellet was then dried under fume hood and solubilized with 0.5 ml Extraction Buffer (40 mM TrisHCl pH 8, 3 % Triton, 1mM PMSF, 1mM Benzamidine, 1M NaCl).

2.5.2 Determination of thiols

Total thiols were determined by derivatization with SBD-F as described in (Masi et al., 2002) and by reversed phase HPLC separation. Fifty µl of acid extract (2.5.1) was buffered with 117 µL borate buffer (1M H_3BO_3 pH 10.5 with KOH) and further incubated 10-15 min at RT with 33 µL TBP 1 % in ddH_2O to allow the thiol reduction. Reduced thiols were derivatized by addition of 33 µL SBD-F 0.3 % in ddH_2O and incubated at 60°C (±1°C) for 1 hour. After cool down the sample, 17 µL 4 M HCl were added to stop the reaction. Aliquots of 20 µl derivatized sample were injected by a System Gold^R 126 Solvent Module (2.1.1) equipped with a Gilson auto-injector 234. The derivatized thiols were separated by reversed phase HPLC using a Luna 3 µ C18 (2) 150 x 4.60 mm column for thiol determination from tissues or Luna 5 µ C18 (2) 150 x 4.60 mm column (2.1.1) for the depletion experiment (3.4). The separation was performed in isocratic condition with 100% of elution buffer (93 % ammonium formiate 75 mM pH 2.9 and 3 % methanol) at a flow rate of 0.3 ml/min (for Luna 3 µ) or of 1 ml/min (for Luna 5 µ) and at room

temperature. Detection of separated thiol-derivatives was achieved by using a Jasco Spectrofluorometer 821-FP (2.1.1) at 516 nm after excitation with 386 nm and identified by comparison with the retention times of standard compounds. The thiols concentration was quantified using a calibration curve and by ChromCard board and software (2.1.3).

2.5.3 GSH depletion in liquid solution

Plants 7-week-old cultivated in hydroponic (2.2.5) were incubated overnight in distilled water to induce a starving condition. The plants were then transferred in 5 ml of 100 µM GSH solution. Whereas for the samples treated with the competitive GGT inhibitor Serine-Borate (SerBor), the plants were pre-incubated for 30 min in 10 mM SerBor solution then 5 µl of 100 mM GSH was added at t 0 time point. Fifty µl from the GSH incubation solution were taken and frozen in liquid nitrogen at 0, 10, 20, 30 min and 1, 3, 6, 8 h time points. The samples were stored at -80 °C and subsequently derivatized for thiols determination (2.5.2).

2.5.4 Ascorbate

The ascorbate content was determined spectrophotometrically by measuring the absorbance at 265 nm from 20 µl of leaf extract, according to the method of (HEWITT and DICKES, 1961).

2.5.5 Determination of free amino acid

The determination of free amino acid was performed by Dr. Ilaria Forieri from Centre for Organismal Studies (COS) of University of Heidelberg. The technique was based on derivatization of amino acids with the fluorescent dye AccQ-Tag™ in a volume of 50 µl containing 0.14 M borate buffer pH 8.8, 30 µg AccQ-Tag and 5 µl of the metabolite extract according to the manufacturer's protocol. Derivatized amino acids were separated by HPLC using a Nova-Pak™ C18, 3.9 × 150 mm column as described in (Hartmann et al., 2004). Derivatized and separated amino acid AccQ-Tag derivatives were detected with Jasco FP-920 fluorescence detector at 395 nm after excitation with 250 nm. Quantification was

performed using the Waters LC control- and analysis software Millenium32. Standardization was carried out by external standards for each individual amino acid.

2.5.6 Analysis of total carbon, nitrogen, and sulfur content

Total carbon, nitrogen, and sulfur contents of mature seeds were measured according to (Khan et al., 2010). Seeds from plants grown on soil in growth chamber (2.2.2) were ground by mortal and pestle in liquid nitrogen. Subsequently the seed powder was dried at 75 °C for 3 days. Two different aliquots of sample, 10 and 30 mg, were used for the elemental analyses.

2.6 Microscopic methods

2.6.1 Slide preparation for enzyme histochemical analysis

Mature green siliques of plants grown in growth chamber (2.2.2) were cut and collect in bundles and placed inside a plastic scaffold. Therefore the siliques bundle was included in optimal cutting temperature medium (OCT 2.1.2) with no prior chemical fixation and frozen in liquid nitrogen. The included siliques were transversal cut in slice 20-25 µm of thickness using a cryomicrotome at -25 °C. Finally sections were placed on a glass slide pretreated with 3-aminopropyltriethoxysilane (APES 2.1.2) and stored at -80 °C.

2.7 Statistical analysis

The normality of each trait, as well as the identification of possible outliers was tested through the visualization of a histogram/density plot and using the Shapiro-Wilk normality test on R statistical software (2.1.3). For the phenotypic characterization time course experiments, the data were analyzed using a mixed model approach using the lme function on nlme package (R, 2015). The model was as follow: $Y_{ijk} = \mu + G_i + T_j + (GxT)_{ij} + TR_k + e_{ijk}$, where Y_{ijk} is the dependent variable, μ is the overall intercept of the model, G_i is the fixed effect of the ith genotype, T_j is the fixed effect of the jth class of time and $(GxT)_{ij}$ is the fixed first

order interaction between genotype and time, TR_k is the random effect of the kth technical replicate ~$N(0,\sigma^2_{TR})$, and e_{ijk} is the random residual ~$N(0,\sigma^2_e)$. For the other phenotypic features the dependent variables were analyzed using the same mixed model approach described before without the fixed effect of Time. A multiple comparison of means was performed for the main effects, using a Tukey's test ($P < 0.05$) through the function "difflsmeans" of the package "lmerTest". All the other statistical analysis was performed using the software SigmaPlot 12.0 (2.1.3). Different data sets were analyzed for statistical significance with the Analysis Of Variance (ANOVA) followed by the Tukey's test. Data with a non-normal distribution were analyzed by non-parametric test (Kruskal-Wallis). Different letters in the figures indicate significant difference ($P < 0.05$). Asterisks in all figures indicate the significance: *, $0.05 \geq p > 0.01$; **, $0.01 \geq p > 0.001$; ***, $p \leq 0.001$.

3 Results

3.1 Selection of *ggt1*/*ggt2* RNAi double mutants

GGT1 and GGT2 are the only enzymes responsible of glutathione degradation in the apoplast. Two T-DNA insertion lines for *GGT1* and *GGT2* were obtained by Salk Institute from NASC: *ggt1* (080363) and *ggt2* (069311). Previously, the same *ggt1* line was used and characterized (Martin et al., 2007) and it was named *ggt1-2*. These two GGT isoforms are located in the same compartment and in some cases are expressed in the same tissues (seed, root, trichome). It is not clear if they are working in concert or separately, but it was shown an overexpression of *GGT2* in *ggt1* root as a compensatory mechanism to restore the absence of GGT1 isoform (Destro et al., 2011). The approach of functional genomic is to find evidences from phenotype of mutants in which one or more genes are knocked out. In these mutants absence of only one of the two isoforms do not cause the complete loss of GGT activity in the apoplast. Therefore a double *ggt1/ggt2* mutant was considered a proper approach to reach this aim and add clues about the function of GGTs in the apoplast. *GGT1* and *GGT2* are consecutive genes and they do not segregate independently, therefore obtaining the double mutant by crossing the relative single lines was not possible. RNA interference application has been considered the best strategy in this case, as exogenous RNA double strand sequence is able to link and lead the degradation of a complementary target mRNA sequence. In this way the gene is knocked down at the transcript level rather than at the genome level.

3.1.1 Construct design, plant transformation and homozygote selection

Construct design and plant transformation were carried out some years ago by Dr. Dinesh Prasad of the Department of Biotechnology BIT Mesra, INDIA (2.3.4). The sequence inserted in the construct was a fragment of *GGT2* gene of 363 bp from nucleotide 104 to 467. This specific fragment was chosen because it conserves the 90 % of identity of *GGT1* gene sequence and can lead the silencing of both genes simultaneously. This fragment was inserted into the hairpin RNA-expressing pWatergate vector (pWG) as an inverted repeat sequence separated by

two introns (Pdk and Cat introns) and under control of the Arabidopsis RbcS promoter (2.3.4.1, Fig. 6). The pWG-GGT vector was further introduced into *Agrobacterium tumefaciens* cells, which were used to transform Arabidopsis plant by vacuum infiltration (2.3.4.2). Seeds from infiltrated plants were germinated and grown on selective medium, and the resultant kanamycin resistant plants (T1 generation) were examined by genomic PCR to verify the integration of the pW-GGT construct (Fig. 6A). Six individuals lines were confirmed to harbor the RNAi construct insertions (L1, L2, L3, L4, L5, L6). At the T2 generation for L2, L4, L5, L6 lines were identified the homozygote individuals by examination of the percentage of the survived seedling in MS supplemented with Kan. The seed batch which had the 100% of seedling survived was considered homozygote. The T3 generation from the homozygote plants was called *ggt1/ggt2* RNAi mutant and was finally used for the further experiments.

3.1.2 Validation of *GGT1* and *GGT2* silencing on RNAi lines

The further step in the generation of *ggt1/ggt2* RNAi double mutant was to demonstrate and quantify the level of silencing in both genes. Since *GGT1* and *GGT2* sequences had high similarity (approx. 80% of genomic identity), specific primers were design accurately to recognize the two isoforms. The sequence with the higher differences in nucleotide was chosen, after aligning *GGT1* and *GGT2* cDNA sequences using Clustal Omega (2.1.3). The GGT1 pair of primers was located between the first and the second exon where RNAi sequence pair with the mRNA, while GGT2 primers were placed between the fourth and the fifth exon (2.1.6). Furthermore the tissue where *GGT1* and *GGT2* expression is in adequate level, was chosen by consulting Genevestigator (2.1.3, Fig. 9). As it was reported in literature (Martin et al., 2007; Ohkama-Ohtsu et al., 2007a; Destro et al., 2011) *GGT1* is expressed in the major part of the tissues while *GGT2* is mainly expressed in seed/silique, pollen and in root. Even if the highest expression level of *GGT2* was found in seed/silique, it did not reach the detectable level by qRT-PCR (2.3.8). This could be explained because the *GGT2* expression is restricted to small anatomical part of the seed and seems stage development dependent as it is shown in Genevestigator and eFP Browser (2.1.3). Finally root tissue of very young seedling was chosen, because in this stage the plant is in active

development and the transcription is fully operated. Therefore mRNA was extracted (2.3.5) from pooled roots of 2-week-old seedlings grown in MS medium in vertical plate and used for cDNA synthesis (2.3.7) and qRT-PCR (2.3.8) with *Protein Phosphatase 2A* (PP2a, 43 and 44, Table 3) as reference gene (Fig. 7). The RNAi lines with the highest level of silencing in both isoforms were L5 and L6. Whereas *GGT2* transcripts (Fig. 7B) were almost knocked down in all the four lines, except L2 that still have 35 % of expression, *GGT1* transcript levels (Fig. 7A) were reduced only for L5 and L6, approx. 70 % less than wild-type, while L2 and L4 are comparable with the wild-type transcript levels. This different silencing predominance between the two isoforms could be due to the RNAi sequence used for the silencing, that originated from *GGT2* cDNA sequence, (2.3.4.1) which do not matched *GGT1* mRNA perfectly and this might influence the level of the silencing. In regard to the single mutants, the overexpression of one isoform when the other was knocked out was confirmed as it was reported in a previous study (Destro et al., 2011). Indeed *GGT2* transcript was almost 4 times more in *ggt1* mutant compared to wild-type and also *ggt2* had 25 % of *GGT1* transcript more than wild-type. From this expression analysis the lines with the highest silencing level were L5 and L6, therefore we used only these two RNAi lines for the further experiments.

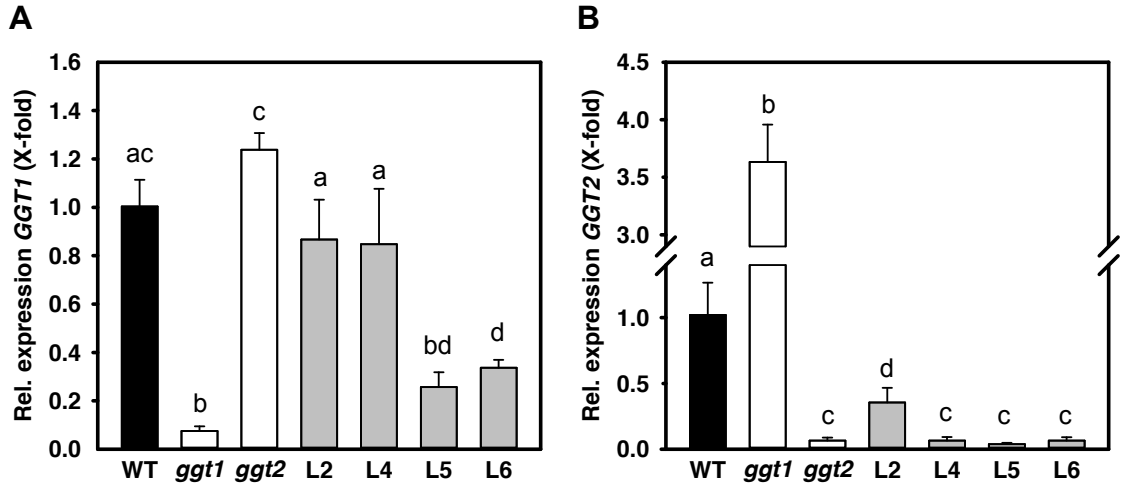

Fig. 7 *GGT1* and *GGT2* relative expression in root of WT, *ggt1, ggt2,* L5 and L6
(A) Transcript level of *GGT1* and (B) *GGT2* in pool of root of 2 – week – old plants grown in Petri dishes. The expression level was determined by qRT-PCR, using *PP2a* (At1g13320) as reference gene. The level in wild-type was set to 1 and the other values were expressed as x-fold of it. Different letters indicate statistically significant differences between lines; (n = 5), (means ± SD).

3.2 *GGT1* and *GGT2* anatomical expression using Genevestigator and eFP Browser

The Web-based software tools rapidly developed in this last century, which provided many information for biologists and facilitated discovery research and hypothesis validation. Genevestigator assembles public expression data for mouse and Arabidopsis into context-related profiles (metaprofiles) and provides easy online access to this database (Hruz et al., 2008). In a previous study (Martin et al., 2007), the earlier version of Genevestigator was already interrogated in order to characterize the expression pattern of all the GGT isoforms. In these last years many improvements and new detailed experiments were added in the new version of Genevestigator data set, therefore it was our interest consulting again the expression pattern of *GGT1* and *GGT2*. The expression pattern data set of both genes was downloaded and the more abundant categories were represented in the graphs (Fig. 9), threshold of 11 for GGT1 and of 8 for GGT2 was used. Moreover the results obtained by Genevestigator were enriched and confirmed in parallel by eFP browser (Winter et al., 2007), which visualizes the gene expression at specific temporal moment of development in specific anatomical part of Arabidopsis organ.

The leaf was the predominant organ for *GGT1* expression with high levels also in cotyledon and sepal. Adult leaves were favorited rather than juvenile and senescent leaves. In the leaf tissues layers *GGT1* was more expressed in epidermal cells, in particular pavement cells and in trichomes, in shoot vascular tissue and bundle sheath cells. These results confirmed the histochemical detection of GGT activity reported in the work of Destro et al. (Destro et al., 2010). Curiously the expression was detected also in the petiole epidermis cells that connect the leaf to the plant stem. In root the elongation zone and the pericycle were the first two most abundant locations were *GGT1* is expressed. The elongation zone is the root region upon the root apex after the transition and the meristematic zone. This zone shows fast cell elongation and is accompanied by drastic and specific cell wall alterations (Verbelen et al., 2006). Several events occur in the cell wall, including a rise in apoplastic pH, callose deposition and cross-linking events steered by reactive oxygen species (De Cnodder et al., 2005). The pericycle is the cells layer just closed to endodermis where the lateral roots are originated and it

is part of the vascular cylinder because it arises from the procambium. In the inflorescence tissues, the chalazal seed coat and the ovule were particular relevant in *GGT1* expression. The chalazal seed coat is the pole linked to the mother plant by the funiculus and represents the connection point for nutrient assimilation and transport (Stadler et al., 2005). In particular the expression of *GGT1* in this seed region seemed increasing during all the stage of development till the mature green (Fig. 8A). In addition at the pre-globular stage *GGT1* expression was distributed in whole coat that surround the seed exactly at the time when nutrient transit from integument and endosperm (Stadler et al., 2005).

GGT1 was strongly expressed in almost all tissues compared to *GGT2*, which in contrast had more fine and specific expression pattern. The seed and the generative tissues were the organ where *GGT2* expression was predominant. The anatomical part where *GGT2* touched the major expression overall was the suspensor, one third more than *GGT1*. Suspensor is the specific structure that connects the embryo to the inner vascular system of the seed, and it is considered the analogous to the placental mammalian's umbilical cord. Both GGT isoforms are expressed here at the globular stage (Fig. 8) within the time the suspensor is simplastically connected to the embryo (Stadler et al., 2005). In addition *GGT2* was high expressed in the endosperm especially in the chalazal and micropylar endosperm and as *GGT1*, in the chalazal seed coat. Intense *GGT2* expression started during the formation of the micropylar endosperm at the pre-globular and globular stage then decreased at the heard stage, whereas simultaneously in the chalazal endosperm increase (Fig. 8B). Moreover, with less intensity, *GGT2* was expressed in pollen, in silique replum, in seed testa and embryo. Interesting was the very high expression of both isoforms in sperm cells which were produced inside the pollen. In the embryo development *GGT2* is expressed at the globular stage and at the heart stage very intense in the root extremity. The only vegetative tissue in which *GGT2* is highly expressed is in the phloem stem, which is fundamental to transport metabolites from leaves to sink tissues. Another connection point in the stem where *GGT2* was expressed was the starch sheath (endodermis) cell. Endodermis is commonly described as starch sheath; its cells are richly deposited with starch grains, without any intercellular spaces. It associated to the Casparian strip that works as hydrophobic barrier that prevents water and any solutes from passing through this layer via the apoplast pathway.

The only way to pass through endodermis is to cross the membrane. It was interesting also observe that *GGT2* expression was focused in the meristematic tissues: in root apical meristem, shoot apex, stem developing meristemoid zone and interfascicular cambium stem cell. Interfascicular cambium represent a continuous ring that bisects the primary xylem and primary phloem, and is composed by undifferentiated meristem cells that divide and originate the secondary vascular tissues. In primary root *GGT2* shared the same expression location of *GGT1* in elongation zone.

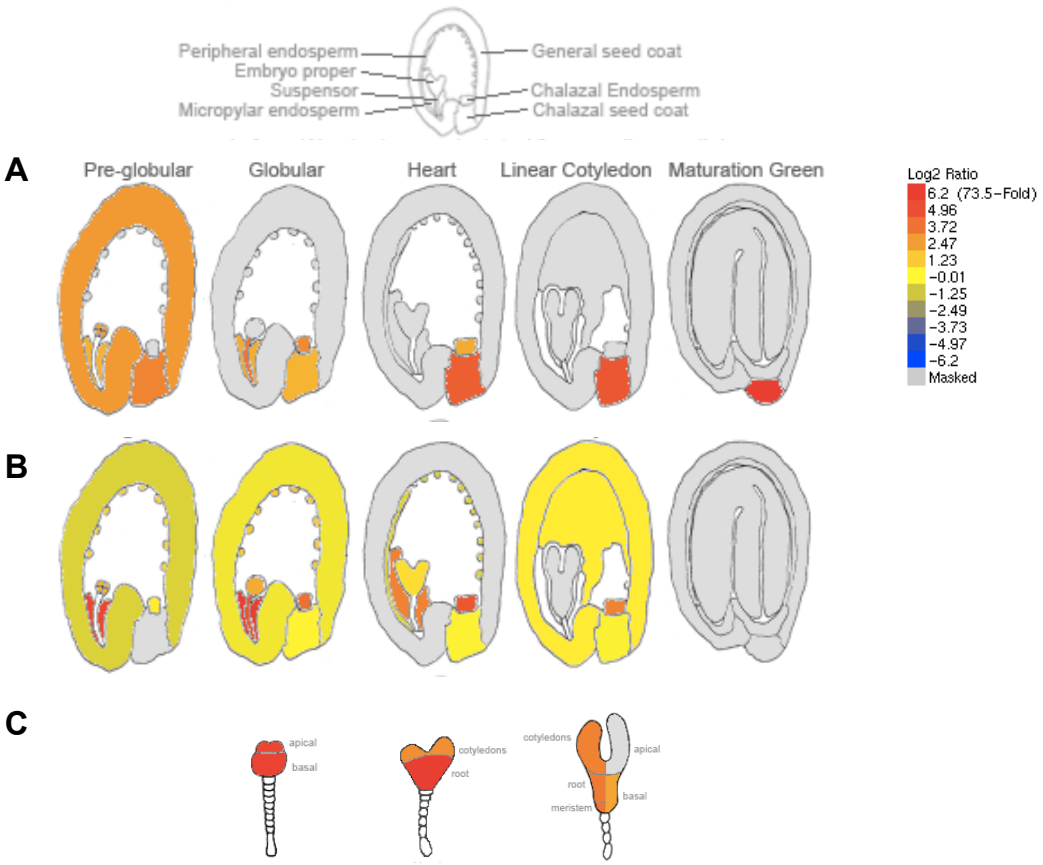

Fig. 8 Temporal and spatial localization of *GGT1* and *GGT2* expression in developing seed using eFP Browser
Levels of (A) *GGT1* and (B) *GGT2* expressions on five seed developmental stages (pre-globular, globular, heart, linear cotyledon, maturation green). (C) *GGT2* expressions on developing embryo; in globular, heart and linear cotyledon. On the top, schematic representation of seed and its anatomical components. On the right side, scale logarithmic base 2 of expression intensity.

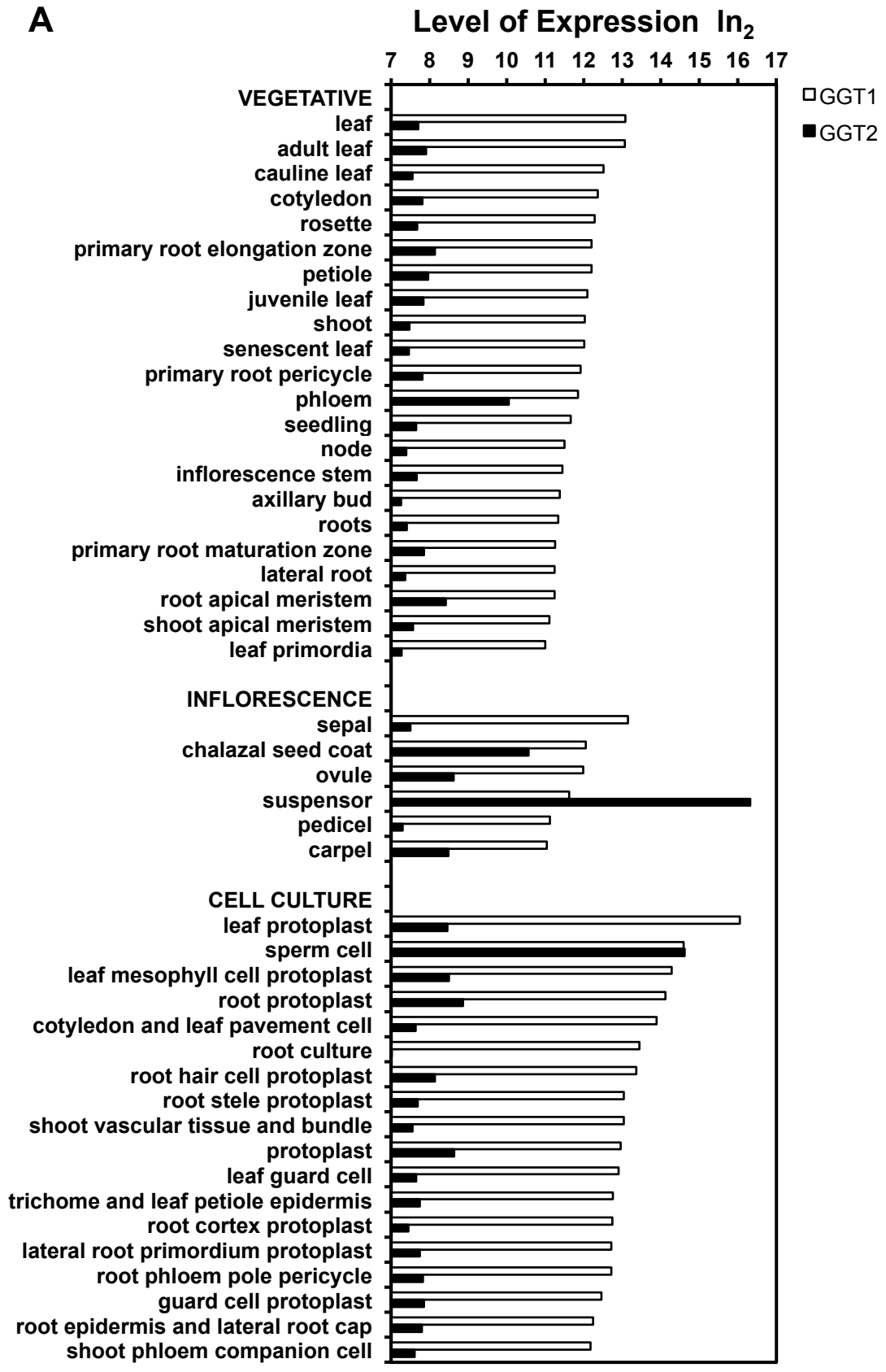
A
Level of Expression ln2
7 8 9 10 11 12 13 14 15 16 17
GGT1
GGT2
VEGETATIVE
leaf
adult leaf
cauline leaf
cotyledon
rosette
primary root elongation zone
petiole
juvenile leaf
shoot
senescent leaf
primary root pericycle
phloem
seedling
node
inflorescence stem
axillary bud
roots
primary root maturation zone
lateral root
root apical meristem
shoot apical meristem
leaf primordia
INFLORESCENCE
sepal
chalazal seed coat
ovule
suspensor
pedicel
carpel
CELL CULTURE
leaf protoplast
sperm cell
leaf mesophyll cell protoplast
root protoplast
cotyledon and leaf pavement cell
root culture
root hair cell protoplast
root stele protoplast
shoot vascular tissue and bundle
protoplast
leaf guard cell
trichome and leaf petiole epidermis
root cortex protoplast
lateral root primordium protoplast
root phloem pole pericycle
guard cell protoplast
root epidermis and lateral root cap
shoot phloem companion cell

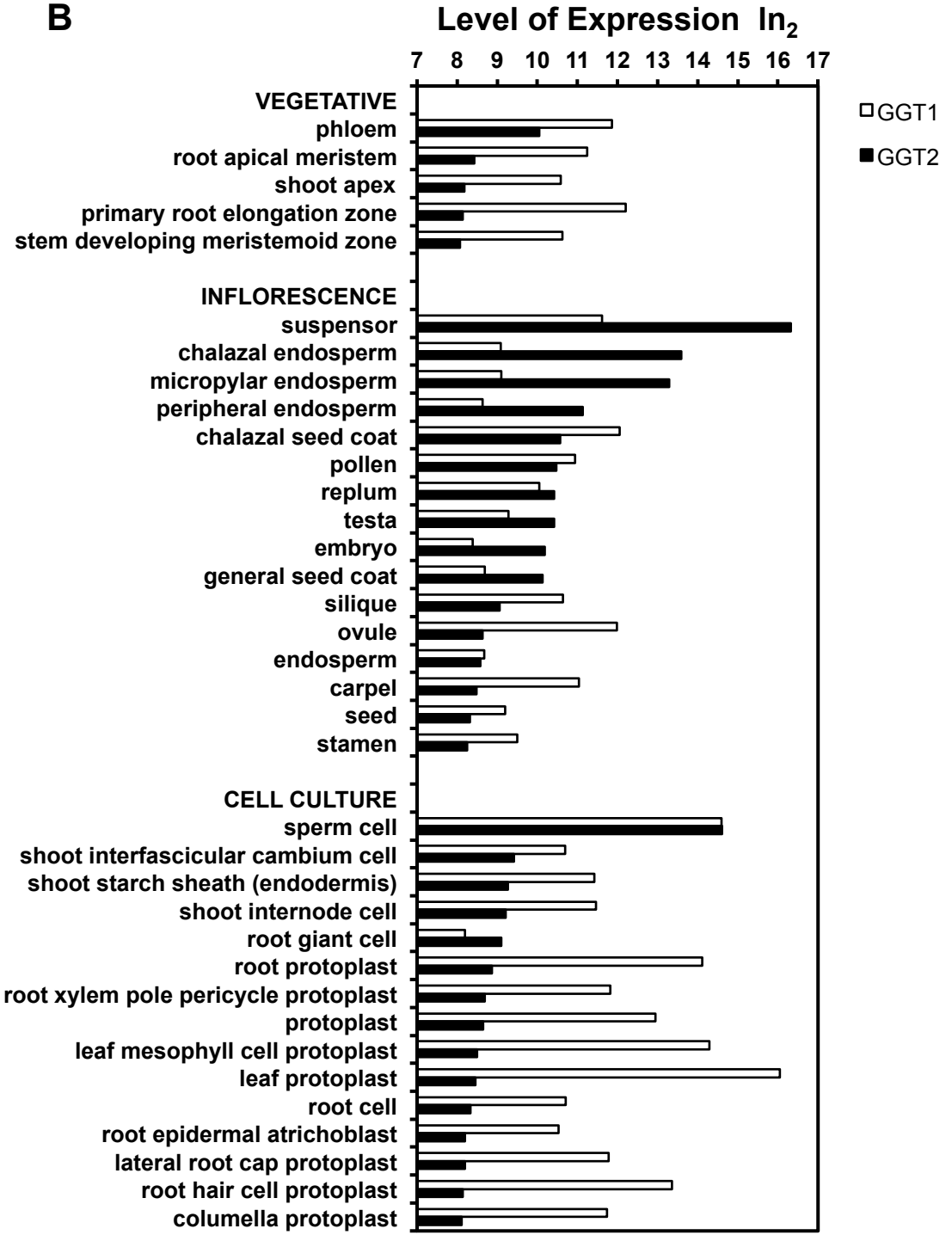

Fig. 9 Anatomical localization of *GGT1* and *GGT2* expression using Genenvestigator®
Level of *GGT1* and *GGT2* expression in anatomical part of the plant. The categories were divided in three groups related to the vegetative, inflorescent or reproductive tissues and the data from experiment in cell culture. The categories were organized in decreasing order of expression of *GGT1* (A) and or of *GGT2* (B) in two different graphs. Values ≥11 for *GGT1* and ≥8 for *GGT2* were selected and represented in the graph. The scale is logarithmic base 2 and started from 7. Data were retrieved from Genevestigator® (2.1.3).

3.3 Phenotypic characterization of generative tissue

3.3.1 Determination of GGT activity in seed

The seed is the tissue where both isoforms are present and one of the few tissues where *GGT2* is expressed. To confirm that GGT activity is knocked down in the *ggt1/ggt2* RNAi lines the total GGT activity was quantified in dry seeds. Total proteins were extracted from dry seeds (2.4.1.2) and the total GGT activity was measured by spectrophotometric method by monitoring the change in absorbance of the release of p-nitroaniline from the artificial γ-glutamyl-p-nitroanilide substrate (2.4.5.1). The GGT activity assay measures the total activity in the whole cell and is not able to discern from which isoforms the activity was originated, therefore activity of the vacuole-localized isoform GGT4 is also included in the total level. In all mutants the GGT activity was reduced compared to wild-type (Fig. 10), L5 showed the lowest level with only 27 % ± 5.1 of total GGT activity remained, L6 and *ggt1* maintained 50 % of activity (L6 55 % ± 14.1; *ggt1* 47 % ± 9.8) and finally *ggt2* was the mutant line which had the highest activity compared to the other lines with 76 % ± 4.6 of activity left.

In order to localize the GGT activity in mature green seeds, enzyme histochemical analysis was performed in transversal section of green siliques. The tissue was included in OCT (2.1.2) without any chemical fixation and then cut in transversal section by cryomicrotome (2.6.1). The slides of tissue were stained by incubation in a solution containing GGMN (2.1.2) as a GGT substrate, gly-gly as a γ-glutamyl acceptor and the diazonium salt Fast Garnet GBC (2.1.2) that will combine with the GGT reaction product. The salt complex GGT-product-Fast Garnet was precipitated as reddish color in the anatomical place where GGT was located. Finally the slides images were acquired by Leica digital microscope (2.1.1). Wild-type showed a strong reddish color due to the salt deposition in the seed inner and outer integument, in the endosperm; in the silique endocarp and sclerenchyma. In all mutant lines the reddish color was reduced, but it did not disappeared completely.

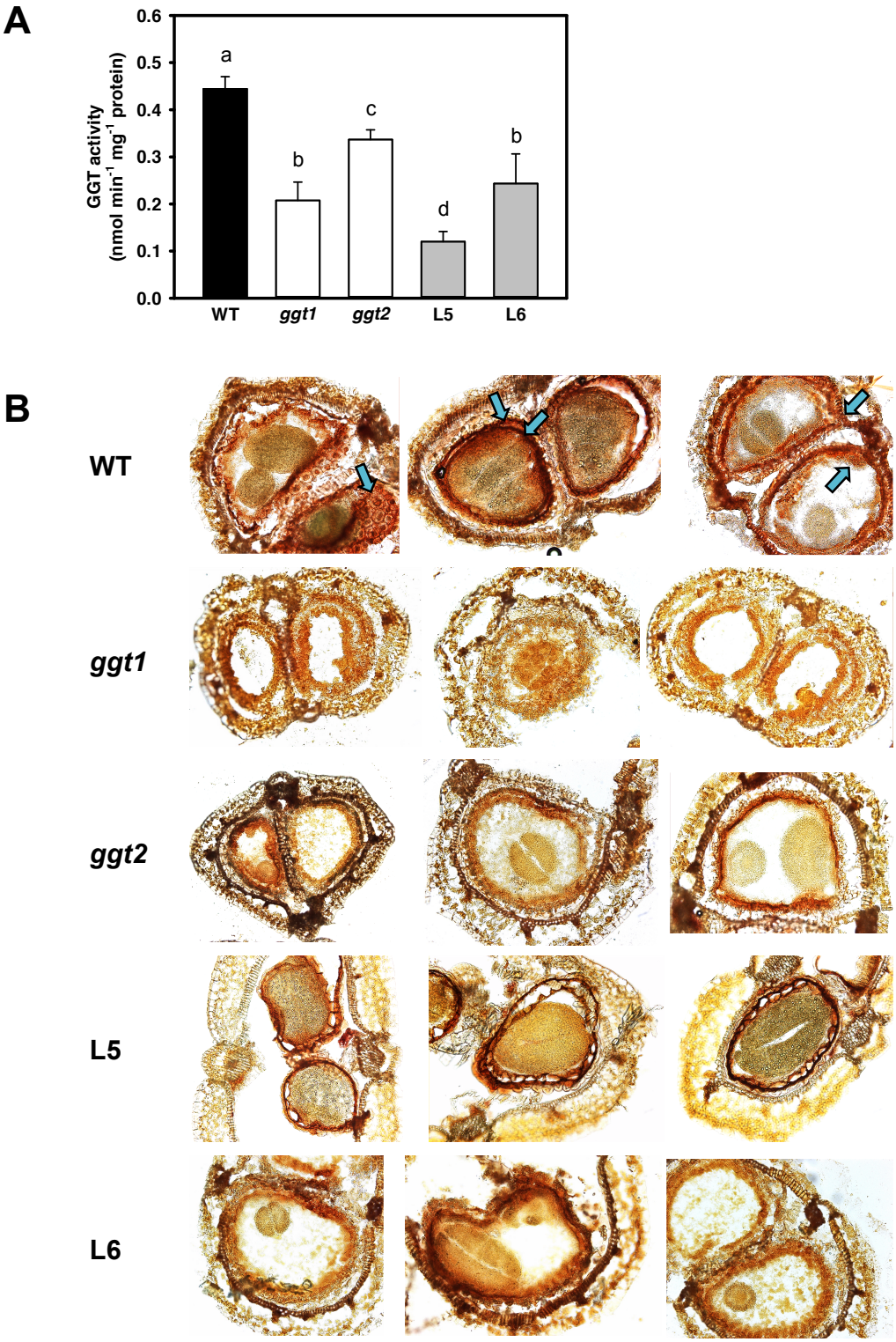

Fig. 10 Detection of GGT activity in dry seed and its localization in transversal section of green silique.
(A) Total GGT activity in dry seed protein extract of wild-type, *ggt1*, *ggt2*, L5 and L6, measured by spectrophotometric method (2.4.5.1); (n = 5), (means ± SD). (B) Enzyme histochemical detection of GGT activity in mature green silique of wild-type, *ggt1*, *ggt2*, L5 and L6. Transversal tissue sections were incubated in a GGMN solution and stained with Fast Garnet GBC (2.4.5.3). Reddish to purplish-brown staining indicates deposition of diazonium salts at the site of GGT activity. The arrows indicate from left to right WT images: endocarp, outer and inner integument, endosperm and sclerenchyma.

3.3.2 Seed yield and influential factors

To investigate the impact of the reduced GGT activity on the seed yield between the different lines, whole sets of seeds per plant were harvested and weighted. Four different dry seed batches, obtained from plants grown in short day conditions until they were 7 – 8 week old and then transferred in long day condition until seed maturation, were used. In average wild-type produced 170 ± 32 seeds per plants, less seeds were produced in RNAi lines L5 (76 ± 38), L6 (60 ± 42), while *ggt1* (110 ± 45) and *ggt2* (115 ± 42) had reduced yield compared to wild-type, but not so strong as the RNAi lines (Fig. 11A). To assess whether weight of individual seeds affected the yield of plant, the weight of a bulk of 100 seeds was determined (Fig. 11B). Only *ggt2* had a slightly significant decrease compared to wild-type. Moreover to find other plant features that could influence the seed yield, the number of side shoots were counted, but no significant differences were observed between wild-type and the mutant lines (Fig. 11C). Pollen viability was investigated (2.2.8) to exclude any impairment in its development and vitality, which could affect the seed yield (Fig. 11A). All the pollen grains in wild-type and in all mutant lines appeared viable (Fig. 11E). The time needed to start bolting was also measure in plants grown in short day condition. All lines started to bolting at the same time (Fig. 11D).

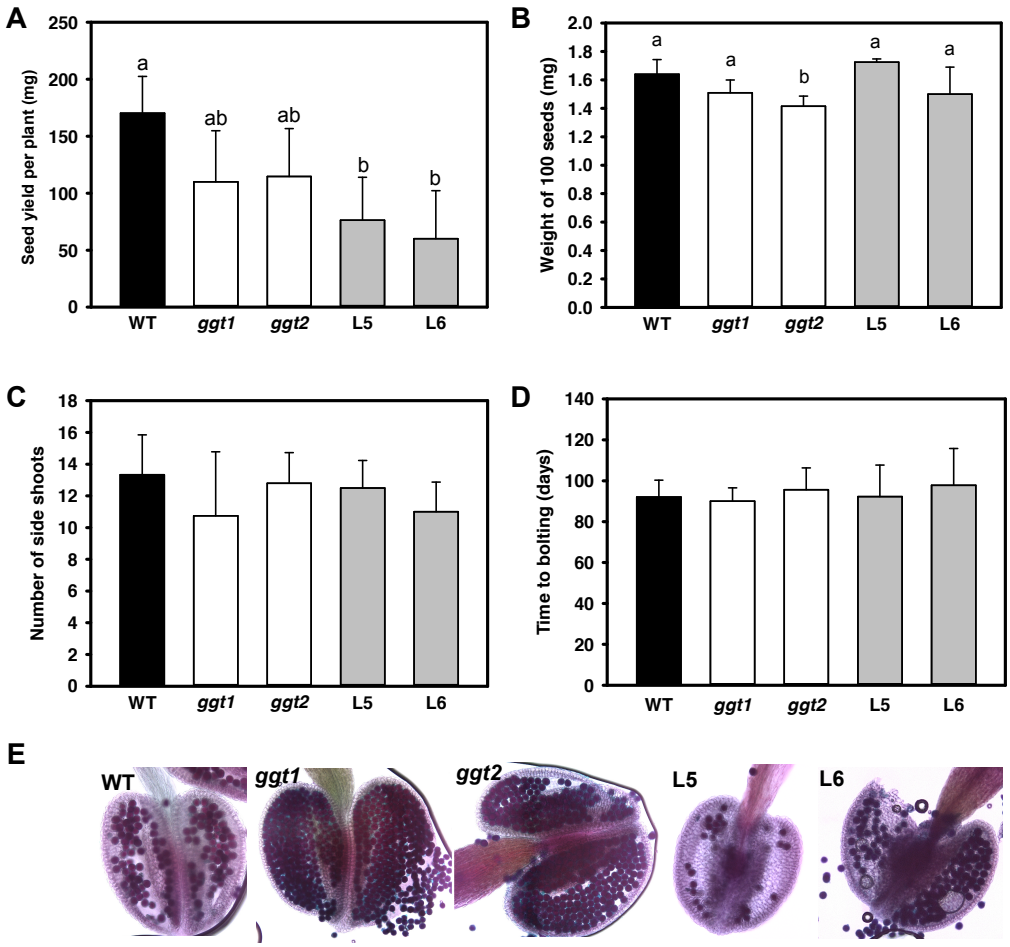

Fig. 11 Seed yield, 100-seed-weight, branches and time to bolting of wild-type, *ggt1*, *ggt2*, L5 and L6
(A) Seed yield was measured as the weight of the whole seed from one plant; (n ≥ 14), (means ± SD). (B) Weight of 100 seeds; (n=4 batches, n ≥ 4 plants), (means ± SE). (C) Number of side shoots per plants; (n ≥ 4), (means ± SD). (D) Time need to start the inflorescence elongation (n ≥ 13), (means ± SD). (E) Images of pollen into anther stained by Alexander's method; magenta-red staining indicates that pollen grains are viable, whereas blue-green staining indicates aborted pollen grains.

3.3.3 Silique characterization

In order to find evidence between the seed yield and silique features, silique characterization was conducted. First the total siliques number produced per plant (Fig. 12A) was counted from two sets of plants grown in growth chamber in different time period (2.2.2). Wild-type plants produced in average 496 ± 21 siliques, as well as *ggt2* (426 ± 81), while significant reduction was found in *ggt1* (307 ± 47), L5 (299 ± 62), L6 (218 ± 87) and this was also visibly detectable (Fig. 12C). One of the possible causes of seed yield reduction could be the reduced silique size. Therefore the length of siliques (Fig. 12B), which were at least 10 days

after flowering (daf), was measured. The RNAi lines were significantly shorter than wild-type and single mutants *ggt1* and *ggt2*. The influence of the siliques length on the number of seeds within silique was further investigated. Seeds were counted from cleared siliques without opening them. Only L6 resulted to have less seeds per silique (Fig. 12D), indeed in some of them empty spaces between seeds (Fig. 12E) and some aborted seeds (Fig. 12F) were found.

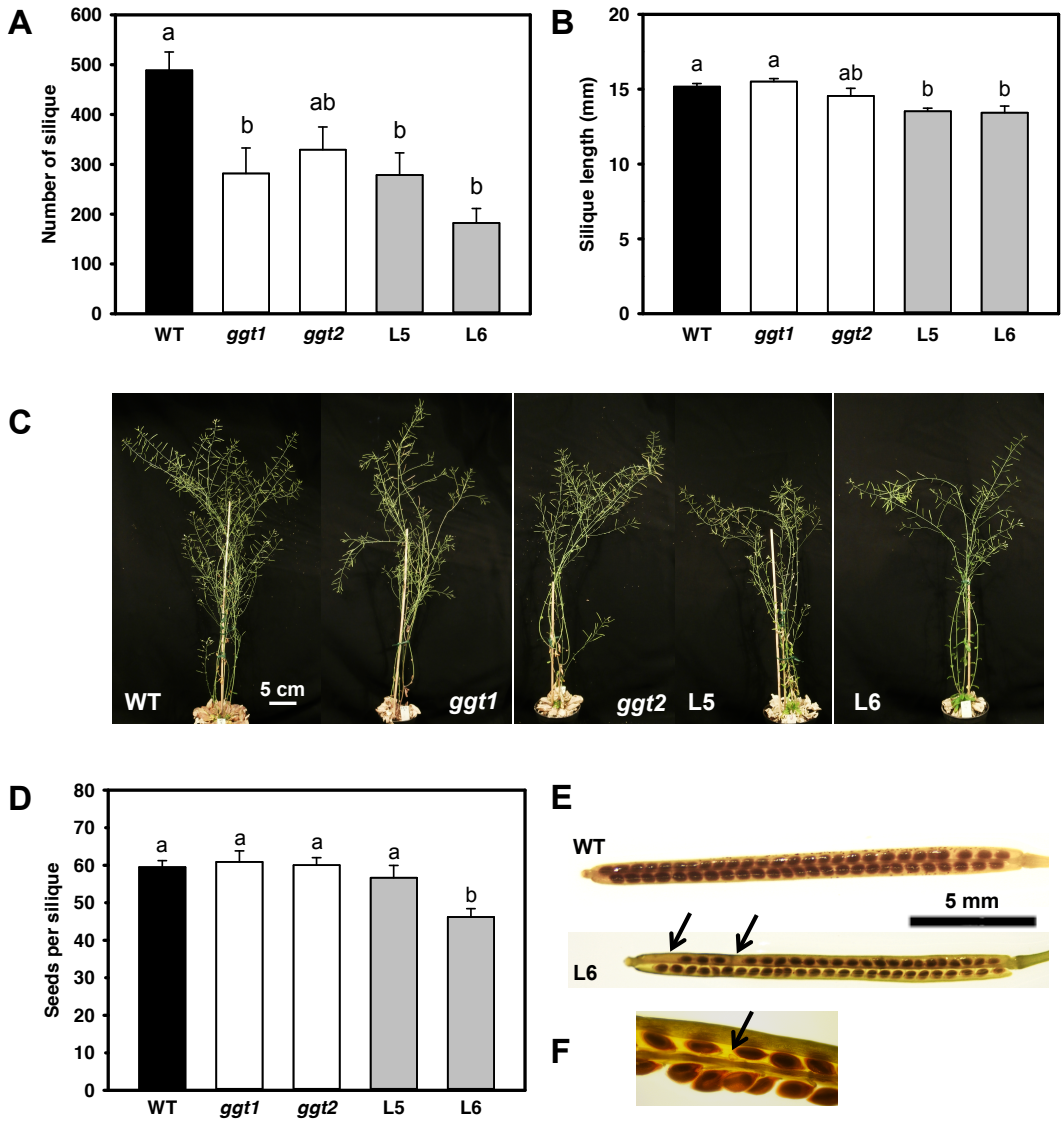

Fig. 12 Silique characterization of wild-type, *ggt1*, *ggt2*, L5 and L6
(A) Number of siliques per plants; (n ≥ 9 plants of n = 2 batches), (means ± SE). (B) Length of siliques was measured at least at 10 daf, from 3 different branches; (n ≥ 30 siliques on n = 5 plants), (means ± SE). (C) Pictures of siliques setting in wild type and *ggt* mutants plants. (D) Number of seeds counted in mature siliques cleared with 0.2 M of NaOH and 1% SDS solution; (n = 3 siliques on n ≥ 5 plants), (means ± SE). (E) Seed setting into wild type and L6 transparent silique. Arrows indicate empty spaces inside L6 silique. (F) The inner L6 silique magnification, arrow indicates aborted seed.

3.3.4 Germination rate

The quality of seed composition and its correct development influence the seed capability to germinate. Therefore germination rate analysis was performed on filter paper without any supplemental elements and the seeds were not sterilized to exclude any germination deficiency due to the sterilization process. Unexpectedly L6 showed the same trend of wild-type and almost the 90% of sowed seed germinated after 4 days. Even if *ggt1* showed a germination delay in the first day, it reached almost the same trend of wild-type after two days. In contrast *ggt2* and L5 showed different germination rate compared to wild-type and at the seventh day they had only 70% of total seeds germinated. Delay in germination was shown in *ggt2* from the second day, while L5 began immediately from the first day to have few seeds germinated. However only L5 trend resulted significantly different from the wild-type trend.

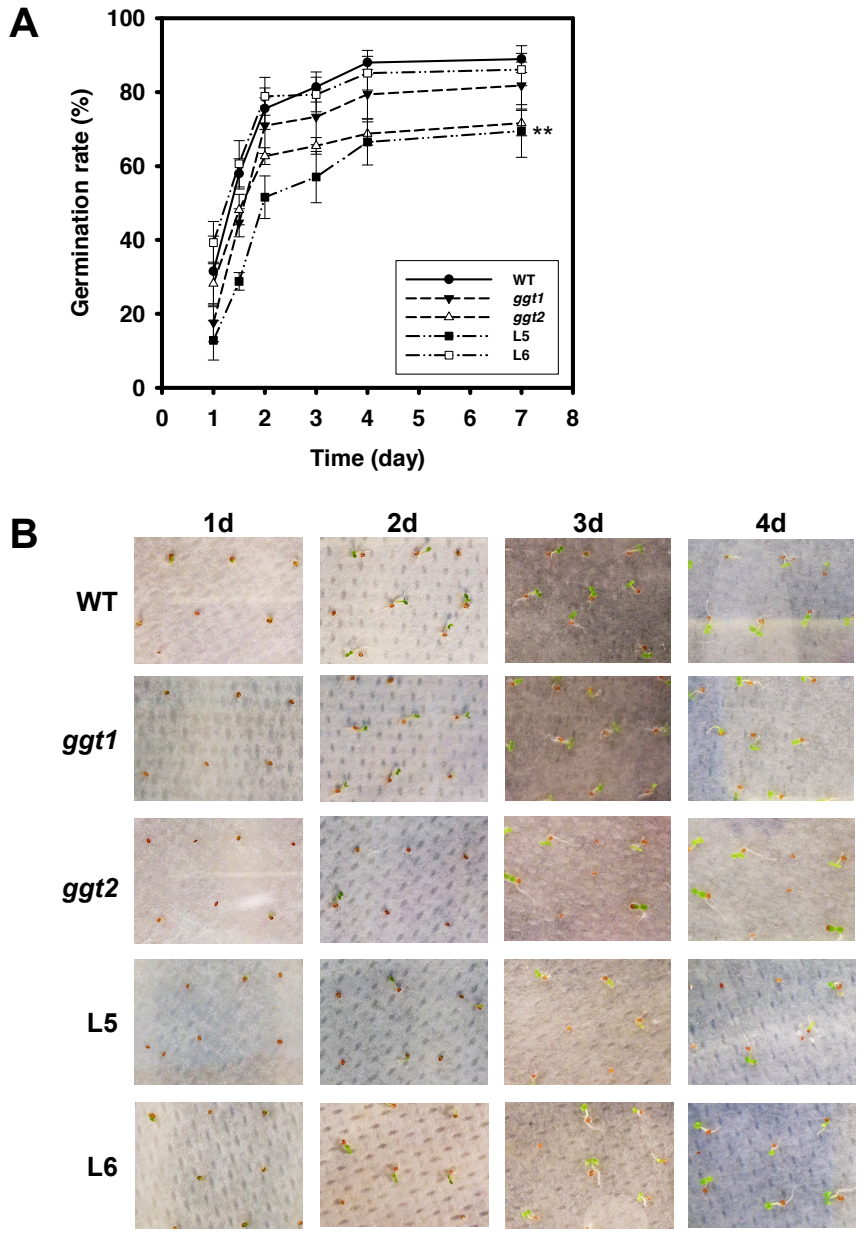

Fig. 13 Germination rate on filter paper
(A) Percentage of seed germinated of at least 50 seeds sowed of wild-type, *ggt1*, *ggt2*, L5 and L6. The number of seeds germinated was converted to a percentage of the total number of seeds sowed, which was assigned to 100; (n = 4), (means ± SD). (B) Pictures of seedlings from seed germinated documented on day 1, 2, 3 and 4 after plate transfer to growth chamber.

3.3.5 Seeds biochemical composition

In order to evaluate the impact of the *GGT*s mutation on the seed quality, the biochemical composition of dry seeds was analyzed. Firstly the total nitrogen, carbon and sulfur contents were quantified, but no significant changes were found between genotypes. Total soluble thiols, without discerning the reduced and the oxidative form, were derivatized with SBDF and separated by reverse

phase HPLC. Glutathione (GSH), cysteinyl-glycine (cys-gly), homocysteine (homocys) and cysteine (cys) were quantified. No changes were observed in all genotypes, only *ggt2* had a slight decrease in cysteine level compared to wild-type. Free amino acids were also determined thanks to the cooperation with the University of Heidelberg where the analysis was performed. The total level of free amino acids did not change between wild-type and the *GGT* mutants. However if we considered the single free amino acids, L5 showed some significant increases in non-polar amino acids: proline (2.6 fold), valine (2.1 fold); and in polar amino acids: glutamine (2.4 fold) and histidine (1.5 fold). Moreover, even if the value was not statistically significant, methionine showed a trend of increase in *ggt2*, L5 and L6 lines.

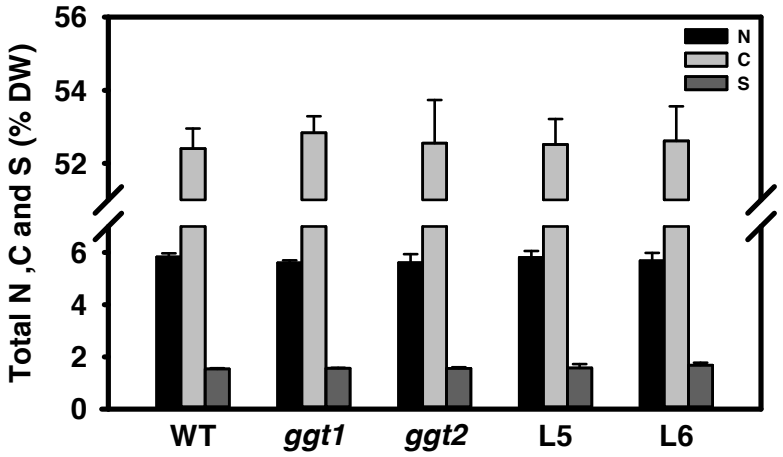

Fig. 14 Total content of nitrogen, carbon and sulfur in mature seed
Percentage of nitrogen (N), carbon (C) and sulfur (S) relative to the dry weight (DW) of seed of wild-type, *ggt1*, *ggt2*, L5 and L6. Two measurements from 10 and 30 mg of dry seed were performed. All the seed batches were from set of plants grown on soil (n = 5), (means ± SD).

Table 8 Thiols content in dry seeds of WT, *ggt1*, *ggt2*, L5 and L6
Levels of glutathione (GSH), cysteinyl-glycine (cys-gly), homocysteine (homocys) and cysteine (cys) nmol g^{-1} FW, from total cell extract derivatized and quantified by reverse phase HPLC (n = 5), (means ± SD).

Genotype	Cys	Homocys	Cysgly	GSH
WT	857.8 ± 187.8	18633.9 ± 1261.9	35.5 ± 7.5	640.6 ± 126.0
ggt1	922.6 ± 219.2	17978.7 ± 1148.4	31.6 ± 5.0	755.7 ± 136.2
ggt2	556.4 ± 122.1	18620.0 ± 1655.5	29.4 ± 2.9	610.0 ± 26.5
L5	858.7 ± 56.5	19414.4 ± 993.4	36.8 ± 8.2	740.9 ± 78.3
L6	1195.3 ± 29.0	19967.9 ± 2361.7	39.9 ± 7.4	825.5 ± 199.9

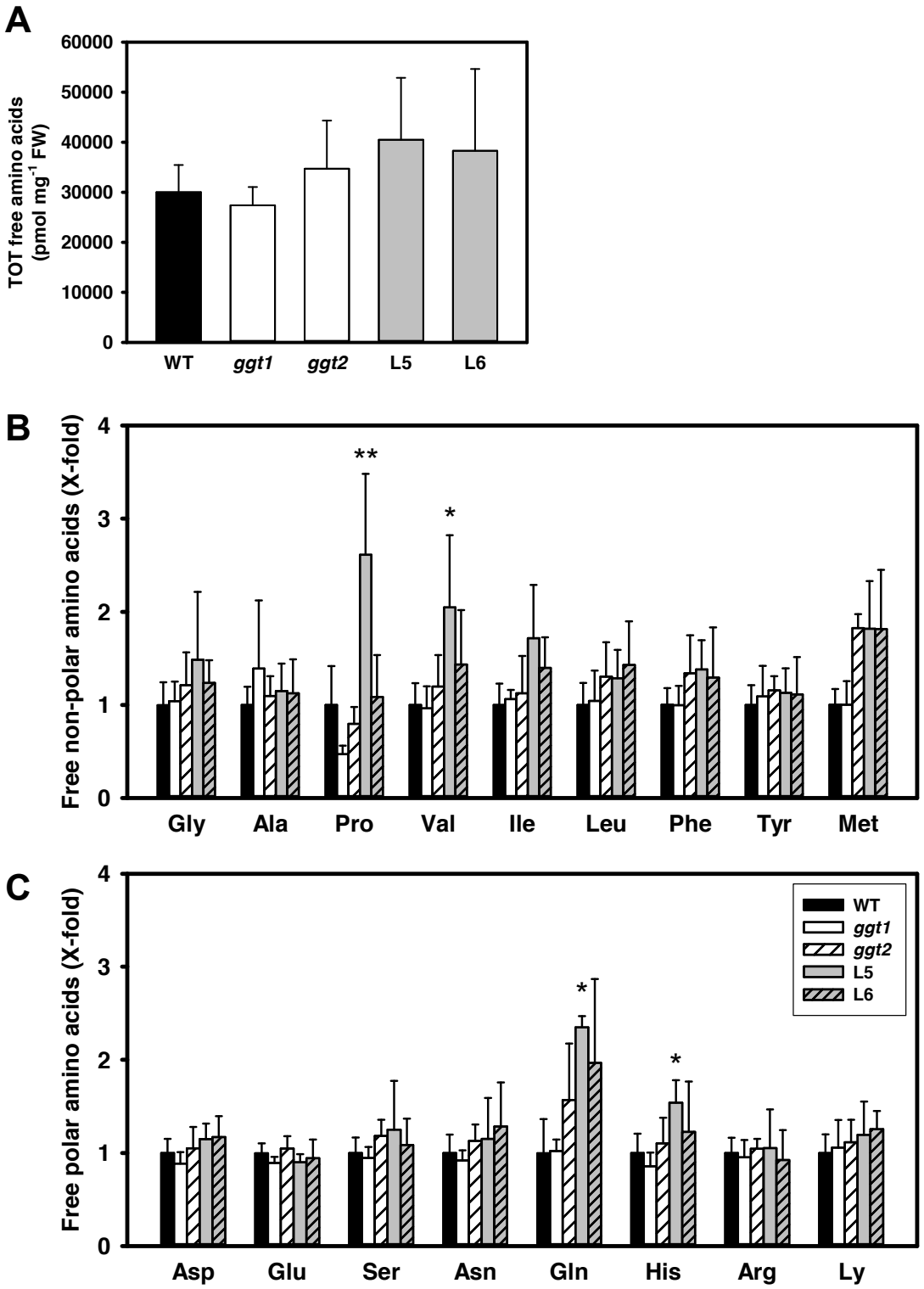

Fig. 15 Free amino acids composition of dry seeds of WT, *ggt1*, *ggt2*, L5 and L6
(A) Total free amino acids obtained by summing up the singular amino acids (n = 5), (means ± SD). (B) Non - polar and (C) polar free amino acids from 10 mg of dry seeds were determined by HPLC. The values were converted into x-fold of the concentration of wild-type, which was assigned to 1. Wild-type concentrations in pmol mg^{-1} FW: Gly=315.3, Ala=482.5, Pro=1860.1, Val=275, Ile=116.3, Leu=118.3, Phe=424.3, Tyr=73.5, Met=30, Asp=1192.4, Glu=2773.2, Ser=397.5, Asn=13368.4, Gln=1262.6, His=310.3, Arg=5741.1, Lys=415.9. The analysis was performed by Dr. Ilaria Forieri (University of Heidelberg).

3.3.6 Protein profile

To determine total protein profile of dry seed, protein extract was loaded and separated by electrophoresis in tricine gel, which was used to guarantee a good separation of the low molecular weight seed storage protein. The two bands in correspondence of 10-11 kDa and 6-7 kDa represented the family of 2S albumins, which are the main seed storage proteins with high sulfur amino acid composition. The band intensity was quantified from the digital image by using Image Lab™ Software (BioRad, 2.1.3) and normalized against the densitometry of the total lane. The protein profile was the same in all genotype and no significant changes were shown from the densitometry of the 2S albumins bands.

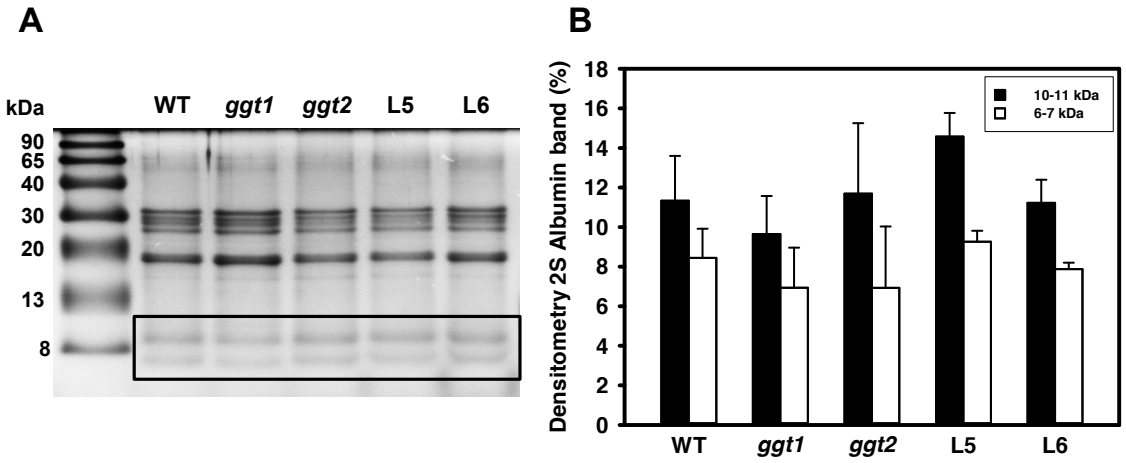

Fig. 16 Seed protein profile
(A) SDS-Tricine gel showing the band profile of protein seed extract of wild-type, *ggt1*, *ggt2*, L5 and L6. The square highlights the last two bands (10-11, 6-7 kDa) which correspond to 2S Albumin family proteins, from which (B) densitometry was performed in order to quantify the band intensity; (n = 4), (means ± SD).

3.3.7 Determination of *GGCT2;1* and *GGT4* transcripts in *ggt1* and *ggt2* seeds

The glutathione degradation involves not only GGT1 and GGT2 enzymes in the apoplast, but also GGCT2;1 in the cytosol and GGT4 in the vacuole. Therefore to investigate whether the expression level of these two genes changed when *ggt1* and *ggt2* were absent, *GGCT2;1* and *GGT4* transcripts were quantified in seeds by qRT-PCR. This expression analysis was conducted only in *ggt1* and *ggt2* seeds, before the double *ggt1/ggt2* RNAi lines were ready to be characterized. RNA was extracted from 100 mg of dry seeds by specifical method (2.3.5) and the level of

gene expression was quantified by qRT-PCR (2.3.8). In both mutants *GGCT2;1* expression (Fig. 17A) was strongly decreased, indeed it was almost ¼ of the wild-type expression. Also GGT4 transcripts (Fig. 17B) were found to be decreased in *ggt1* with just 26 % ± 11 of wild-type expression and in *ggt2*, even if almost twice more than *ggt1*, with 54% ± 5 of wild-type expression. Therefore glutathione degradation inside the cell seemed down-regulated when *ggt1* or *ggt2* were absent.

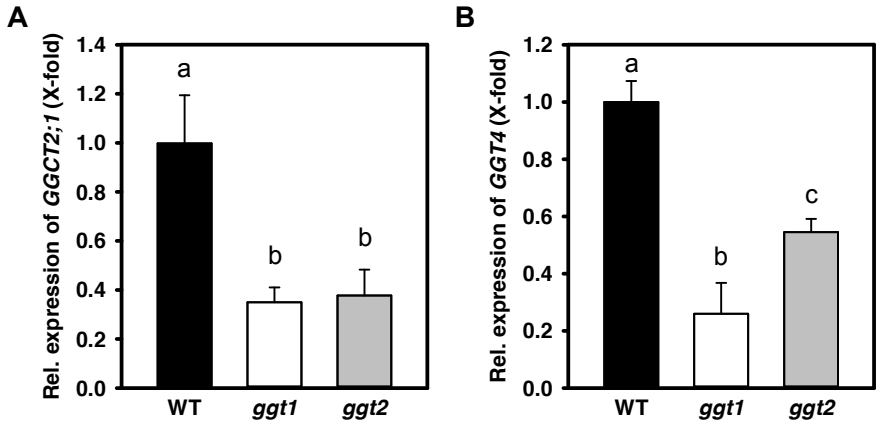

Fig. 17 *GGCT2;1* and *GGT4* relative expression in mature seed of WT, *ggt1* and *ggt2*
((A) Transcript level of *GGCT2;1* and (B) *GGT4* in mature seeds were determined by qRT-PCR using *PP2a* as reference genes. The level in wild-type was set to 1 and the other values are expressed as x-fold of it. Asterisks indicate the statistical significance difference relative to wild-type; (n = 4), (means ± SD).

3.4 Root biochemical and phenotypic characterization

3.4.1 Depletion of GSH from external solution

In previous studies (Ferretti et al., 2009; Destro et al., 2011) the depletion of GSH from external solution by Arabidopsis roots was performed. This analysis is based on the fact that GGT is localized in the apoplast that is readily accessed by the external solution where the root is immersed. Therefore we thought that the root capability to degrade glutathione by GGT activity would be interesting to investigate in *ggt* mutants. The degradation of glutathione (GSH) (Fig. 18A) and the releasing of cysteinyl-glycine (cys-gly) (Fig. 18B) by the GGT activity were measured at 0, 10, 20, 30 min and at 1, 3, 6, 8 h (2.5.3) in 7 – week – old hydroponically grown plants (2.2.5). In wild type glutathione decreased after 30 min – 1 h as well as the increase of cys-gly production. After almost 5 h the 50 %

of GSH was depleted and after 8 h just 20 % remained. Simultaneously cys-gly concentration increased 3 times more after 8 h. Wild-type root previously incubated with Serine-Borate (SerBor), a competitive inhibitor of GGT, was used as negative control. In this condition neither GSH decrease nor cys-gly releasing was detected, but there was rather GSH tendency to increase. The same incapability to degrade GSH was found in *ggt1*; indeed in the solution where *ggt1* was incubated, the initial concentration of GSH was maintained stable for all the 8 h. A slightly decrease of GSH was shown after 1 h in *ggt2* and simultaneously cys-gly was increased by 0.5% compared to the initial level. However after 3 h GSH concentration was stable at 85 – 90 % of the initial concentration and did not seem to decrease anymore. The trend of the two RNAi lines was unexpectedly in the middle between wild-type and *ggt2* trend. Somehow L5 and L6 root maintained the capability to degrade GSH to cys-gly even if in reduced level compared to wild-type.

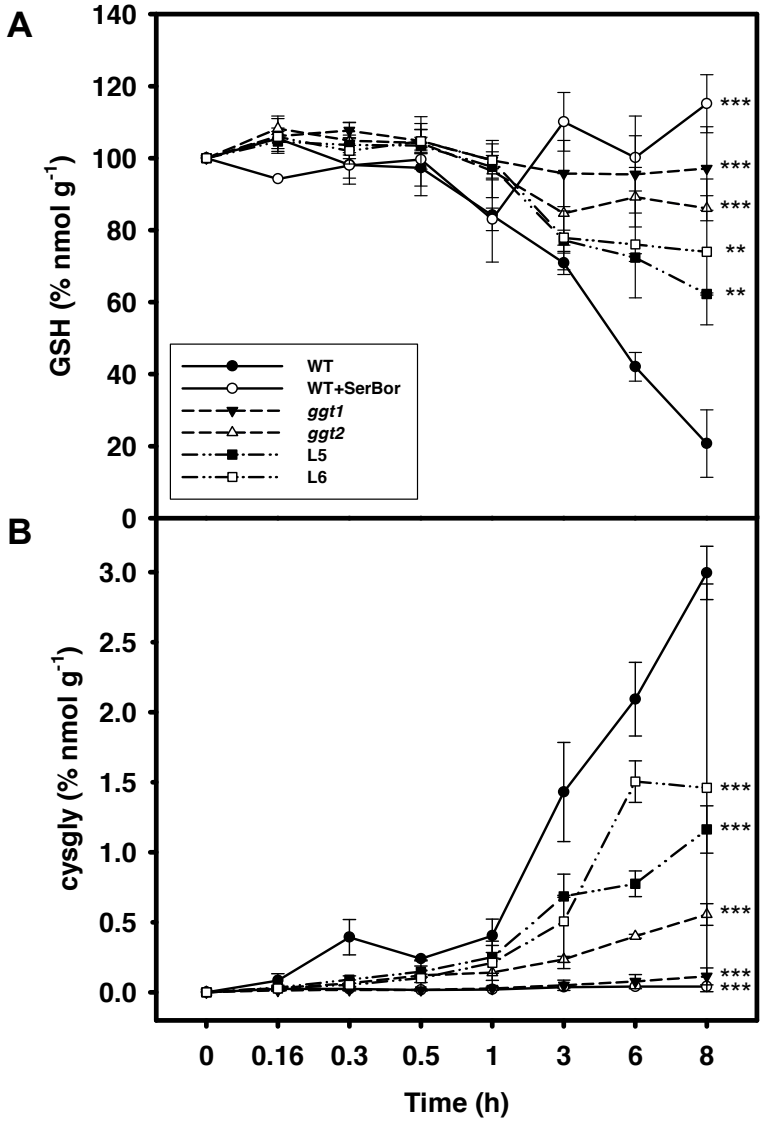

Fig. 18 Percentage of glutathione degradation and cys-gly releasing by root of wild-type, *ggt1*, *ggt2*, L5 and L6 plant
(A) GSH and (B) cys-gly levels (% nmol g^{-1}) at 0, 10, 20, 30 min and 1, 3, 6, 8 h measured in 100 µM GSH aqueous solution where root of 7 – week – old plant was incubated. The thiols were derivatized and separated by reverse phase HPLC (2.5.2). The t 0 was set to 100 for GSH and to 0.01 for cys-gly and the other values are expressed as percentage of them; (n=3), (means ± SD).

3.4.2 GGT activity *in vivo* and *in vitro* in root

In order to elucidate the capability of the different mutants to degrade glutathione from an external solution (3.4.1), the level of GGT activity in roots of 4 – week – old plants was measured *in vitro* (Fig. 19 black bar) and *in vivo* (Fig. 19 white bar). The total GGT activity was measured *in vitro* (2.4.5.1) following the same protocols used for seeds (3.3.1). Strong decrease of GGT activity was shown

in *ggt1,* which had just the 10% activity of the wild type left, whereas *ggt2* had the same level of the wild-type activity and L5 and L6 maintain the 75 % of the wild type. GGT activity *in vivo* was assayed in Arabidopsis root according to the works of Ferretti and Destro (Ferretti et al., 2009; Destro et al., 2011). The experiment is an adaptation of the *in vitro* assay and consists in circulating the reaction solution from the test tube, where the roots are immersed, to the cuvette placed into the spectrophotometer (2.4.5.2). In this method it is assumed that the external solution is *in continuum* compartment with the apoplast, therefore the GGT activity measured was only apoplastic from GGT1 and GGT2 isoforms. Indeed the activity detected in wild-type (47.7 nmol min $^{-1}$ g^{-1} ± 11.5) was lower compared to the activity measured *in vitro* (102.7 nmol min $^{-1}$ g^{-1} ± 17.6). This gap could be due to GGT4, which is also expressed in roots and was included in the total GGT activity detected *in vitro*. Also for *ggt2* (45.4 nmol min $^{-1}$ g^{-1} ± 6), L5 (35.5 nmol min $^{-1}$ g^{-1} ± 6.1) and L6 (42.3 nmol min $^{-1}$ g^{-1} ± 8.6) the activity was almost the half of the level measured *in vitro* (*ggt2* = 94.6 nmol min $^{-1}$ g^{-1} ± 8.5; L5 = 75.7 nmol min $^{-1}$ g^{-1} ± 3.7; L6 = 76.2 nmol min $^{-1}$ g^{-1} ± 4.8). However in *ggt1* the level detected *in vivo* (10.8 nmol min $^{-1}$ g^{-1} ± 1.3) was the same compared to the level measured *in vitro* (11.6 nmol min $^{-1}$ g^{-1} ± 2.3), and showed a strong reduction of the activity level, whereas no significant changes were shown in *ggt2*, L5 and L6 compared to wild-type.

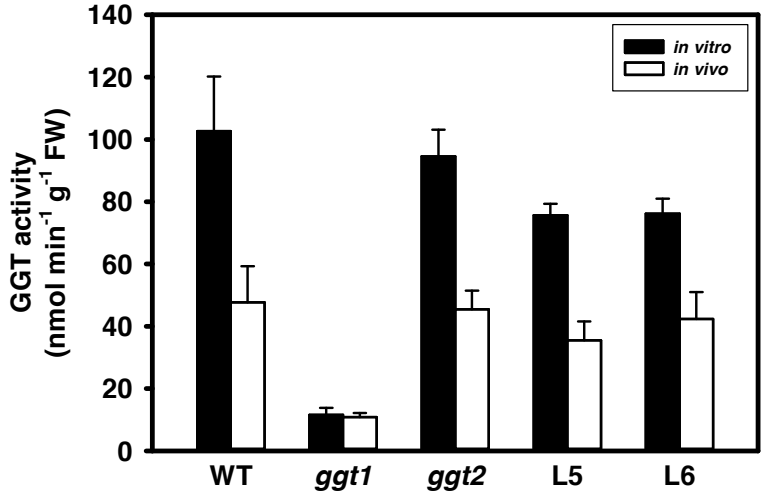

Fig. 19 GGT activity in root of wild-type, *ggt1*, *ggt2*, L5 and L6
Level of GGT activity (nmol min^{-1} g^{-1} FW) measured *in vitro* (black) and *in vivo* (white) spectrophotometrically, from poll of root of 4 – week – old plant grown in petri dishes; (n = 5), (means ± SD).

3.4.3 GST activity in root

In proteomic study the up-regulation of four glutathione S-transferases (GSTs) in *ggt1* leaves was shown(Tolin et al., 2013). Therefore to investigate if the same difference was present in roots, the total GST activity was measured in wild-type and *ggt* mutants. In all the four lines the GST activities were comparable to wild-type (39.5 nmol min $^{-1}$ mg^{-1} ± 6.4): *ggt1* (40.3 nmol min $^{-1}$ mg^{-1} ± 11.1), *ggt2* (35.1 nmol min $^{-1}$ mg^{-1} ± 9.3), L5 (37.1 nmol min $^{-1}$ mg^{-1} ± 8.9), L6 (37.5 nmol min $^{-1}$ mg^{-1} ± 6.4).

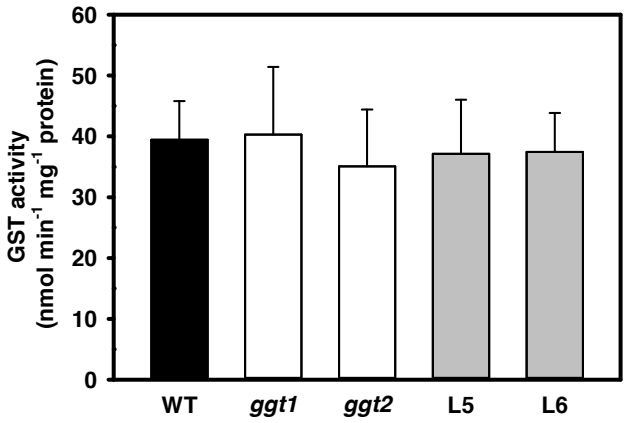

Fig. 20 GST activity in root of wild-type, *ggt1*, *ggt2*, L5 and L6
Level of GST activity (nmol min $^{-1}$ mg^{-1} of protein) measured *in vitro* spectrophotometrically, from pool of roots of 4 – week – old plant grown in petri dishes; (n = 5), (means ± SD).

3.4.4 Root morphological and growth characterization

In order to elucidate if the root growth and its structure were modified in the mutants, a morphological and growth characterization was conducted in roots of plants cultivated in Petri plate (2.2.4). The root growth was monitored twice a week for 4 weeks by image scanning and several root parameters were elaborated by winrhizo software (2.1.3). For root length and area a growth curve was drawn (Fig. 21). Only the length trend of L5 resulted significantly lower than wild-type, while all the other lines were like wild-type. No significant differences were shown in root area between the different lines even if after 4 weeks there was a tendency for *ggt1* (6.1 cm^2 ± 0.9) and L5 (6.2 cm^2 ± 0.7) to have a lower area compared to wild-type (7.9 cm^2 ± 0.2). Also the number of tips and forks, the root

diameter and the ratio length to fork showed that there were not significant changes in root structure between lines.

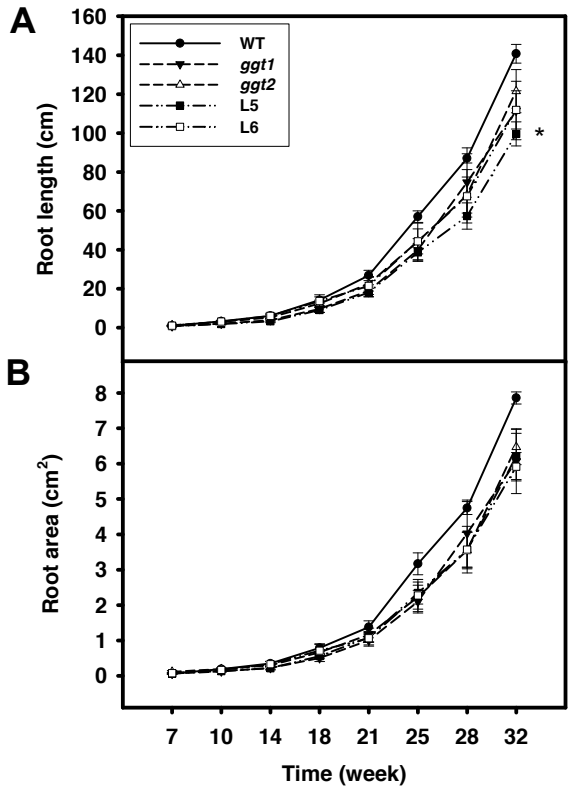

Fig. 21 Root growth curves
(A) Growth rate of root length (cm) and (B) area (cm^2) monitored from 7 to 32 days after sowing of wild-type, *ggt1*, *ggt2*, L5 and L6 plants. Plants were grown on ½ MS media in Petri dishes; (n = 6 plants, n = 5 plates), (means ± SE).

Table 9 Root structure parameters
Number of tips (n), forks (n), length/fork ratio (cm/n) and diameter (mm) of root of 18 – day – old plants of wild-type, *ggt1*, *ggt2*, L5 and L6. Plants were grown on ½ MS media in Petri dishes; (n = 6 plants, n = 5 plates), (means ± SE).

Genotype	Tip	Fork	Lenght/Fork	Diameter
WT	27.88 ± 5.69	27.88 ± 6.08	0.42 ± 0.15	0.18 ± 0.01
ggt1	16.40 ± 1.90	14.30 ± 3.01	0.55 ± 0.16	0.16 ± 0.01
ggt2	25.01 ± 3.96	17.37 ± 2.83	0.65 ± 0.17	0.17 ± 0.02
L5	21.42 ± 3.59	20.12 ± 3.26	0.39 ± 0.11	0.20 ± 0.02
L6	19.63 ± 5.39	16.25 ± 3.77	0.87 ± 0.16	0.17 ± 0.01

3.5 Phenotypic characterization in vegetative tissues

Vegetative tissues were also characterized in order to investigate the presence of some impairment in plant growth and leaf composition in the RNAi lines.

3.5.1 Rosette growth

Rosette growth was documented weekly from plants grown in short day condition (2.2.2) by measuring the rosette diameter (2.2.6). After 5 weeks *ggt2*, L5 and L6 showed slight smaller rosette compared to wild-type, but afterwards first *ggt2,* at the ninth week, and then L5, at the eleventh week, reached the same diameter of the wild-type. L6 instead maintained a significant slower rosette growth rate than wild-type, with almost one week of delay in vegetative growth.

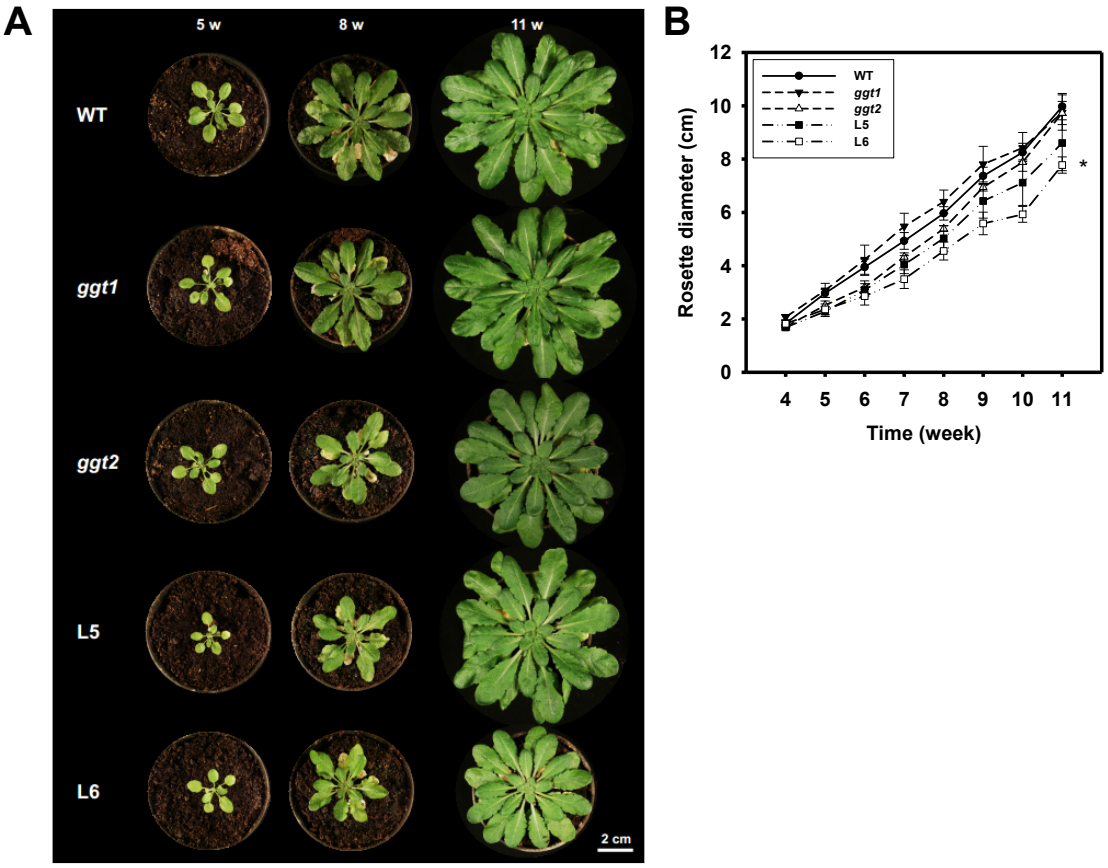

Fig. 22 Rosette growth phenotype
(A) Rosettes pictures of wild type, *ggt1*, *ggt2*, L5 and L6 were taken after 5, 8 and 11 weeks. (B) Growth rate of rosette diameter (cm) of plants grown in short day condition (2.2.2). The diameter was measured 3 times every week till the eleven weeks after sowing; (n = 5), (means ± SE).

3.5.2 Trichomes

Trichomes are the small, fine hair present on the surface of plant leaves and as it was reported (Gutiérrez-Alcalá et al., 2000; Wienkoop et al., 2004; Frerigmann et al., 2012) they have high glutathione content which is supposed to be related with detoxification processes and defense responses. Moreover GUS expression under control of GGT1 and GGT2 promoter in immature trichomes was shown(Martin et al., 2007). Taking these evidences into account, the number of trichome of the different *ggt* mutant lines was considered interesting to investigate. Trichomes were counted from the first two leaves when trichomes initiation started at the time when the leaves have the same dimension. The lines with significant decrease in the number of trichomes were *ggt2*, L5, L6; wild-type had in average 23.1 ± 0.7, *ggt1* 20.4 ± 0.7, *ggt2* 18.4 ± 0.5, L5 17.5 ± 0.9, L6 19 ± 0.9 trichomes per leaf.

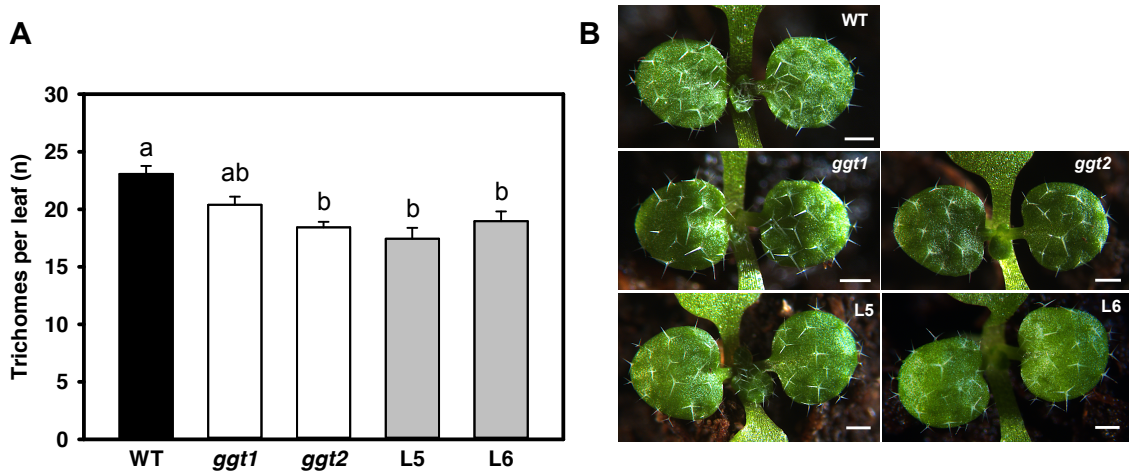

Fig. 23 Trichomes in first true leaves
(A) Number of trichomes per leaf counted from the first true leaves of wild-type, *ggt1*, *ggt2*, L5 and L6 plants; (n = 2 leaves, n ≥ 10), (means ± SE). (B) First true leaves of 2 – weeks – old plants grown in short day condition; (bars = 0.5 mm).

3.5.3 Metabolites: thiols, ascorbate

In order to quantify the level of the main antioxidants, total thiols and ascorbate were measured in leaves. Total glutathione, cysteinyl-glycine, homocysteine, cysteine were determined from total cell extract and no significant changes were shown between mutants, even if cys-gly was slightly decreased in *ggt1* and L5

compared to wild-type. Similarly the level of ascorbate was the same in all genotypes.

Table 10 Thiols and ascorbate levels in leaves of wild-type, *ggt1*, *ggt2*, L5 and L6
Levels of glutathione (GSH), cysteinyl-glycine (cys-gly), homocysteine (homocys) and cysteine (cys) (nmol g^{-1} FW), from total cell extract derivatized and quantified by reverse phase HPLC. In the last column level of total ascorbate determined spectrophotometrically (µmol g^{-1} FW); (n = 7), (means ± SD).

Genotype	Cys	Homocys	Cysgly	GSH	Ascorbate
WT	90.2 ± 14.0	490.1 ± 46.9	2.4 ± 0.4	147.9 ± 21.0	2.2 ± 0.3
ggt1	106.7 ± 15.7	593.2 ± 78.9	1.8 ± 0.4	159.8 ± 28.0	2.6 ± 0.2
ggt2	107.4 ± 12.6	444.6 ± 33.9	2.5 ± 0.3	143.9 ± 19.5	2.3 ± 0.2
L5	101.2 ± 14.8	418.5 ± 104.3	1.8 ± 0.4	145.3 ± 27.0	2.5 ± 0.3
L6	102.9 ± 9.90	544.2 ± 219.1	2.8 ± 0.7	144.7 ± 26.6	2.6 ± 0.6

3.6 Double mutants using *ggt1*, *ggt2*, *sir1-1*, *ggct2;1*

New crossbreeding were obtained, involving *ggt1* and *ggt2* with *sir1-1* and *ggct2;1,* two mutants related to the key genes of sulfur assimilation and glutathione degradation. The knockdown mutant *sir1-1* is relative to sulfite reductase (SiR), the enzyme responsible of the sulfite reduction to sulfide in the sulfur assimilation pathway. SiR has a key role in the regulation and control of sulfur assimilation and flux as a bottleneck function in the assimilatory reduction pathway (Khan et al., 2010). Moreover proteomic analyses in *sir1-1* seeds revealed that the storage proteins were the most affected category, with strong decrease in 2S albumin (Allboje Samami, 2011). In addition to GGT, another enzyme able to degrade glutathione exists in the cytosol and it is called GGCT. This enzyme degrades glutathione in its singular amino acids in different manner than GGT (Ohkama-Ohtsu et al., 2008; Paulose et al., 2013). However GGCT and GGT1 share the same expression pattern (Paulose et al., 2013). Taken into account these evidences, the influence of reduced sulfur flux on plants already affected by impaired glutathione degradation was considered interesting to investigate. To this purpose, *ggt* mutants were crossed with *sir1-1* or with *ggtc2;1*

mutant lines to generate double mutants. In addition the double mutants with both apoplastic (*ggt1* and *ggt2*) and cytosolic (*ggct2;1*) glutathione degradation pathway knocked out could help defining better their respective role in plant cell. The mutant lines *sir1-1* and *ggct2;1* were provided by the research group of Prof. Hell of the University of Heidelberg, where the crossings were performed. The procedure and the combination of the breeding were explained in the paragraph 2.2.9. Seeds of F2 from all the five combination of crossed plants were obtained and screened by sowing in selective media. The survived seedling were isolated and subsequently genotyped by PCR, except for *ggct2;1/ggt2* mutant because no seedling survived in selective media and most of the seeds did not germinate. The individuals with the mutation in homozygosis for both genes were found for all the combinations and the relative plants were collected and maintained for seed propagation. Preliminary phenotypic observation showed that all the double mutants in combination with *sir1-1* inherited the impairment in vegetative growth and the delay to start flowering typical of *sir1-1*. Indeed the rosette diameter was significantly smaller than wild-type. This mean that neither the absence of *GGT1* nor of *GGCT2;1* could rescue the *sir1-1* phenotype. Differently the double mutant *ggt1/ggct2;1* did not show any difference of growth profile compared to wild-type. Further phenotypic characterization would be necessary to elucidate in detail the differences between double mutants and wild-type and the relative single mutants from which they derived.

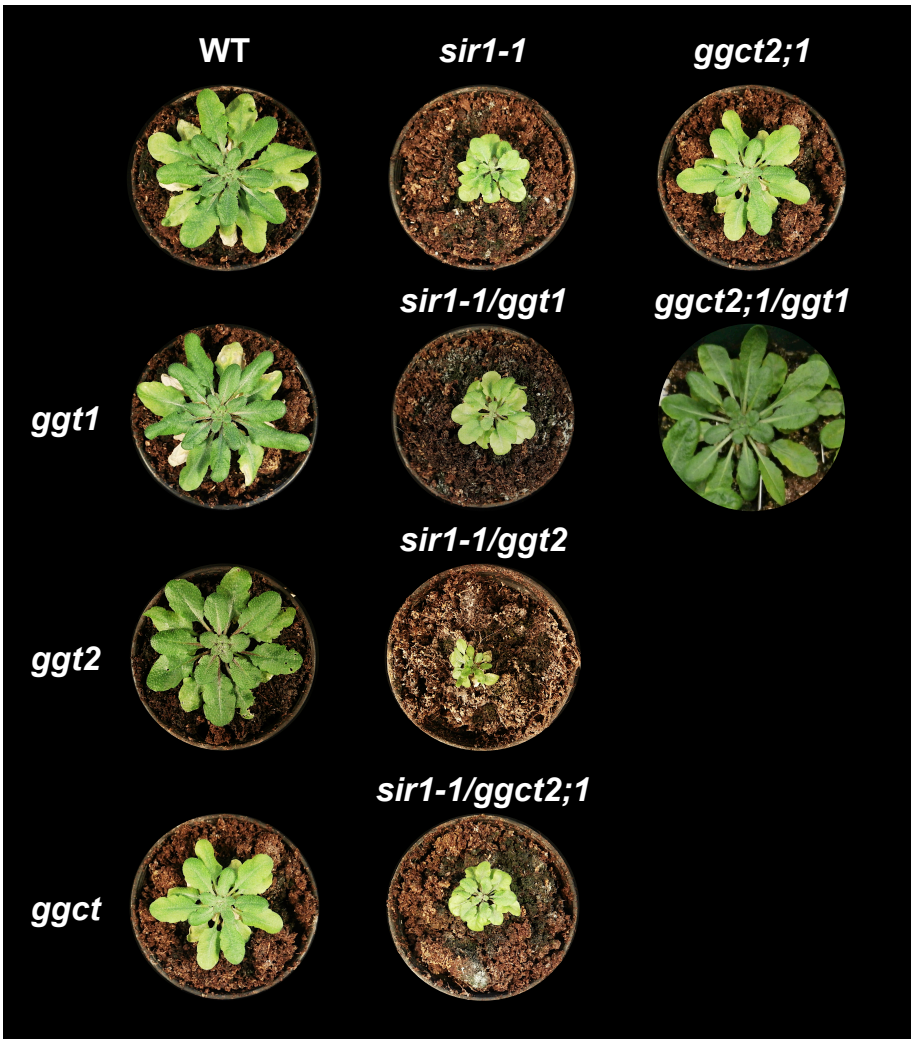

Fig. 24 Rosette comparison between single and relative double mutants
Rosette pictures of the single mutants *ggt1*, *ggt2*, *ggct2;1*, *sir1-1* and the relative combination of double mutants *sir1-1/ggt1*, *sir1-1/ggt2*, *sir1-1/ggct2;1* and *ggct2;1/ggt1*. Plants were grown in growth chamber, and the pictures were taken 7 weeks after sowing.

4 Discussion

The silencing of both GGT1 and GGT2 is a functional genetic approach useful to add new clues on the role of apoplastic GGT, leaving out any compensatory effect between the two isoforms. In this work the affections provoked by the silencing were investigated in several plant organs and compared to wild-type and the relative knock out single mutants.

4.1 GGT and seed development

Glutathione is the main source of reduced sulfur circulating in the phloem and is one of the most important redox regulators. Seeds are par excellence sink organs with high nutrient demand and during development undergo a complex scenario. Previous studies proposed GGT as responsible of GSH unloading from phloem to sink tissues (Ohkama-Ohtsu et al., 2007a), therefore we were interested in investigating whether the double silencing of GGT1 and GGT2 affects seed production and composition. Seed is one of the few organs where both GGT1 and GGT2 are expressed. However detection of GGT1 and 2 transcripts in mature seed and siliques are at limit of detection by using qRT-PCR as it was observed in this study (data not shown) and in others (Destro et al., 2011). Expression analyses by consulting Genevestigator and eFP Browser showed that GGT1 and GGT2 are restricted to specific small anatomical part of the seed and in narrow time interval of development (Fig. 8, Fig. 9). However, the measurement of total GGT activity (3.3.1) *in vitro* allows to have an idea of the single isoforms contribution. The high GGT activity remained in *ggt2* mature seed seems to indicate that this isoform is a secondary protagonist in this stage, whereas in *ggt1* just half of activity was maintained (Fig. 10A). However the remaining 50 % of wild-type activity detected in green seeds of both mutants (Martin et al., 2007) suggests that GGT2 participates during the seed development rather at the mature stage. Indeed large part of total expression of GGT2 in seed is ascribed to the suspensor that disappears completely at the mature stage, whereas GGT1 in this stage is still highly expressed at the chalazal coat (Fig. 8). It is important not to forget that GGT4 contributes to the total activity, explaining the residual activity remained in double *ggt1/ggt2* RNAi (Fig. 10A). However in L5 the GGT activity is resulted less than in the single mutants. However it is not excluded that a little percentage of

GGT1 activity might be still present in *ggt1/ggt2* RNAi since the relative transcript was not completely knocked down, especially in L6 (Fig. 7A). This was shown also by histochemical GGT activity localization where the reddish product deposition decreased in *ggt1/ggt2* RNAi compared to wild-type and did not disappear completely (Fig. 10B).

The silencing of GGT1 and GGT2 in *ggt1/ggt2* RNAi mutants showed less seed yield (Fig. 11A) as a consequence of less siliques production (Fig. 12A) and short silique length (Fig. 12B). Decrease of seed yield was also shown in the single mutants, but not so strong to be statistically different than wild-type, indicating that only when both GGT1 and GGT2 are silenced severe deficiency emerges. Seed composition seemed not compromised; sulfur, nitrogen and carbon content were equal in all lines (Fig. 14), no changes were found in the amount of total free amino acids (Fig. 15A) and seed storage proteins (Fig. 16). It appears that the plant strategy to cope with the mutation is to develop less seeds but with good composition. In any mutant lines the fertility was not compromised, pollen resulted viable (Fig. 11E), suggesting that the problem was restricted within the time of seed development.

All these evidences suggest certain impairment in seed development that could be due to nutritional deficiency or to sort of inability in development progression.

4.1.1 GTT leads cys to the seed

One of the several roles that have been proposed for GGT is the delivery of cysteine to the seeds by GSH degradation. This hypothesis is based on the fact that GSH is considered one of the most important storage molecules of reduced sulfur. No mechanism has been found yet that lead GSH unloading to the seeds and GGT may represent a good candidate to accomplish this role (Ohkama-Ohtsu et al., 2007a). GSH has been found in the phloem sap (Kuzuhara et al., 2000) and intense GSH-MCB labeling was detected in the funiculus and in the chalazal seed coat at which the funiculus is attached; it has been observed also in the seed outer integument, but very weak in the inner integument and absent in the endosperm, whereas in the developing embryo is labeled (Cairns et al., 2006). All these evidences indicate that intact GSH reaches the seed at the level of the interface between outer and inner integument then it is broken down. This is compatible with the observation of Stadler et al. (Stadler et al., 2005) who describes the

existence of a symplastic way that covers the entire outer integument but not the inner integument or the endosperm, therefore the only possibility to cross these last two regions is through the apoplast. GGT is the only enzyme able to degrade glutathione in the apoplast and in particular *GGT1* is expressed in the integument during the early stage of seed development as the eFP results (Fig. 8A) and the histochemical localization of GGT activity showed (Fig. 10B), hence GGT could be directly involved in cysteine translocation to the endosperm by GSH degradation. The possible involvement of glutathione transporter (Zhang et al., 2015) seems to be excluded by the fact that GSH labeling ended to the outer integument. Moreover the *GGT2* expression in the suspensor and in the adjacent micropylar endosperm during the early stages when suspensor is connect to the embryo (Fig. 8B), suggests that GGT2 could participate in glutathione translocation between endosperm and suspensor since their cells are not simplastically connected. Previous study has evidenced that glutathione biosynthesis within the embryo is fundamental since loss of the first enzyme (GSH1) in the biosynthetic pathway confers embryo-lethal phenotype. While *gsh1* homozygote mutation is lethal, *gsh1* heterozygote seed is able to cover the early stages of development but it dies later, between heart and torpedo stage (Cairns et al., 2006). This suggests that the GSH received from the maternal plant is important support during the earlier stages of seed development that corresponds to the time of *GGT* expression (Fig. 8). However the amount of cysteine, glutathione and thiols in general were not changed in *ggt1/ggt2* RNAi mature seeds (Table 8), suggesting that GGT is not essential to provide cysteine through glutathione degradation. Indeed sulfate (Tabe and Droux, 2001) and S-methyl methionine (Tan et al., 2010) are other possible source of sulfur that can reach the seed by phloem. In facts, even if not statistically significant, the level of free methionine in *ggt2* and in *ggt1/ggt2* RNAi mutants tends to increase (Fig. 15B), suggesting that this amino acid might be a possible integration of sulfur from phloem. Moreover, it has been demonstrated that developing cotyledon of lupin seed is able to reduce sulfate and performs all the steps for cysteine biosynthesis (Tabe and Droux, 2001). However, during seed development high level of nutrients are required and independent cysteine biosynthesis is not sufficient to satisfy completely the seed necessities. During leaf senescence, salvage of nutrients occurs and nutrients are targeted to seeds by long distance transport through the phloem, indeed in

Arabidopsis leaves a consistent decrease in the level of S (66.6 %) has been seen during their senescence (Himelblau and Amasino, 2001). The premature yellowing of *ggt1* leaves noticed by different research groups (Martin et al., 2007; Ohkama-Ohtsu et al., 2007a) and in *ggt1/ggt2* RNAi mutants observed in this thesis work (data not shown), might be due to the urgency to mobilize in advance the nutrient and in particular sulfate, because these mutants have a deficiency in the degradation of GSH. Therefore GSH could help to integrate the elevated seed demand, indeed in *sult3;4* mutant seeds, where the capacity to assimilate sulfate is reduced, over accumulation of a membrane Ala peptidase that degrades cysteinyl-glycine is found (Zuber et al., 2010). This indicates that the product of degradation of GSH by GGT (cys-gly) is used as sulfur source when sulfate transport to the seed is reduced.

In summary *ggt1/ggt2* RNAi mutants generate the quantity of seed that are sure to sustain completely then induce a metabolic readjustments leading to allocate the resources to less, but fully viable seeds. Finally this mutants results to have low seed yield.

However no changes in thiols content in whole seed (Table 8) does not exclude that changes in the apoplastic spaces occurred. It is known that glutathione in apoplast is just 1-2% of the total cellular pool in leaf (Foyer et al., 2001; Ohkama-Ohtsu et al., 2007a; Tolin et al., 2013), therefore it is not possible to recognize minimal differences occurring in apoplast from total cellular extract. Further experiments will be addressed to quantify thiols from extracellular fluid in *ggt1/ggt2* RNAi mutants.

4.1.2 GGT as ROS modulator in seed development

On the other hand the reduced silique length, the empty space (Fig. 12E) and aborted seeds observed in L6 (Fig. 12F), and to a lesser extent in L5 siliques could suggest a sort of impairment in the mechanism that regulates seed development. Many pathway and regulatory mechanisms operate in concert to coordinate the sophisticated development of all seed regions and subregions. Glutathione biosynthesis within the embryo is essential for embryo development and seed maturation (Cairns et al., 2006) and glutathione reductase mutant is embryo lethal with development arrest at early stages (Tzafrir et al., 2004). These evidences emphasize the importance that glutathione metabolism and redox

homeostasis assumes for embryo development. In addition several evidences have highlighted the relevance of ROS signaling generated in the apoplast during embryogenesis (Western et al., 2000; Bozhkov et al., 2005; Bailly et al., 2008); ROS tight modulation and spatial regulation of their production result in different messages for the cell, which could be transduced through H_2O_2 or perceived by several classes of receptor-like protein kinases with cysteine-rich extracellular domains (CRKs) (Shiu and Bleecker, 2003; Wrzaczek et al., 2010). GGT could be an additional ROS regulatory element induced by the cell to modulate ROS signaling by glutathione degradation in the apoplast. Indeed there are many evidences, both in plant and in animal, that suggest such a contribute of GGT in redox sensing (Paolicchi et al., 2002; Masi et al., 2015; Trentin et al., 2015).

GGT2 in the suspensor evocates particular attention, because here it reaches the major level of expression as ever seen in other organs (Fig. 9B). Suspensor contribution in embryogenesis is limited and after the heart stage suspensor undergoes progressive degeneration and finally at the mature stage it disappears. Programmed cell death has been found crucial for suspensor degeneration (Yeung and Meinke, 1993). GGT2 is mainly expressed at the globular stage before suspensor degenerates. In animals, GGT pro-oxidant role has been suggested, in order to maintain continue H_2O_2 production which acts as a sort of survival message that supports proliferation and prevents apoptosis (Del Bello et al., 1999). The same mechanism might happen in the suspensor: when GGT2 is expressed at the globular stage, the development is sustained; at the heart stage when GGT2 lacks, the system cracks toward the PCD. This hypothesis is in line also for the seed coat where GGT1 is expressed in the pre-globular stage (Fig. 8A), and it is known that differentiation in this subregion involves a highly regulated series of events in the apoplast that might be coordinated by ROS (Western et al., 2000). Indeed PCD occurs very early for two inner integument cell layers (Nakaune et al., 2005) and by maturity all seed coat cells are dead (Haughn and Chaudhury, 2005). However to support this hypothesis the verification of the integrity of suspensor and the seed coat in *ggt* mutants is necessary.

On the other hand, cell wall remodeling has been shown to be related with GGT. Previous study in *ggt1* leaves proteome reported that several proteins involved in

this process were downregulated (Trentin et al., 2015). Cell wall and membrane structures characterize both suspensor and seed coat: cell-wall ingrowths, haustorial outgrowths, numerous plasmodesmata enhance the suspensor ability to transfer molecules (Kawashima and Goldberg, 2010); whereas cell wall thickening and secretion of mucilage occur during seed coat differentiation (Western et al., 2000). These evidences are in line with the localization of both *GGT1* and *GGT2* expression (Fig. 8, Fig. 9) suggesting their involvement in cell wall remodeling during seed development.

4.1.3 Oxidative stress in seed and germination

Free amino acids profile in mature seed evidenced that L5 accumulates consistent level of proline (Pro) (Fig. 15B). Proline accumulation has been reported as a marker of stress in plant, numerous reviews have assumed that accumulation of proline in stressed plants has a beneficial effect (Kishor et al., 2005; Szabados and Savouré, 2010; Verslues and Sharma, 2010). In particular accumulation of proline has been shown in drought stress and in tissue with low water content (Schwacke et al., 1999), where it works as osmolyte that recruits water or metabolites acting as protection. High level of proline has been found also in reproductive tissue to sustain metabolically the high energy demand (Mattioli et al., 2009). Moreover proline biosynthesis is coupled with the pentose phosphate pathway. Proline biosynthesis generates high level of $NADP^+$ that is needed to support the oxidative pentose phosphate pathway to regenerate NADPH, on the other hand proline catabolism releases NADPH that is further used for antioxidant reactions. Hence this metabolic cycle of proline can be modulated as a sort of redox buffering (Kishor et al., 2005). Not only proline was shown enhanced in L5, but also glutamine (Gln) and histidine (His) (Fig. 15C). Both these two amino acids are interdependent with the proline pathway: proline is recycled in glutamate (Glu), which is converted in glutamine and finally histidine is biosynthesized by using both glutamate and glutamine. In particular proline and glutamine are strictly connected, indeed mutant deficient in glutamine synthesis have reduced proline level (Díaz et al., 2010) and glutamine level changes in parallel with proline's one while the intermediate glutamate remains unchanged due to its rapid turn over (Brugiere et al., 1999). All these evidences suggest that L5 accumulate proline and glutamine as a response to overcome such

a stress. However L6 did not exhibit the same accumulation of free amino acids shown in L5. The higher level of GGT activity present in L6 seed (Fig. 10A) than L5, might be sufficient to not affect the amino acids profile.

In addition L5, together with *ggt2*, showed low germination rate (Fig. 13A). It is largely known that an increase of ROS cellular level and protein oxidation occurs during seed maturation and germination (Job et al., 2005). There is a defined "oxidative window" within ROS acting as signaling molecule and beyond it ROS exceed leading to oxidative stress, damages and germination inhibition (Bailly et al., 2008). To overcome an uncontrolled ROS production the cell deploys a large variety of detoxifying enzymes (e.g. catalase, glutathione reductase) and antioxidant compounds such as glutathione, ascorbate and tocopherols (vitamin E) to confer stress tolerance to the seed (FOYER and NOCTOR, 2005). Furthermore the genes involved in the pentose phosphate pathway have been shown to be progressively up-regulated during germination to provide NADPH used against oxidative stress (Fait et al., 2006). On the other hand ROS are signaling molecules leading to important processes during seed desiccation and germination: degeneration of aleurone layer by PCD, endosperm weakening by loss of cell wall, protection against pathogen during seedling emergence, regulation of gene expression, protein oxidation and carbonylation, dormancy alleviation and sensing the favorable environment condition (Bailly, 2004; Job et al., 2005; Savage and Metzger, 2006). In summary, proline accumulation suggests that L5 seed is under oxidative stress and the delay in germination observed could be associated with the time necessary to setup the antioxidant machinery in order to escape oxidative stress. The high level of proline and glutamine could contribute to accelerate the pentose phosphate pathway and provides elevated reserves of NADPH necessary for antioxidant reaction led by ascorbate and glutathione. In addition, downregulation of the other genes involved in glutathione degradation, GGCT in the cytosol and GGT4 in the vacuole, resulted in *ggt1* and *ggt2* mature seed (Fig. 17), suggesting a tendency to preserve free glutathione into the cell to overcome an imminent oxidative stress. It would be interesting to perform the GGCT and GGT4 expression analyses also in L5 seed, to add new clues about its redox state.

4.2 GGT and glutathione in vegetative tissues development

4.2.1 Root

The characterization of root growth and morphology showed a slower elongation rate of L5 compared to wild-type, however also for the other lines there is a root growth tendency to slow down (Fig. 21A). This result suggests a possible relationship between GGT and regulation of root growth. Intense GGT activity and expression is observed in vascular bundle of whole plant including root (Martin et al., 2007; Ohkama-Ohtsu et al., 2007a; Destro et al., 2011); in addition glutathione is transported from the shoot to the root and constitutes important regulator for root growth (Herschbach and Scheerer, 2010). Therefore GGT might recruit glutathione from the vascular tissue to root zones that are under development. In fact in a global view GGT has been revealed to be highly expressed in tissues in active development: shoot apex, cotyledon of young seedling, elongation zone of root seedling, floral stem (Martin et al., 2007). Histochemical localization of GGT activity has shown intense reddish color in root tip of *Arabidopsis thaliana* (Destro et al., 2011), *Hordeum vulgare* (Ferretti et al., 2009) and *Zea mays* (Masi et al., 2007). Genevestigator showed both *GGT1* and *GGT2* expressed in the pericycle (Fig. 9), a meristematic tissue where lateral root originates. Coherently with these observations, several studies underlined the importance of glutathione in root growth. Glutathione is required for the initiation and maintenance of cell division in Arabidopsis root apex. The *root meristemless1* (*rml1),* mutant of *GSH1,* has low GSH level and extremely short root and lateral root due to abnormal growth in the root tip after germination (Vernoux et al., 2000). In contrast with this, extracellular GSH accumulation, induced by GGT activity inhibition, triggers ROS enhancement and root growth inhibition (Tamás et al., 2015). All these evidences together suggest GGT acts as a coordinator of glutathione level in root meristematic zone. However the silencing of both *GGT1* and *GGT2* does not affect severely root phenotype, indeed many factors play a role in this context and GGT might be just one of the elements involved in a fine root growth regulation.

The other root morphological factors characterized did not show any significant differences between lines. Root hairs, as trichomes in leaf, are originated from one epidermal cell. Root hair development depends on generation of ROS in the

apoplast by NADPH oxidase (NOX) (Foreman et al., 2003). Adjusting of ROS level by antioxidant as glutathione and ascorbate is thought to be crucial to modulate the growth of the root hair in response to changes of environmental conditions (Sánchez-Fernández and Fricker, 1997). Therefore since GGT is a modulator of glutathione and indirectly of ROS level in the apoplast, it might have a relationship with root hair development. However root hairs are invisible to the naked eye and root characterization performed in this thesis work does not allow to recognize them. Since trichomes are analogous to the root hair in leaves and they were less abundant in *ggt1/ggt2* RNAi than wild-type (Fig. 23) we presume that also root hair might be affected by *ggt1/ggt2* silencing. Further future studies will be focused on the characterization of this aspect.

The presence of GGT activity in roots can be tested by measuring GSH depletion and cys-gly release by roots immersed in a GSH containing solution. This experiment has been performed previously in different works (Ferretti et al., 2009; Destro et al., 2011) and it was repeated here with all *ggt* mutant lines in order to define the roles of the single isoforms in roots (Fig. 18). Genevestigator results (Fig. 9) and previous studies (Martin et al., 2007) showed that in root *GGT1* is largely more expressed than *GGT2*. The analysis of GGT activity in root showed that wild-type and *ggt2* had the same level of activity (Fig. 19); together with the incapability of *ggt1* to efficiently deplete GSH (Fig. 18A), leads us to assume that GGT1 is the main isoform in root. Moreover GGT activity measured in *ggt1/ggt2* RNAi mature seed (Fig. 10A) was considerable lower than those registered in root, where 25-30% of residual GGT1 transcript level remained (Fig. 7A). This indicates that low level of GGT1 mRNA in root was sufficient to translate the amount of protein necessary to reach the same activity of the wild-type. However the slow GSH depletion found in *ggt2* (Fig. 18A) demonstrates that GGT1 alone is unable to reach the wild-type trend even if *ggt2* root had the same level of activity of the wild-type. This suggests that GGT1 and GGT2 need to work together to deplete glutathione efficiently. In agreement with this finding, in *ggt1/ggt2* RNAi mutants, where both *GGT1* and *GGT2* were knocked down (transcripts not completely eliminated) and assuming that the residual transcripts led to functional proteins, glutathione depletion was more rapid than in the single mutants.

Enhancement of GGT2 transcript and activity in wild-type root incubated with GSH solution has been reported (Destro et al., 2011). The strong positive feedback on GGT2 expression in *ggt1* seems more inducted by GSH accumulation in the apoplast rather than a stimulus to compensate the absence of GGT1. Indeed, differently than what has been shown in Destro et al. (Destro et al., 2011), neither GGT activity (Fig. 19) nor the capacity to deplete GSH from external solution is enhanced in *ggt1* (Fig. 18). This apparent discrepancy could be due to differences in developmental stage, since in this work we used younger seedlings.

4.2.2 Leaves and trichome

In leaves GGT1 is the isoform that contributes to overall apoplastic activity. Vascular system and all the minor veins spread in the whole leaf surface are the predominant locations of GGT1 expression (Martin et al., 2007; Ohkama-Ohtsu et al., 2007a) and activity (Destro et al., 2011). Indeed the GGT1 expression in leaf vascular cell laser microdissected was over 17 times greater than the whole leaf (Ohkama-Ohtsu et al., 2007a). GGT1 expression has been found also in all other structures that connect different organs as petiole (stem with leaf) and pedicel (stem with silique). Genevestigator showed GGT1 expression also in companion cells (Fig. 9A). Companion cells are specialized in transferring solutes between phloem and source or sink cells during loading and unloading processes. These cells are simplastically connected by plasmodesmata with the vascular system, but the apoplastic way is also used to absorb nutrients by the enhanced membrane surface characterized by numerous invaginations. It is interesting to observe that phloem is the unique vegetative shoot tissue where GGT2 is adequately expressed (Fig. 9). Therefore GGT is at the interface between conductive elements and other tissues, therefore it might be assumed as a mediator between these two compartments. The growth rate of *ggt1/ggt2* RNAi rosettes resulted slower than in the other lines (Fig. 22), indicating that absence of the two isoforms affects the rapidity to grow.

More interest assume trichomes, which are defined as the hairs on the leaf surface. Both GGT1 and GGT2 are found expressed during their development (Martin et al., 2007) and in the first true leaves of *ggt1/ggt2* RNAi and *ggt2* mutants trichomes were significantly reduced (Fig. 23). The function of trichomes is still under debate, however several findings suggest their involvement in

detoxification process and plant defense. It has been reported that glandular trichomes secrete a broad range of natural products, which are known to have properties for plant defense (Gershenzon et al., 1992). Total GSH content in trichomes is more than 300-fold higher than in the basement and epidermal cells (Gutiérrez-Alcalá et al., 2000) and it has been assumed that GSH is important in the detoxification of xenobiotics and heavy metals. Indeed glutaredoxin and glutathione S-conjugate translocator have been identified in trichomes by proteomic analysis (Wienkoop et al., 2004). GGT could be involved in this process too in order to degrade GSH S-conjugates as it happens in animals (Shi et al., 2001) . On the other hand elevated levels of glutathione are necessary in this organ and GGT might contribute to recruit glutathione from the phloem. In trichomes of Arabidopsis leaves the main genes (Gutiérrez-Alcalá et al., 2000) and proteins (Wienkoop et al., 2004) related to cysteine and GSH biosynthesis have been shown to be expressed at high levels. It has been suggested that sulfide, or other intermediates of sulfur metabolism, is provided by the basement cell, whereas cysteine and then glutathione are biosynthesized in the trichome. However, high demand of glutathione is required in trichomes and GGT might integrate glutathione biosynthesis *in loco* by providing additional cysteine. The decision to produce lower amount of trichomes in *ggt1/ggt2* RNAi and *ggt2* mutant might be due to the inability to reach a physiologically adequate level of glutathione.

Trichomes have been considered a useful model for studying plant cell differentiation because of their characteristic development. Trichome is originated from single epidermal cell that further expands out and differentiates in the typical shape with three branches (Larkin et al., 1996). GGTs are expressed in immature trichomes and in particular GGT2:GUS expression in the basal regions of the leaf primordium has been shown (Martin et al., 2007), exactly where trichomes began to form (Marks, 1994). During the early stage of development, the trichome cell, after increasing its size, undergoes expansion perpendicular to the plane of the leaf. It seems relevant that expansion occurs also in root hairs, a phenomenon that is controlled in the apoplast by ROS produced by NOX (Foreman et al., 2003). In this scenario GGT might contribute to modulate indirectly ROS level in the apoplast by glutathione degradation.

5 Conclusion

In this work two independent lines of *ggt1/ggt2* RNAi double mutant were obtained in homozygosis and with good level of silencing. The simultaneous *GGT1* and *GGT2* silencing induces the decrease in the number of organs with high GSH demand (seed and trichome), but seemingly without changes in level of sulfur-containing molecules (glutathione, cysteine, 2S-albumin). This suggests that sulfur assimilation machinery is sufficient to provide normal level of sulfur-containing compounds, although to a lower number of seeds. Hence, GGT role is to integrate the elevated sulfur demand by means of GSH degradation that allows increasing the yield.

Accumulation of proline in L5 *ggt1/ggt2* RNAi seeds reveals that a stress condition is present and this is likely the cause of germination delay. Here it has been proposed that GGT acts as a modulator of redox status in the apoplast, and in turn that it might regulate the development mechanisms through ROS signaling. Additional experiments will be performed in order to quantify the ROS level in several tissues of *ggt1/ggt2* RNAi mutants. Further investigations will be addressed to explain the slight slowdown of vegetative growth in *ggt1/ggt2* RNAi mutants, focusing on root and root hair. Finally it has been shown that to deplete GSH from external solution by root the simultaneous presence of both *ggt* isoforms is necessary even if at low level. The future characterization of the double *ggt* mutants in the *sir1-1* and *ggct2;1* mutant background obtained in this work will provide new evidences about GGT. In particular the reduced flux of sulfur imposed by *sir1-1* mutation will highlight the contribution of GGT in cysteine delivery to the seed and in other organ; while *ggct2;1* mutation will elucidate new aspects on glutathione degradation and on the relation between cytosolic and apoplastic pathway.

6 References

Alexander MP (1969) Differential staining of aborted and nonaborted pollen. Stain technology **44**: 117–22

Allboje Samami A (2011) Lowered sulfite reduction affects metabolism and seed composition in Arabidopsis thaliana . University of Heidelberg, Germany, Combined Faculties for the Natural Sciences and for Mathematics of the Ruperto-Carola

Anderson J, Fitzgerald M (2001) Physiological and metabolic origin of sulphur for the synthesis of seed storage proteins. Journal of Plant Physiology **158**: 447–456

Baehrecke EH (2002) How death shapes life during development. Nat Rev Mol Cell Biol **3**: 779–87

Bailly C, Bailly C (2004) Active oxygen species and antioxidants in seed biology. Seed Sci Res **14**: 93–107

Bailly C, El-Maarouf-Bouteau H, Corbineau F (2008) From intracellular signaling networks to cell death: the dual role of reactive oxygen species in seed physiology. C R Biol **331**: 806–14

Becker, Hsu, Harada (2014) Genomic dissection of the seed. Front Plant Sc **5:**464

Belmonte MF, Kirkbride RC, Stone SL (2013) Comprehensive developmental profiles of gene activity in regions and subregions of the Arabidopsis seed. PNAS **14**:E435-E444

Bick JA, Setterdahl AT, Knaff DB, Chen Y, Pitcher LH, Zilinskas BA, Leustek T (2001) Regulation of the plant-type 5'-adenylyl sulfate reductase by oxidative stress. Biochemistry **40**: 9040–8

Bienert GP, Schjoerring JK, Jahn TP (2006) Membrane transport of hydrogen peroxide. Biochim Biophys Acta **1758**: 994–1003

Bolle C (2009) Phenotyping of Arabidopsisi Mutants for Developmental Effect of Gene Deletions. pp 17–34

Bourgis F, Roje S, Nuccio ML, Fisher DB, Tarczynski MC, Li C, Herschbach C, Rennenberg H, Pimenta MJ, Shen TL, et al (1999) S-methylmethionine plays a major role in phloem sulfur transport and is synthesized by a novel type of methyltransferase. Plant Cell **11**: 1485–98

Boyes D, Zayed A, Ascenzi R, McCaskill A, Hoffman N, Davis K, Görlach J (2001) Growth stage-based phenotypic analysis of Arabidopsis: a model for high throughput functional genomics in plants. Plant Cell **13**: 1499–510

Bozhkov PV, Suarez MF, Filonova LH (2005) Cysteine protease mcII-Pa executes programmed cell death during plant embryogenesis. PNAS **102**:40 14463-14468

Bradford MM (1976) A rapid and sensitive method for the quantitation of microgram quantities of protein utilizing the principle of protein-dye binding. Anal Biochem **72**: 248–54

Brisson LF, Tenhaken R, Lamb C (1994) Function of Oxidative Cross-Linking of Cell Wall Structural Proteins in Plant Disease Resistance. Plant Cell **6**: 1703–1712

Brugiere, Dubois, Limami AM, Lelandais, Roux, Sangwan RS, Hirel (1999) Glutamine synthetase in the phloem plays a major role in controlling proline production. Plant Cell **11**: 1995–2012

Cairns N, Pasternak M, Wachter A, Cobbett C, Meyer A (2006) Maturation of arabidopsis seeds is dependent on glutathione biosynthesis within the embryo. Plant physiology **141**: 446–55

Chang S, Puryear J, Cairney J (1993) A simple and efficient method for isolating RNA from pine trees. Plant molecular biology reporter **11**: 113–116

Chikhi N, Holic N, Guellaen G, Laperche Y (1999) Gamma-glutamyl transpeptidase gene organization and expression: a comparative analysis in rat, mouse, pig and human species. Comp Biochem Physiol B, Biochem Mol Biol **122**: 367–80

Circu M, Aw T (2008) Glutathione and apoptosis. Free radical research **42**: 689–706

De Cnodder T, Vissenberg K, Van Der Straeten D, Verbelen J-PP (2005) Regulation of cell length in the Arabidopsis thaliana root by the ethylene precursor 1-aminocyclopropane-

1-carboxylic acid: a matter of apoplastic reactions. New Phytol **168**: 541–50

Corti A, Paolicchi A, Franzini M, Dominici S, Casini AF, Pompella A (2005) The S-thiolating activity of membrane gamma-glutamyltransferase: formation of cysteinyl-glycine mixed disulfides with cellular proteins and in the cell microenvironment. Antioxid Redox Signal **7**: 911–8

Del Bello B, Paolicchi A, Comporti M, Pompella A, Maellaro E (1999) Hydrogen peroxide produced during gamma-glutamyl transpeptidase activity is involved in prevention of apoptosis and maintainance of proliferation in U937 cells. FASEB J **13**: 69-79.

Destro T, Prasad D, Martignago D, Bernet I, Trentin A, Renu I, Ferretti M, Masi A (2011) Compensatory expression and substrate inducibility of γ-glutamyl transferase GGT2 isoform in Arabidopsis thaliana. Journal of Experimental Botany **62**: 805–814

Diaz Vivancos P, Wolff T, Markovic J, Pallardó FV, Foyer CH (2010) A nuclear glutathione cycle within the cell cycle. Biochem J **431**: 169–78

De Donatis GM, Moschini R, Cappiello M, Del Corso A, Mura U (2010) Cysteinyl-glycine in the control of glutathione homeostasis in bovine lenses. Mol Vis **16**: 1025–33

Edwards, Johnstone, Thompson C (1991) A simple and rapid method for the preparation of plant genomic DNA for PCR analysis. Nucleic acids research **19**: 1349

Fait A, Angelovici R, Less H, Ohad I, Urbanczyk-Wochniak E, Fernie A, Galili G (2006) Arabidopsis seed development and germination is associated with temporally distinct metabolic switches. Plant physiology **142**: 839–854

Ferretti, Destro, Tosatto S, Rocca L, Rascio, Masi (2009) Gamma-glutamyl transferase in the cell wall participates in extracellular glutathione salvage from the root apoplast. New Phytologist **181**: 115–126

Foreman J, Demidchik V, Bothwell JH, Mylona P, Miedema H, Torres MA, Linstead P, Costa S, Brownlee C, Jones JD, et al (2003) Reactive oxygen species produced by NADPH oxidase regulate plant cell growth. Nature **422**: 442–6

FOYER C, NOCTOR G (2005) Oxidant and antioxidant signalling in plants: a re-evaluation of the concept of oxidative stress in a physiological context. Plant Cell Environ **28**: 1056–1071

Foyer C, Theodoulou F, Delrot S (2001) The functions of inter- and intracellular glutathione transport systems in plants. Trends Plant Sci **6**: 486–492

Franco R, Cidlowski JA (2009) Apoptosis and glutathione: beyond an antioxidant. Cell Death & Differentiation **16**:1303-1314

Frerigmann, Böttcher, Baatout (2012) Glucosinolates are produced in trichomes of Arabidopsis thaliana. Front Plant Sci **3**: 242

Fry SC (1998) Oxidative scission of plant cell wall polysaccharides by ascorbate-induced hydroxyl radicals. Biochem J **332 (Pt 2)**: 507–15

Galant A, Preuss M, Cameron J, Jez J (2011) Plant Glutathione Biosynthesis: Diversity in Biochemical Regulation and Reaction Products. Frontiers in Plant Science. **2**: 45

Gapper C, Dolan L (2006) Control of plant development by reactive oxygen species. Plant Physiology. **141**: 341-345

Gechev TS, Breusegem VF, Stone JM, Denev I (2006) Reactive oxygen species as signals that modulate plant stress responses and programmed cell death. BioEssays **28**: 1091-1101

Gechev TS, Minkov IN, Hille J (2005) Hydrogen peroxide-induced cell death in Arabidopsis: transcriptional and mutant analysis reveals a role of an oxoglutarate-dependent dioxygenase gene in the cell death process. IUBMB Life **57**: 181–8

Gershenzon J, McCaskill D, Rajaonarivony JI, Mihaliak C, Karp F, Croteau R (1992) Isolation of secretory cells from plant glandular trichomes and their use in biosynthetic studies of monoterpenes and other gland products. Anal Biochem **200**: 130–8

Gomez LD, Noctor G, Knight MR, Foyer CH (2004) Regulation of calcium signalling and gene expression by glutathione. J Exp Bot **55**: 1851–9

Grzam A, Martin M, Hell R, Meyer A (2007) gamma-Glutamyl transpeptidase GGT4 initiates vacuolar degradation of glutathione S-conjugates in Arabidopsis. FEBS letters **581**:

3131–8

Gutiérrez-Alcalá G, Gotor C, Meyer AJ (2000) Glutathione biosynthesis in Arabidopsis trichome cells. PNAS **97**: 11108-11113

Habig W, Pabst M, Jakoby W (1974) Glutathione S-transferases the first enzymatic step in mercapturic acid formation. Journal of biological Chemistry **249**: 7130–7139

Hanigan MH (2014) Gamma-glutamyl transpeptidase: redox regulation and drug resistance. Adv Cancer Res **122**: 103–41

Hanigan MH, Frierson HF (1996) Immunohistochemical detection of gamma-glutamyl transpeptidase in normal human tissue. J Histochem Cytochem **44**: 1101–8

Hartmann T, Hönicke P, Wirtz M, Hell R, Rennenberg H, Kopriva S (2004) Regulation of sulphate assimilation by glutathione in poplars (Populus tremula x P. alba) of wild type and overexpressing gamma-glutamylcysteine synthetase in the cytosol. J Exp Bot **55**: 837–45

Haughn G, Chaudhury A (2005) Genetic analysis of seed coat development in Arabidopsis. Trends Plant Sci **10**: 472–7

Hell R, Wirtz M (2011) Molecular Biology, Biochemistry and Cellular Physiology of Cysteine Metabolism in Arabidopsis thaliana. Arabidopsis Book **9**: e0154

Herschbach C, van der Zalm E, Schneider A (2000) Regulation of sulfur nutrition in wild-type and transgenic poplar over-expressing γ-glutamylcysteine synthetase in the cytosol as affected by atmospheric H2S. Plant Physiology **124**: 461-473

Herschbach, Scheerer (2010) Redox states of glutathione and ascorbate in root tips of poplar (Populus tremula× P. alba) depend on phloem transport from the shoot to the roots. Journal of Experimental Botany **61**: 1065–1074

HEWITT EJ, DICKES GJ (1961) Spectrophotometric measurements on ascorbic acid and their use for the estimation of ascorbic acid and dehydroascorbic acid in plant tissues. Biochem J **78**: 384–91

Himelblau, Amasino (2001) Nutrients mobilized from leaves of Arabidopsis thaliana during leaf senescence. J. Plant Physiol. **158**: 1317 – 1323

Höller K, Király L, Künstler A, Müller M, Gullner G, Fattinger M, Zechmann B (2010) Enhanced glutathione metabolism is correlated with sulfur-induced resistance in Tobacco mosaic virus-infected genetically susceptible Nicotiana tabacum plants. Mol Plant Microbe Interact **23**: 1448–59

Hruz T, Laule O, Szabo G, Wessendorp F (2008) Genevestigator v3: a reference expression database for the meta-analysis of transcriptomes. Advances in Bioinformatics

Huseby, Strömme (1974) Practical points regarding routine determination of gamma-glutamyl transferase (gamma-GT) in serum with a kinetic method at 37 degrees C. Scandinavian journal of clinical and laboratory investigation **34**: 357–63

Job C, Rajjou L, Lovigny Y, Belghazi M, Job D (2005) Patterns of protein oxidation in Arabidopsis seeds and during germination. Plant Physiol **138**: 790–802

Kawashima T, Goldberg RB (2010) The suspensor: not just suspending the embryo. Trends in plant science. 1360-1385

Khan MS, Haas FH, Samami AA, Gholami AM, Bauer A, Fellenberg K, Reichelt M, Hänsch R, Mendel RR, Meyer AJ, et al (2010) Sulfite reductase defines a newly discovered bottleneck for assimilatory sulfate reduction and is essential for growth and development in Arabidopsis thaliana. The Plant cell **22**: 1216–31

Kim I, Kobayashi K, Cho E (2005) Subdomains for transport via plasmodesmata corresponding to the apical–basal axis are established during Arabidopsis embryogenesis. PNAS **102**: 11945–11950

Kishor P, Sangam S, Amrutha RN, Laxmi PS (2005) Regulation of proline biosynthesis, degradation, uptake and transport in higher plants: its implications in plant growth and abiotic stress tolerance. Curr Sci

Kocsis MG, Ranocha P, Gage DA, Simon ES (2003) Insertional inactivation of the methionine S-methyltransferase gene eliminates the S-methylmethionine cycle and increases the methylation ratio. Plant Phisyol. **131**: 1808-1815

Kopriva S, Rennenberg H (2004) Control of sulphate assimilation and glutathione synthesis:

interaction with N and C metabolism. J Exp Bot **55**: 1831–42

Kuzuhara Y, Isobe A, Awazuhara M, Fujiwara T, Hayashi H (2000) Glutathione levels in phloem sap of rice plants under sulfur deficient conditions. Soil Science and Plant Nutrition **46**: 265270

Lappartient AG, Touraine B (1996) Demand-driven control of root ATP sulfurylase activity and SO42-uptake in intact canola (the role of phloem-translocated glutathione). Plant Physiology. doi: 10.1104/pp.111.1.147

Larkin JC, Young N, Prigge M, Marks MD (1996) The control of trichome spacing and number in Arabidopsis. **122**: 997–1005

Lee Y-II, Yeung EC (2010) The osmotic property and fluorescent tracer movement of developing orchid embryos of Phaius tankervilliae (Aiton) Bl. Sex Plant Reprod **23**: 337–41

Lieberman MW, Wiseman AL, Shi ZZ, Carter BZ, Barrios R, Ou CN, Chévez-Barrios P, Wang Y, Habib GM, Goodman JC, et al (1996) Growth retardation and cysteine deficiency in gamma-glutamyl transpeptidase-deficient mice. Proc Natl Acad Sci USA **93**: 7923–6

Liszkay A, van der Zalm E, Schopfer P (2004) Production of reactive oxygen intermediates (O(2)(.-), H(2)O(2), and (.)OH) by maize roots and their role in wall loosening and elongation growth. Plant Physiol **136**: 3114–23; discussion 3001

Marks MD (1994) Plant development. The making of a plant hair. Curr Biol **4**: 621–3

Martin M, Saladores P, Lambert E, Hudson A, Leustek T (2007) Localization of Members of the ^{3}-Glutamyl Transpeptidase Family Identifies Sites of Glutathione and Glutathione S-Conjugate Hydrolysis. PLANT PHYSIOLOGY **144**: 17151732

Masi A, Ghisi R, Ferretti M (2002) Measuring low-molecular-weight thiols by detecting the fluorescence of their SBD-derivatives: application to studies of diurnal and UV-B induced changes in Zea mays L. Journal of Plant Physiology **159**: 499–507

Masi A, Destro T, Turetta L, Varotto S, Caporale G, Ferretti M (2007) Localization of gamma-glutamyl transferase activity and protein in Zea mays organs and tissues. Journal of Plant Physiology **164**: 15271535

Masi A, Trentin AR, Agrawal GK, Rakwal R (2015) Gamma-glutamyl cycle in plants: a bridge connecting the environment to the plant cell? Front Plant Sci **6**: 252

Mattioli R, Costantino P, Trovato M (2009) Proline accumulation in plants: not only stress. Plant Signal Behav **4**: 1016–8

May MJ, Vernoux T, Leaver C (1998) Glutathione homeostasis in plants: implications for environmental sensing and plant development. Journal of Experimental Botany **49:** 649–667

Meister, A., and Anderson, M. E. (1983). Glutathione. Annu. Rev. Biochem **52**: 711–760.

Mendoza-Cózatl D, Butko E, Springer F, Torpey J, Komives E, Kehr J, Schroeder J (2008) Identification of high levels of phytochelatins, glutathione and cadmium in the phloem sap of Brassica napus. A role for thiol-peptides in the long-distance transport of cadmium and the effect of cadmium on iron translocation. The Plant Journal **54**: 249–259

Morley-Smith ER, Pike MJ, Findlay K, Köckenberger W, Hill LM, Smith AM, Rawsthorne S (2008) The transport of sugars to developing embryos is not via the bulk endosperm in oilseed rape seeds. Plant Physiol **147**: 2121–30

Mou Z, Fan W, Dong X (2003) Inducers of plant systemic acquired resistance regulate NPR1 function through redox changes. Cell **113**: 935–44

Nakaune S, Yamada K, Kondo M, Kato T, Tabata S, Nishimura M, Hara-Nishimura I (2005) A vacuolar processing enzyme, deltaVPE, is involved in seed coat formation at the early stage of seed development. Plant Cell **17**: 876–87

NOCTOR G (2006) Metabolic signalling in defence and stress: the central roles of soluble redox couples. Plant Cell Environ **29**: 409–425

NOCTOR G, MHAI A, CHAOUCH S, HAN, NEUKERMANS J, MARQUEZ-GARCIA B, QUEVAL G, FOYER C (2012) Glutathione in plants: an integrated overview. Plant, Cell & Environment **35**: 454–484

Noctor G, Queval G, Mhamdi A, Chaouch S, Foyer C (2011) Glutathione. The Arabidopsis book / American Society of Plant Biologists.

Ohkama-Ohtsu N, Oikawa A, Zhao P, Xiang C, Saito K, Oliver DJ (2008) A gamma-glutamyl transpeptidase-independent pathway of glutathione catabolism to glutamate via 5-oxoproline in Arabidopsis. Plant Physiol **148**: 1603–13

Ohkama-Ohtsu N, Radwan S, Peterson A, Zhao P, Badr AF, Xiang C, Oliver DJ (2007a) Characterization of the extracellular gamma-glutamyl transpeptidases, GGT1 and GGT2, in Arabidopsis. Plant J **49**: 865–77

Ohkama-Ohtsu N, Zhao P, Xiang C, Oliver DJ (2007b) Glutathione conjugates in the vacuole are degraded by gamma-glutamyl transpeptidase GGT3 in Arabidopsis. Plant J **49**: 878–88

Paolicchi, Dominici, Pieri, Maellaro (2002) Glutathione catabolism as a signaling mechanism. Biochemical Pharmacology Biochemical Pharmacology **64**: 1027-1035

Pasternak M, Lim B, Wirtz M, Hell R, Cobbett C, Meyer A (2008) Restricting glutathione biosynthesis to the cytosol is sufficient for normal plant development. The Plant Journal **53**: 999–1012

Paulose B, Chhikara S, Coomey J, Jung H-II, Vatamaniuk O, Dhankher OP (2013) A γ-glutamyl cyclotransferase protects Arabidopsis plants from heavy metal toxicity by recycling glutamate to maintain glutathione homeostasis. Plant Cell **25**: 4580–95

Perego P, Paolicchi A, Tongiani R (1997) The cell-specific anti-proliferative effect of reduced glutathione is mediated by g-glutamyl transpeptidase-dependent extracellular pro-oxidant reactions. Int. J. Cancer: **71**: 246–250

Pompella A, Corti A, Paolicchi A, Giommarelli C (2007) γ-Glutamyltransferase, redox regulation and cancer drug resistance. Current Opinion in Pharmacology **7**:360–366

Rennenberg H, Herschbach C (2014) A detailed view on sulphur metabolism at the cellular and whole-plant level illustrates challenges in metabolite flux analyses. J Exp Bot **65**: 5711–24

Rodríguez AAA, Grunberg KA, Taleisnik EL (2002) Reactive oxygen species in the elongation zone of maize leaves are necessary for leaf extension. Plant Physiol **129**: 1627–32

Rutenburg AM, Kim H, Fischbein JW, Hanker JS, Wasserkrug HL, Seligman AM (1969) Histochemical and ultrastructural demonstration of gamma-glutamyl transpeptidase activity. J Histochem Cytochem **17**: 517–26

Sagi M, Davydov O, Orazova S, Yesbergenova Z, Ophir R, Stratmann JW, Fluhr R (2004) Plant respiratory burst oxidase homologs impinge on wound responsiveness and development in Lycopersicon esculentum. Plant Cell **16**: 616–28

Sánchez-Fernández R, Fricker M (1997) Cell proliferation and hair tip growth in the Arabidopsis root are under mechanistically different forms of redox control. Proc. Natl. Acad. Sci. USA **94**: 2745–2750

Savage W, Metzger G (2006) Seed dormancy and the control of germination. New phytologist **171**: 501–523

Schägger H (2006) Tricine-SDS-PAGE. Nat Protoc **1**: 16–22

Schopfer P, Liszkay A, Bechtold M, Frahry G, Wagner A (2002) Evidence that hydroxyl radicals mediate auxin-induced extension growth. Planta **214**: 821–8

Schwacke R, Grallath S, Breitkreuz KE, Stransky E, Stransky H, Frommer WB, Rentsch D (1999) LeProT1, a transporter for proline, glycine betaine, and gamma-amino butyric acid in tomato pollen. Plant Cell **11**: 377–92

Shapiguzov A, Vainonen J, Wrzaczek M, Kangasjärvi J (2012) ROS-talk – how the apoplast, the chloroplast, and the nucleus get the message through. Front Plant Sci. **3**: 292

Shi ZZ, Han B, Habib GM, Matzuk MM, Lieberman MW (2001) Disruption of gamma-glutamyl leukotrienase results in disruption of leukotriene D(4) synthesis in vivo and attenuation of the acute inflammatory response. Mol Cell Biol **21**: 5389–95

Shiu SH, Bleecker AB (2003) Expansion of the receptor-like kinase/Pelle gene family and receptor-like proteins in Arabidopsis. Plant Physiol **132**: 530–43

Stadler R, Lauterbach C, Sauer N (2005) Cell-to-Cell Movement of Green Fluorescent Protein Reveals Post-Phloem Transport in the Outer Integument and Identifies Symplastic

Domains in Arabidopsis Seeds and Embryos. PLANT PHYSIOLOGY **139**: 701–712

Stark AA, Zeiger E, Pagano DA (1988) Glutathione mutagenesis in Salmonella typhimurium is a gamma-glutamyltranspeptidase-enhanced process involving active oxygen species. Carcinogenesis **9**: 771–7

Stark AA, Zeiger E, Pagano DA (1993) Glutathione metabolism by gamma-glutamyltranspeptidase leads to lipid peroxidation: characterization of the system and relevance to hepatocarcinogenesis. Carcinogenesis **14**: 183–9

Storozhenko S, Belles-Boix E, Babiychuk E, Hérouart D, Davey M, Slooten L, Montagu M, Inzé D, Kushnir S (2002) Gamma-glutamyl transpeptidase in transgenic tobacco plants. Cellular localization, processing, and biochemical properties. Plant physiology **128**: 1109–19

Szabados L, Savouré A (2010) Proline: a multifunctional amino acid. Trends Plant Sci **15**: 89–97

Tabe L, Droux M (2001) Sulfur assimilation in developing lupin cotyledons could contribute significantly to the accumulation of organic sulfur reserves in the seed. Plant Physiology **126**: 176–187

Takahashi H, Kopriva S, Giordano M, Saito K, Hell R (2011) Sulfur assimilation in photosynthetic organisms: molecular functions and regulations of transporters and assimilatory enzymes. Annu Rev Plant Biol **62**: 157–84

Tamás L, Alemayehu A, Mistrík I, Zelinová V (2015) Extracellular glutathione recycling by γ-glutamyl transferase in barley root tip exposed to cadmium. Environmental and Experimental Botany **118**: 3239

Tan Q, Zhang L, Grant J, Cooper P, Tegeder M (2010) Increased phloem transport of S-methylmethionine positively affects sulfur and nitrogen metabolism and seed development in pea plants. Plant Physiol **154**: 1886–96

Tolin S, Arrigoni G, Trentin AR, Veljovic-Jovanovic S, Pivato M, Zechman B, Masi A (2013) Biochemical and quantitative proteomics investigations in Arabidopsis ggt1 mutant leaves reveal a role for the gamma-glutamyl cycle in plant's adaptation to environment. Proteomics **13**: 2031–45

Trentin AR, Pivato M, Mehdi SMM, Barnabas LE, Giaretta S, Fabrega-Prats M, Prasad D, Arrigoni G, Masi A (2015) Proteome readjustments in the apoplastic space of Arabidopsis thaliana ggt1 mutant leaves exposed to UV-B radiation. Front Plant Sci **6**: 128

Tzafrir I, Pena-Muralla R, Dickerman A, Berg M, Rogers R, Hutchens S, Sweeney TC, McElver J, Aux G, Patton D, et al (2004) Identification of genes required for embryo development in Arabidopsis. Plant Physiol **135**: 1206–20

Vanacker, Carver TL, Foyer CH (1998) Pathogen-induced changes in the antioxidant status of the apoplast in barley leaves. Plant Physiol **117**: 1103–14

Vauclare P, Kopriva S, Fell D, Suter M, Sticher L, von Ballmoos P, Krähenbühl U, den Camp RO, Brunold C (2002) Flux control of sulphate assimilation in Arabidopsis thaliana: adenosine 5'-phosphosulphate reductase is more susceptible than ATP sulphurylase to negative control by thiols. Plant J **31**: 729–40

Verbelen J-PP, De Cnodder T, Le J, Vissenberg K, Baluska F (2006) The Root Apex of Arabidopsis thaliana Consists of Four Distinct Zones of Growth Activities: Meristematic Zone, Transition Zone, Fast Elongation Zone and Growth Terminating Zone. Plant Signal Behav **1**: 296–304

Vernoux T, Wilson RC, Seeley KA, Reichheld JP, Muroy S, Brown S, Maughan SC, Cobbett CS, Van Montagu M, Inzé D, et al (2000) The ROOT MERISTEMLESS1/CADMIUM SENSITIVE2 gene defines a glutathione-dependent pathway involved in initiation and maintenance of cell division during postembryonic root development. Plant Cell **12**: 97–110

Verslues PE, Sharma S (2010) Proline metabolism and its implications for plant-environment interaction. Arabidopsis Book **8**: e0140

Western TL, Skinner DJ, Haughn GW (2000) Differentiation of mucilage secretory cells of the Arabidopsis seed coat. Plant Physiol **122**: 345–56

Wienkoop S, Zoeller D, Ebert B, Simon-Rosin U (2004) Cell-specific protein profiling in

Arabidopsis thaliana trichomes: identification of trichome-located proteins involved in sulfur metabolism and detoxification. Phytochemistry **65**: 1641–1649

Winter D, Vinegar B, Nahal H, Ammar R, Wilson GV, Provart NJ (2007) An "Electronic Fluorescent Pictograph" browser for exploring and analyzing large-scale biological data sets. PloS one **2**: e718–e718

Wrzaczek M, Brosché M, Salojärvi J, Kangasjärvi S, Idänheimo N, Mersmann S, Robatzek S, Karpiński S, Karpińska B, Kangasjärvi J (2010) Transcriptional regulation of the CRK/DUF26 group of receptor-like protein kinases by ozone and plant hormones in Arabidopsis. BMC Plant Biol **10**: 95

Yeung EC, Meinke DW (1993) Embryogenesis in Angiosperms: Development of the Suspensor. Plant Cell **5**: 1371–1381

Zechmann B (2014) Compartment-specific importance of glutathione during abiotic and biotic stress. Frontiers in Plant Science. **5**: 566

Zechmann, Mauch, Sticher, Müller (2008) Subcellular immunocytochemical analysis detects the highest concentrations of glutathione in mitochondria and not in plastids. Journal of Experimental Botany **59**: 4017–4027

Zhang X, Henriques R, Lin S-SS, Niu Q-WW, Chua N-HH (2006) Agrobacterium-mediated transformation of Arabidopsis thaliana using the floral dip method. Nature protocols **1**: 641–6

Zhang, Xie, Jobe, Kau, Wang, Li (2015) Identification of AtOPT4 as a Plant Glutathione Transporter. Molecular Plant

Zuber H, Davidian J-CC, Aubert G, Aimé D, Belghazi M, Lugan R, Heintz D, Wirtz M, Hell R, Thompson R, et al (2010) The seed composition of Arabidopsis mutants for the group 3 sulfate transporters indicates a role in sulfate translocation within developing seeds. Plant Physiol **154**: 913–26

Publications

Trentin A.R., Pivato M., Mehdi M.S., Barnabas L.E., Giaretta S., Fàbrega M., Prasad D., Masi A (2015) Proteome readjustments in the apoplastic space of Arabidopsis thaliana ggt1 mutant leaves exposed to UV-B radiation. Front. Plant Sci. 6:128. doi: 10.3389/fpls.2015.00128

Poster

Anna Rita Trentin, Serena Tolin, Micaela Pivato, Sabrina Giaretta, Marta Fabrega-Prats, Mehdi Syed Muhammad Muntazir, Giorgio Arrigoni, Dinesh Prasad, Antonio Masi (2013). "Functions of the Gamma-Glutamyl Cycle in Plant Metabolism Explored by Proteomic Analysis of Arabidopsis Mutants". 8th ITPA Congress, Padova 18-21 June 2013.

A.R. Trentin, M. Pivato, S. Giaretta, M. Fabrega-Prats, G. Arrigoni, D. Prasad, A. Masi (2013) "GGT-assisted glutathione degradation is functional to apoplastic redox control and seed storage proteins accumulation" 11°International POG conference Reactive Oxygen and nitrogen species in plants Warsaw, 17-19 luglio 2013.

Trentin A., Pivato M., Ebinezer L.B., Giaretta, S., Prasad D., Fabrega-Prats M., Masi A (2014). "Role of apoplastic GGT1 in plant's response to UV-B radiation" The final network conference of COST Action FA0906, UV4 Growth. Bled, 30 March, 2 April 2014.

Trentin A., Pivato M., Giaretta S., Fabrega-Pratz M., Ebinezer L.B., Mehdi M.S., Masi A. (2014) "Involvement of extracellular glutathione degradation in the response to UV-B radiation in A. thaliana wild-type and ggt1 mutant". 9th International Workshop: Sulfur Metabolism in Plants, 14-17 April 2014.

Trentin A.R., Sharma N., Giaretta S., Fabrega-Prats M., , Arrigoni G., Masi A. (2015). "gamma-glutamyl cycle and oxidative stress: investigations on apoplastic proteome composition in ggt1 mutants" 12° International POG conference Reactive Oxygen and nitrogen species in plants Verona, 24-26 giugno 2015.

Sabrina Giaretta, Anna Rita Trentin, Marta Fabrega-Prats, Antonio Masi (2015). "PROPERTIES AND FUNCTIONS OF THE γ-GLUTAMYL CYCLE IN PLANTS: AN OVERVIEW". From Molecules to the Field BOTANIKERTAGUNG 2015 30.8. – 3.9.2015 Ludwig-Maximilians-Universität & Technische Universität München, Freising – Germany.

Acknowledgment - Ringraziamenti

Prima di tutto vorrei ringraziare il mio supervisore Prof. Antonio Masi per avermi dato la possibilità di intraprendere questi tre anni di dottorato; inoltre lo ringrazio per i suoi consigli e per avermi dato l'opportunità di arricchire la mia esperienza anche all'estero.

Ringrazio i membri che hanno fatto parte del nostro gruppo di ricerca durante questi tre anni: la Dr.ssa Anna Rita Trentin per essere sempre stata disponibile ad aiutarci in laboratorio, Marta Fabrega-Prats per aver condiviso insieme questa esperienza di dottorato portando un po' di allegria e la Dr.ssa Micaela Pivato per i suoi numerosi consigli.

In particolare ringrazio coloro che hanno contribuito alla elaborazione di questa tesi: Dr. Dinesh Prasad per aver generato i mutanti RNAi, Dr.ssa Ilaria Forieri per l'analisi al CNS e degli aminoacidi e per aver letto e corretto questa tesi, Paolo Gottorado e Veronica Vendramin per la statistica, Prof. Teofilo Vamerali e Cristian Dal Cortivo per l'analisi radicale, Giovanni Caporale per l'ottenimento delle sezioni tissutali per l'istochimica.

I would like to express my gratitude to Prof. Dr. Rüdiger Hell and Dr. Markus Wirtz of University of Heidelberg for the supervision during the time spent in Germany and for giving me the opportunity to work in their research group. I would like also to thank all the members and the students of AG Hell lab: Anna, Catrin, Eric, Eva Maria, Francy, Gernot, Ilaria, Michael, Monika, Stefan, Sundas and Yihan.

Ringrazio gli studenti e dottorandi con i quali ho collaborato e mi hanno aiutato nel lavoro di laboratorio: Martina Gianbruno, Simone Masala, Syed M. M. Mehdi, Nisha Sharma e Alba Sturaro.

Un pensiero di ringraziamento va a tutti i dottorandi del XXVIII ciclo con cui ho condiviso le gioie e le pene del dottorato: Matteo Bergamaschi, Marco Birolo, Chiara Broccanello, Chiara De Lucchi, Marta Fabrega-Prats, Paolo Gottardo, Laura Maccarana, Federica Tinello, Veronica Vendramin.

Infine voglio ringraziare i miei genitori per avermi sempre sostenuto nei miei studi e a mia sorella che ha letto e corretto con criticità la mia tesi.